July 16, 1978

Final Report

DEVELOPMENT OF METHODS OF CHARACTERIZING COAL IN ITS PLASTIC STATE

William G. Lloyd
Institute for Mining and Minerals Research
Kentucky Center for Energy Research Laboratory

University of Kentucky
Lexington, Kentucky 40506

work performed under
California Institute of Technology Contract No. 954920
(Subcontract under NASA Contract NAS7-100)
Technical Manager:
Dr. Raymond Kushida, Jet Propulsion Laboratory

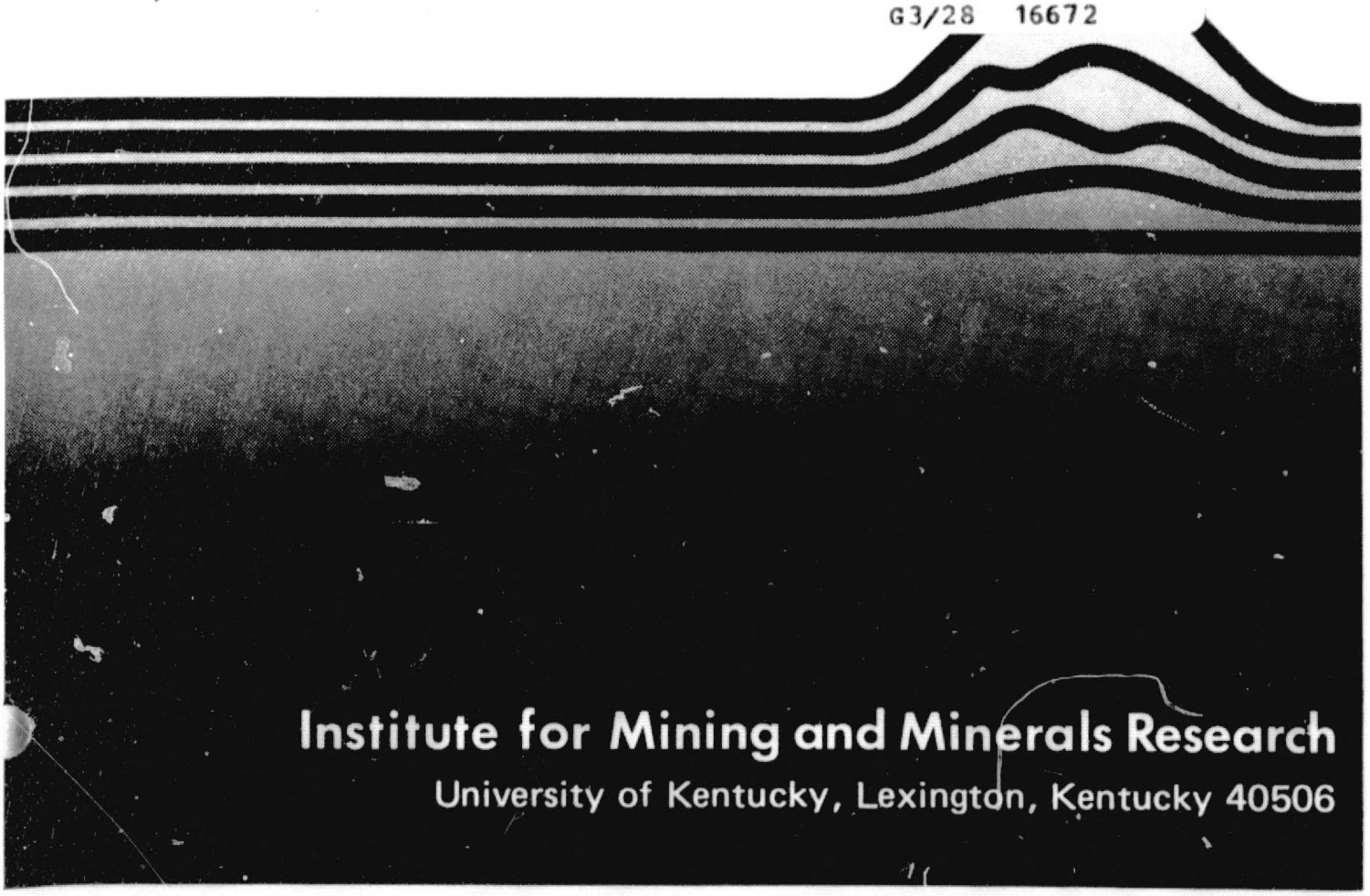

Institute for Mining and Minerals Research
University of Kentucky, Lexington, Kentucky 40506

INSTITUTE FOR MINING AND MINERALS RESEARCH

University of Kentucky

Lexington, Kentucky

The Institute for Mining and Minerals Research has these objectives:

to conduct research programs and projects of direct interest to mining and minerals

function as a coordinating body between the elements of the University of Kentucky, state and federal agencies, and local and private agencies

be responsible for the direction of research participation, training grants, and similar academic-research cooperation

provide information on industrial, technological, social and health aspects of coal production and usage

distribute information through published reports, monographs, news releases, seminars, conferences, and similar means of dissemination

provide direction and technical assistance to related projects conducted by other organizations

---

Technical Reports are published by the Office of Research and Engineering Services at the University of Kentucky to report progress and accomplishments in its program of investigation and research.

For additional copies or information address correspondence to:

ORES Publications
College of Engineering
University of Kentucky
Lexington, Kentucky 40506

A PUBLICATION OF THE OFFICE OF RESEARCH AND ENGINEERING SERVICES

College of Engineering
University of Kentucky

DEVELOPMENT OF METHODS OF CHARACTERIZING COAL IN ITS PLASTIC STATE

Final Report

William G. Lloyd

Institute for Mining and Minerals Research

University of Kentucky

July 16, 1978

work performed under

California Institute of Technology Contract No. 954920

(Subcontract under NASA Contract NAS7-100)

Technical Manager: Dr. Raymond Kushida, Jet Propulsion Laboratory

DEVELOPMENT OF METHODS OF CHARACTERIZING COAL IN ITS PLASTIC STATE

TABLES PAGE

FIGURES PAGE

1. SUMMARY

Coal in its plastic state (typically 400-460°C) has been examined by the isothermal Gieseler plastometry of seven selected coals of widely varying plastic properties. A kinetic model has been proposed for the isothermal plastometric curves.

This plastic behavior has been compared with a variety of laboratory analyses and characterizations of these coals, including classical coal analysis, mineral analysis, microstructural analysis (extractable fractions, surface area measurements, and petrographic analysis), and thermal analysis (thermogravimetric analysis, thermomechanical analysis, and differential scanning calorimetry).

The phenomenon of a sharp, large, poorly reproducible exotherm in the differential scanning calorimetric analysis of coking coals has been examined. It is concluded that this is a method artifact.

Examination of several coal extrudates shows mineral distribution, organic maceral composition and overall calorific value to be little affected by 800°F extrusion. Volatile matter and plastic properties are moderately reduced, and the network structure (as gauged by extractables) appears to be slightly degraded in the extrusion process.

2. INTRODUCTION

This study of the development of methods of characterizing coal in its plastic state was authorized under California Institute of Technology Contract No. 954920 (Subcontract under NASA Contract NAS7-100), dated November 16, 1977.

In consultation with the Technical Contract Manager, Jet Propulsion Laboratory, we have selected a small group of coals for detailed laboratory characterization. Each of these coals has been or is to be the subject of an extrusion experiment using JPL's 1.5-inch screw extruder. Our laboratory has undertaken a comprehensive characterization of each of these coals, and of a number of coal extrudate samples supplied by JPL, with the objective of better understanding the melting phenomenon and the nature of the plastic state, and of seeking laboratory analytical techniques of useful predictive value with regard to the thermoplastic behavior of coals.

The coals selected for this study are:

Pittsburgh #8	(PA)
Ohio #9	(OH)
Lower Kittanning	(PA)
Kentucky #11	(KY)
Pocahontas #3	(WV)
Amax (Wyoming)	(WY)
Elkhorn #1	(KY)

They range in rank from low volatile bituminous (Pocahontas #3) to subbituminous C (Amax), with free swelling indexes from 0 to 8, and with a substantial range of values for other properties. Three of these coals are quite plastic, two are slightly plastic, and two are nonplastic, as characterized by Gieseler fluidity.

The experimental study of these coals and of selected coal extrudates is reported in Section 3. The classical analyses used for the characterization of coals (proximate and ultimate analyses, free swelling index, calorific value) are given in Section 3.1. Mineral analyses, and related information on high- and low-temperature ashing, are reported in Section 3.2. The plastic behavior of these coals, in terms of both ASTM and isothermal Gieseler measurements, is described in Section 3.3. Several indicators of microstructural characteristics -- extractable fractions, SEM micrography and elemental mapping, surface areas by gas and vapor adsorption, and petrographic analysis -- are given in Section 3.4. The results of thermal analysis, using thermogravimetric analysis, thermomechanical analysis, and differential scanning calorimetry, are reported in Section 3.5.

Section 4 presents a brief discussion of these findings, under three headings. Section 4.1 describes a simple model for the isothermal plastometric curve. Section 4.2 discusses the utility of several kinds of laboratory analysis from the standpoint of predictability of the plastic behavior of coals. Section 4.3 discusses two serious problem areas. Section 4.4 notes some suggestions for future work.

Section 6 is a tabulation of raw analytical data obtained with these coals and coal extrudates.

3. EXPERIMENTAL

3.1 Proximate and Ultimate Analyses

(work performed by Gerald A. Thomas and Henry E. Francis)

The proximate and ultimate analyses of the seven coals comprising this study are reported in Table 3.1-1. Also included in this table are the calorific values (heating values in Btu/lb by adiabatic bomb calorimetry) and FSI values (ASTM free swelling indices) of these coals.

The moisture, ash, volatile matter, fixed carbon, total sulfur, calorific value, and FSI value determinations are conducted in accordance with the standards recommended by Committee D-5 (Coal and Coke) of the American Society for Testing and Materials (ASTM). Carbon, hydrogen and nitrogen are determined by a semimicro combustion analysis (Perkin-Elmer Model 240 Elemental Analyzer). Oxygen is determined by difference, as noted below. All of these analyses are the averages of duplicate or triplicate determinations. The raw analytical data are given in Appendix Table 6.1-1.

Several practices are in current or recent usage with regard to correction of hydrogen and oxygen contents for moisture or ash present. In this report the following practice is followed (cf. ASTM D3180):

The as-received (ar) hydrogen data are not corrected for moisture content; i.e., part of the ar hydrogen is that associated with the moisture present in the coal sample.

The as-received oxygen data are calculated from the other ar data, simply by subtratcting from 100% the percentages found for carbon, hydrogen, nitrogen, sulfur and ash. As is generally recognized, ar oxygen is a rather arbitrary number. It does not include the oxygen which is an important part of the ash, and hence tends to be low; on the other hand the oxygen content of the ash is materially different from that associated with the mineral phases of a coal prior to ashing. The ar oxygen reported here follows common current usage but is of questionable meaning.

Table 3.1-1

Proximate and Ultimate Analyses of Seven Coals[1,2]

Coal Seam	Proximate Analysis, Percent				Ultimate Analysis, Percent						
	Moisture	Ash	Volatile Matter	Fixed Carbon	Carbon	Hydrogen	Nitrogen	Sulfur	Oxygen	Calorific Value	FSI
Pittsburgh #8	0.79	8.65 (8.72)	40.85 (45.11)	49.71 (54.89)	76.82 (84.83)	5.06 (5.49)	1.30 (1.44)	2.64 (2.92)	5.53 (5.33)	13845 (15,288)	7½
Ohio #9	2.15	18.87 (19.28)	39.40 (49.89)	39.58 (50.11)	62.72 (79.41)	4.43 (5.30)	0.89 (1.13)	4.25 (5.38)	8.84 (8.78)	11065 (14,009)	3
Lower Kittanring	1.95	10.76 (10.97)	26.57 (30.44)	60.72 (69.56)	76.56 (87.71)	4.51 (4.92)	1.19 (1.36)	1.67 (1.91)	5.32 (4.10)	13150 (15,065)	8
Kentucky #11	1.97	8.34 (8.51)	41.19 (45.92)	48.50 (54.08)	73.73 (82.21)	5.09 (5.43)	1.22 (1.36)	3.16 (3.52)	8.47 (7.48)	13242 (14,765)	7
Pocahontas #3	0.47	9.68 (9.73)	17.40 (19.37)	72.45 (80.63)	80.95 (90.09)	3.77 (4.14)	0.92 (1.02)	0.65 (0.72)	4.03 (4.02)	13936 (15,510)	4½
Amax Wyoming	29.12	5.34 (7.53)	33.07 (50.46)	32.47 (49.54)	50.52 (77.08)	3.90 (0.98)	0.55 (0.84)	0.45 (0.69)	39.24 (20.41)	8581 (13,092)	0
Elkhorn #1	2.45	14.80 (15.17)	35.53 (42.94)	47.22 (57.06)	69.28 (83.72)	4.74 (5.40)	1.27 (1.53)	0.78 (0.94)	9.13 (8.40)	12070 (14,586)	3½

1. Data Without parentheses are ar basis: data with parentheses on maf basis, except ash on a dry basis. Reference ASTM D3180-74.

2. Oxygen is by difference.

The figures given in parentheses in Table 3.1-1 and in following tables are on a moisture- and ash-free (maf) basis (except for percent ash itself, which is calculated on a moisture-free basis). The hydrogen value is first corrected by subtracting from ar hydrogen that amount associated with the moisture present, then multiplying the net hydrogen by the factor which adjusts for the contribution of moisture and ash to the original mass:

$$f = \frac{100}{(100 - \% \text{ ash} - \% \text{ moisture})}$$

Oxygen on a maf basis is similarly calculated, that is, by subtracting from ar oxygen the amount associated with the moisture present, then multiplying net oxygen by the above factor. Oxygen on this basis may also be calculated by difference, by subtracting the maf values for carbon, hydrogen, nitrogen and sulfur from 100%. The maf oxygen value defines the amount of oxygen associated with the organic portion of the original coal, and is likely to be more meaningful than ar oxygen.

Other maf values given in these tables (volatile matter, fixed carbon, % carbon, % nitrogen, % sulfur and calorific value) are calculated simply by multiplying the ar values by the above factor f.

Similar analyses have been carried out on samples of coal extrudate, i.e., samples of coal which had been extruded through the Jet Propulsion Laboratory's 1.5-inch extrusion pump, typically at 425-625°C. These analyses are presented in Tables 3.1-2 and 3.1-3.

The first four extrudates listed in these tables are pairs: extrudates 1A and 1B are both from Pittsburgh #8 seam coal, collected from the same extrusion run, and ostensibly identical in composition; and extrudates 2A and 2B are both from Ohio #9 seam coal, also collected from the same run and ostensibly identical. An examination of the replicate raw analyses indicates that the differences between the paired samples in Tables 3.1-2 and 3.1-3 are considerably greater than the differences in replicate analyses of the same samples. For example, the ash contents of samples 1A and 1B are 8.89% and 8.54%, respectively, indicating a dif-

Table 3.1-2

Proximate Analyses, FSI and Calorific Values of Coal Extrudates*

Extrudate Source	Moisture	Ash	Volatile Matter	Fixed Carbon	Calorific Value	FSI
Pittsburgh #8 1/78 (1A)	0.00	8.89 (8.89)	36.26 (39.80)	54.85 (60.20)	13,947 (15,308)	8
Pittsburgh #8 1/78 (1B)	0.10	8.54 (8.55)	34.68 (37.96)	56.68 (62.04)	13,829 (15,137)	7 1/2
Ohio #9 1/78 (2A)	0.27	25.02 (25.09)	29.10 (38.95)	45.62 (61.06)	10,876 (14,557)	2 1/2
Ohio #9 1/78 (2B)	0.31	25.58 (25.66)	28.75 (38.79)	45.37 (61.22)	10,724 (14,470)	1 1/2
Kentucky #11 4/78	0.00	15.60 (15.60)	32.77 (38.83)	51.63 (61.17)	12,397 (14,688)	6 1/2
Kentucky #11 5/78	0.00	11.93 (11.93)	35.42 (40.22)	52.65 (59.78)	13,143 (14,923)	4
Pittsburgh #8 4/78 - 800°F	0.00	7.83 (7.83)	36.21 (39.29)	55.96 (60.71)	13,930 (15,113)	8
Pittsburgh #8 4/78 - 900°F	0.17	8.27 (8.28)	31.35 (34.24)	60.21 (65.76)	13.646 (14,904)	6
Pittsburgh #8 4/78 - 1000°F	0.00	8.25 (8.25)	34.75 (37.87)	57.00 (62.13)	13,764 (15,002)	7 1/2
Pittsburgh #8 4/78 - 1100°F	0.12	8.13 (8.14)	35.63 (38.83)	56.12 (61.17)	13,945 (15,199)	8
Pittsburgh #8 4/78 - 1200°F	0.10	8.36 (8.37)	36.91 (40.32)	54.63 (59.68)	13,857 (15,138)	7 1/2

---

* See footnote to Table 3.1-1

Table 3.1-3

Ultimate Analyses of Coal Extrudates*

Extrudate source	% C	% H	% N	% S	% O
Pittsburgh #8 1/78 (1A)	77.22 (84.75)	4.94 (5.42)	1.61 (1.77)	2.79 (3.06)	4.56 (4.99)
Pittsburgh #8 1/78 (1B)	76.98 (84.26)	4.87 (5.32)	1.58 (1.73)	2.78 (3.04)	5.26 (5.65)
Ohio #9 1/78 (2A)	62.51 (83.67)	3.89 (5.17)	1.10 (1.47)	4.36 (5.84)	3.12 (3.86)
Ohio #9 1/78 (2B)	61.52 (83.01)	3.73 (4.99)	1.22 (1.65)	4.47 (6.03)	3.49 (4.32)
Kentucky #11 4/78	68.69 (81.39)	4.29 (5.08)	1.29 (1.53)	4.51 (5.34)	5.62 (6.66)
Kentucky #11 5/78	72.94 (82.82)	4.85 (5.51)	1.28 (1.45)	3.42 (3.88)	5.58 (6.34)
Pittsburgh #8 4/78 - 800°F	77.85 (84.46)	4.95 (5.37)	1.26 (1.37)	2.27 (2.46)	5.84 (6.34)
Pittsburgh #8 4/78 - 900°F	77.68 (84.84)	4.55 (4.95)	1.34 (1.46)	2.16 (2.36)	6.00 (6.39)
Pittsburgh #8 4/78 - 1000°F	77.64 (84.62)	4.78 (5.21)	1.26 (1.37)	2.39 (2.60)	5.68 (6.19)
Pittsburgh #8 4/78 - 1100°F	77.45 (84.41)	4.90 (5.33)	1.24 (1.35)	2.12 (2.31)	6.16 (6.60)
Pittsburgh #8 4/78 - 1200°F	77.74 (84.92)	4.95 (5.40)	1.26 (1.38)	2.21 (2.41)	5.48 (5.89)

---

* See footnote to Table 3.1-1.

ference of 0.35%; while the standard deviation of ash analysis for this set of data is only 0.03%. Thus there appear to be real compositional variations among different samples of extrudate from the same extrusion run. In most of the instances shown here, however, these differences are relatively small.

The two samples of Kentucky #11 extrudate represent different runs (April 19, 1978 and May 4, 1978) conducted under different conditions. These extrudates are markedly different from one another (and from the parent coal) in ash content and elemental composition.

The five extrudates at the bottom of Tables 3.1-2 and 3.1-3 represent successive extrudates taken from a single extrusion run in which the die temperature was successively increased from about 425°C (800°F) to about 650°C (1200°F).

In the process of heating and extruding coal (1) a significant amount of volatile matter is formed and released; coal extrudates are typically brittle friable porous solids of low bulk density, quite unlike raw whole coal. Expectations were that coal extrudate would prove to be markedly lower in volatile matter, free swelling index, and calorific value than its parent whole coal. It was also expected that these differences would be accentuated by extrusion at progressively higher temperatures. These expectations are given only slight support by the data. Volatile matter (maf) does decrease by some 6-7% for Pittsburgh #8 and Kentucky coals, and by over 10% for Ohio #9, but there is little evidence of a systematic trend in extrusions conducted at varying temperatures. For these three coals the FSI value appears to be decreased by an average of about one unit, perhaps marginally significant; and again there is no systematic decrease with increase of extrusion temperature. The maf calorific values show no significant change for any of these extrudates.

Among the quality control techniques of the Materials Analysis Department is the practice of sending sample splits to commercial analytical laboratories. Two of the coals in the present study have been selected for such comparison analyses. Results are reported in Tables 3.1-4 and 3.1-5. In both of these tables "Laboratory A" is this Institute's Materials Analysis Department. Agreement in general among these three analytical laboratories is good, with the marked exception of the volatile matter/fixed carbon results. The large discre-

Table 3.1-4

Interlaboratory Comparison of Analyses
of Pittsburgh #8 Seam Coal*

	Laboratory						
Ultimate Analysis	A			B		C		Median Value
% Moisture	0.82	0.76		0.76	0.76	0.64	0.69	0.76
% Carbon	76.82	77.13	76.52	76.80	76.99	76.17	75.79	76.80
% Hydrogen	5.05	5.07	5.07	5.20	5.25	5.31	5.26	5.20
% Nitrogen	1.31	1.29	1.29	1.44	1.51	1.47	1.45	1.44
% Chlorine		0.09		0.10	0.09	-----	-----	0.09
% Sulfur	2.64	2.65		2.56	2.51	2.73	2.72	2.65
% Ash	8.62	8.68		8.51	8.52	8.50	8.50	8.52
% Oxygen (by diff.)		4.64		4.63	4.37	5.18	5.59	4.54
Proximate Analysis								
% Moisture	0.82	0.76		0.76	0.75	0.64	0.69	0.76
% Ash	8.62	8.68		8.51	8.52	8.50	8.50	8.52
% Volatile Matter	40.60	41.09		29.50	29.07	37.24	36.35	36.80
% Fixed Carbon	49.96	49.47		61.23	61.66	53.64	54.46	53.92
Sulfur Forms								
% Pyritic				0.97	1.00	1.18	1.25	1.09
% Sulfate				0.04	0.04	0.03	0.03	0.04
% Organic				1.55	1.47	1.54	1.46	1.51
% Total				2.56	2.51	2.75	2.74	2.64
BTU/lb	13,849	13,841		13,853	13,853	13,785	13,803	13,845

* as received basis. Hydrogen figure includes hydrogen content of moisture; oxygen estimate is by difference and excludes oxygen content of moisture.

Table 3.1-5

Interlaboratory Comparison of Analyses of
Kentucky #11 Seam Coal*

	Laboratory						
Ultimate Analysis	A			B		C		Median Value
% Moisture		1.95	1.99	2.06	2.10	2.06	1.98	2.02
% Carbon	73.77	73.87	73.57	74.66	74.55	72.87	72.93	73.77
% Hydrogen	5.01	5.11	5.14	5.27	5.00	5.05	4.97	5.05
% Nitrogen	1.21	1.22	1.24	1.44	1.47	1.40	1.42	1.40
% Chlorine		0.18		0.23	0.27	------	-----	0.23
% Sulfur		3.15	3.17	3.09	3.11	3.20	3.20	3.16
% Ash		8.37	8.30	8.27	8.18	8.31	8.43	8.31
% Oxygen (by diff.)		6.25		4.98	5.32	7.11	7.07	6.06
Proximate Analysis								
% Moisture		1.95	1.99	2.06	2.10	2.06	1.98	2.03
% Ash		8.37	8.30	8.27	8.18	8.31	8.43	8.34
% Volatile Matter		41.12	41.26	29.11	28.91	37.13	37.22	37.18
% Fixed Carbon		48.45	48.56	60.56	60.81	52.50	52.37	52.45
Sulfur Forms								
% Pyritic				1.15	1.11	1.34	1.35	1.25
% Sulfate				0.08	0.07	0.07	0.09	0.08
% Organic				1.86	1.93	1.86	1.82	1.86
% Total				3.09	3.11	3.27	3.26	3.11
BTU/lb		13,245	13,239	13,367	13,373	13,299	13,265	13,255

* as received basis. Hydrogen figure includes hydrogen content of moisture; oxygen estimate is by difference and excludes oxygen content of moisture.

pancies among these particular data probably reflect significantly different temperature ramps and ceilings in this fast pyrolysis determination.

Ashing of coals in the standard ASTM procedure is a high-temperature process, wherein coals are heated in the presence of air to about 725°C. All of the ashing data reported thus far has been obtained using this standard high temperature ashing (HTA) technique. Another means for separation of the inorganic portion of coal is to subject the pulverized coal to oxygen plasma ashing (2,3). In this technique the coal is placed in contact with RF-excited oxygen at about 1 torr pressure and is only very moderately heated in the process of the oxidation of the organic portion (a manufacturer's estimate is that sample temperature does not exceed 100°C). This has become a standard low temperature ashing (LTA) technique, of value for inorganic and mineralogical analysis. Since heat-labile compounds such as inorganic carbonates are not decomposed by LTA, the percent ash obtained by LTA is always appreciably greater than that obtained by HTA.

Samples of the seven coals used in the present study, and of seven extrudates, have been subjected to low temperature ashing. A comparison of HTA and LTA results is shown in Table 3.1-6. The ratio LTA/HTA is 1.2-1.3 for most of the coals in this study. The extrudates show a generally lower LTA/HTA ratio, suggestive that their mineral matter may have undergone a partial thermal decomposition during the extrusion process. The two least plastic eastern coals show LTA/HTA ratios of less than 1.15.

Table 3.1-6

Comparison of Ash Contents by HTA and LTA Methods*

Coal or Extrudate	%Ash (HTA)	%Ash (LTA)	Ratio LTA/HTA
Pittsburgh #8	8.72	10.84	1.24
Ohio #9	19.28	23.69	1.23
Lower Kittanning	10.97	14.58	1.33
Kentucky #11	8.51	10.88	1.28
Pocahontas #3	9.73	11.01	1.13
Amax Wyoming	7.53	9.43	1.25
Elkhorn #1	15.17	17.29	1.14
Pittsburgh #8 1/78 (1A)	8.22	9.50	1.16
Ohio #9 1/78 (2A)	25.38	28.40	1.12
Pittsburgh #8 4/78 - 800°F	7.83	9.25	1.18
Pittsburgh #8 4/78 - 900°F	8.27	9.68	1.17
Pittsburgh #8 4/78 - 1000°F	8.25	9.67	1.17
Pittsburgh #8 4/78 - 1100°F	8.13	9.80	1.20
Pittsburgh #8 4/78 - 1200°F	8.36	9.12	1.09

*All data are dry basis. HTA denotes high temperature (ASTM furnace) ashing; LTA denotes low temperature oxygen plasma ashing, sample temperature estimated to reach approximately 100°C.

3.2 Mineral Analysis

(work performed by Karen C. Moore, Sayre N. Russell, and Henry E. Francis)

Quantitative mineral analysis is most commonly conducted by atomic absorption spectrometry. (4) In recent years x-ray fluoresence has come into use as a rapid qualitative and semiquantitative method, especially for the preliminary analysis of whole coals. (5 , 6) Both techniques have been used in the present study.

The results of a low-energy (14 KeV) x-ray fluorescence analysis of the seven coals comprising this study are shown in Table 3.2-1. Under these conditions the major fluorescence is Kα radiation from lighter elements (atomic numbers 11-26). The strongest signals for most of these coals are from sulfur and iron; however, Pocahontas#3 is unusually rich in titanium, Elkhorn #1 is rich in potassium, and the Amax western coal exhibits a very strong calcium peak. Ohio #9 coal shows a relatively strong manganese peak, while the coals from West Virginia, Pennsylvania and Kentucky show little or no manganese.

Results of a parallel set of x-ray fluorescence analyses at higher energies (40 KeV) are shown in Table 3.2-2. Fluorescence signals in this energy range are considerably weaker. Many of these elements are heavier group homologs of more abundant elements, and are to be expected, for instance, Rb in the presence of Na and K, Sr in the presence of Mg and Ca. The presence of weak copper and zinc signals (less than 1 cps) may be a system artifact, since the radiation chamber is brass-lined.

The data in these tables are of use to give the 'lay of the land' with regard to the mineral elemental composition of these coals; and indeed, rough comparisons may be made among coals on the basis of relative intensities. Owing to several complex interactions of photons in thick matrices, however, it is not possible to make a simple linear regression analysis; element concentrations cannot be assumed to be directly proportional to fluorescent signal intensities.

Table 3.2-1

X-Ray Fluorescence Analysis of Seven Coals At 14 KeV*

Fluorescent Intensities in Counts per Second

Element	Pittsburgh #8	Ohio #9	Lower Kittanning	Kentucky #11	Pocahontas #3	Amax Wyoming	Elkhorn #1
Al	3.2	5.2	4.7	2.6	4.0	1.9	6.8
Si	20.9	36.9	22.7	23.4	23.9	8.0	41.7
P	ND	ND	0.7	ND	ND	9.2	ND
S	166.	205.	95.2	200.	54.6	41.1	43.0
K	11.0	31.7	18.3	19.7	3.9	1.4	56.8
Ca	45.3	95.8	25.2	11.9	9.4	294.	25.8
Ti	24.3	26.4	39.1	20.2	67.8	28.0	38.8
Cr	1.8	2.2	1.4	2.7	1.5	1.0	1.5
Mn	ND	38.	0.1	ND	ND	3.3	2.0
Fe	408.	723.	503.	569.	184.	188.	498.

---

* Determined by triplicate averages of 1000-sec counting periods, using a commercial rhodium-targeted tube-excited x-ray fluorescence spectrometer (Finnigan Corp. Model 9008) with 14.0 KeV excitation, 0.40 milliamperes, vacuum path, no filter, and 1024 channels set at -0.03 to +8.01 KeV span, with 0.1-mil mylar windows. ND = not detectable.

Table 3.2-2

X-Ray Fluorescence of Seven Coals at 40.0 KeV*

Fluorescent Intensities in Counts per Second

Element	Pittsburgh #8	Ohio #9	Lower Kittanning	Kentucky #11	Pocahontas #3	Amax Wyoming	Elkhorn #1
Cu	0.2	0.2	0.3	0.3	0.7	0.6	0.9
Zn	0.2	0.5	0.8	1.6	ND	0.3	0.3
As/Pb	ND	0.7	2.2	ND	0.5	ND	ND
Br	1.4	0.1	2.8	1.2	4.1	ND	1.6
Rb	0.5	1.2	ND	1.8	ND	ND	2.3
Sr	18.9	6.4	20.4	5.1	7.4	13.9	6.2
Y	ND	ND	ND	ND	12.7	ND	0.6
Zr	9.6	5.7	10.2	ND	2.0	5.2	6.7

* Determined by triplicate averages of 1000-sec counting periods, using a commercial rhodium-targeted tube-excited x-ray fluorescence spectrometer (Finnigan Corp. Model 900B) with 40.0 KeV excitation, 0.050 milliamperes, air path, rhodium foil filter, and 1024 chanels set at -0.05 to +18.97 KeV span with 0.1 -mil mylar windows. ND = not detectable. At low concentrations (less than about 0.0005%) the As Kα and Pb Lα peaks are not distinguished by energy-dispersive systems.

For quantitative information portions of these seven coals have been ashed, then re-ashed to assure complete removal of organic matter, then dissolved in acid, diluted and buffered appropriately, and the aqueous solutions analyzed by atomic absorption spectrometry. In addition, two coal extrudates were similarly treated. Determinations were carried out for ten elements commonly present as minor components of coals. The best average data are reported in Table 3.2-3.

These data show that the mineral components of all of these coals are rich in silica and alumina, the chief components of clays. Most coals contain a substantial amount of iron. The earlier observations concerning titanium in Pocahontas #3, potassium in Elkhorn #1, and calcium in the Amax coal are confirmed and quantified in this table.

Eight of the ten elements tabulated in Table 3.2-3 as their oxides are nonvolatile under the ashing conditions used. The ninth element, sulfur, is of course volatile and forms volatile oxides. The data in this table show the amount of sulfur remaining in the high-temperature ash, and do not measure the total sulfur content of the coal. [If all of the sulfur of Pittsburgh #8 coal has remained as bound SO_3 in the ash, this component would have comprised over 80% of the ash!] From these data it may be suggested that retained sulfur appears to be most closely related to the levels of Group IIA oxides (MgO and CaO) in the ashes. Thus Ohio #9 and Amax coals are the richest in these alkaline earth oxides, their ashes containing nearly tenfold more than the ashes of Pocahontas #3 and Kentucky #11; and indeed the former coal ashes contain nearly ten times the levels of SO_3 found in the ashes of the latter coals.

The quality control practice of sending sample splits to commercial laboratories for comparison analyses has been noted in the preceding section. This has also been done with regard to mineral analyses of ashes by atomic absorption spectrometry. Interlaboratory comparison data for Pittsburgh #8 and Kentucky #11 seam coals are reported in Tables 3.2-4 and 3.2-5.

As before, Laboratory A is the Materials Analysis Department of the Institute; Laboratories B and C are experienced commercial laboratories which we have found to be generally reliable. Based upon the best consensus values, the iron data from our laboratory may be consistently low by 8-10%, and our

Table 3.2-3

Atomic Absorption Analysis of the Ashes of Seven Coals
Concentration in Reignited Ash, %

Coal Seam	Fe_2O_3	SiO_2	Al_2O_3	CaO	MgO	K_2O	Na_2O	TiO_2	SO_3	P_2O_5
Pittsburgh #8	15.9	50.5	23.4	3.35	0.86	1.27	0.93	1.53	3.12	0.34
Ohio #9	16.86	43.2	18.8	5.34	3.84	2.23	0.27	0.76	6.00	0.34
Lower Kittanning	12.2	48.5	29.2	1.07	0.56	1.75	0.18	1.95	1.00	1.12
Kentucky #11	20.5	50.6	20.1	0.93	0.75	2.36	0.48	1.51	0.63	0.19
Pocahontas	2.84	58.1	31.6	0.54	0.37	0.44	0.65	4.33	0.54	0.21
Amax Wyoming	5.47	31.9	15.8	22.8	3.36	0.24	1.69	1.62	5.33	0.64
Elkhorn #1	8.37	67.9 70.2*	26.1	0.88	1.71	4.09	0.30	1.82	0.65	0.11
Pittsburgh #8 Extrudate 1A	17.0	45.2	22.6	4.50	0.81	1.09	0.96	----	3.69	------
Ohio #9 Extrudate 2A	15.9	37.1	16.7	7.02	4.55	1.90	0.38	----	9.35	------

*Best two of three determinations.

Table 3.2-4

Interlaboratory Comparison of Mineral Analyses of Pittsburgh #8 Seam Coal*

(Composition of the Reignited Ash by Atomic Absorption Spectrometry)

Component	Laboratory A	Laboratory B	Laboratory C	Median Value
Fe_2O_3	16.28% 15.42	18.17% 18.07	17.6% 17.5	17.55%
SiO_2	52.49 48.45	45.49 45.68	49.3 49.5	48.88
Al_2O_3	23.66 23.02 23.54 23.25	25.43 25.68	19.0 19.0	23.40
CaO	3.36 3.12 3.44 3.47	3.75 3.64	3.33 3.20	3.40
MgO	0.85 0.81 0.86 0.90	0.79 0.82	0.91 0.93	0.86
K_2O	1.22 1.20 1.34 1.32	0.93 0.97	1.22 1.25	1.22
Na_2O	0.80 0.75 1.04 1.11	0.43 0.40	1.06 1.08	0.92
TiO_2	1.57 1.48	3.13 2.99	1.45 1.45	1.53
SO_3	3.08 3.16	0.77 0.76	3.63 3.73	3.12
P_2O_5	0.34	0.21 0.22	0.39 0.39	0.31

*AA methods are compared for all elements except SO_3 and P_2O_5 (see footnote to Table 3.2-3).

Table 3.2-5

Interlaboratory Comparison of Mineral Analyses of Kentucky #11 Seam Coal*

(Composition of the Reignited Ash by Atomic Absorption Spectrometry)

Component	Laboratory A	Laboratory B	Laboratory C	Median Value
Fe_2O_3	20.64% 20.28	22.91% 22.69	22.3% 22.0	22.15%
SiO_2	50.11 50.99	48.48 48.81	49.1 49.3	49.2
Al_2O_3	20.22 20.14 20.02 20.19	21.77 21.98	19.9 20.0	20.17
CaO	0.80 0.88 0.94 1.08	1.05 0.96	0.84 0.83	0.91
MgO	0.68 0.68 0.78 0.75	0.69 0.77	0.80 0.78	0.76
K_2O	2.34 2.32 2.38 2.41	2.11 2.03	2.47 2.48	2.36
Na_2O	0.61 0.54 0.42 0.34	0.28 0.31	0.35 0.36	0.36
TiO_2	1.57 1.45	2.10 2.01	1.50 1.55	1.56
SO_3	0.64 0.62	0.17 0.15	0.60 0.53	0.57
P_2O_5	0.19	0.06 0.07	0.18 0.21	0.13

*AA methods are compared for all elements except SO_3 and P_2O_5 (see footnote to Table 3.2-3).

sodium values show a larger spread than we like. In general, however, these intercomparison tables indicate our mineral analysis data to be acceptably good, and for several elements to be closer to median than the data of either commercial laboratory.

Individual analyses by x-ray fluorescence and atomic absorption are tabulated in section 6.2 of this report.

The atomic absorption analyses of the ashes of the two extrudates show sulfur retention by the extrudate ashes to be significantly greater than that found for the parent coal ash. This is suggestive of a mineralogical change (perhaps carbonate decomposition) as a result of the extrusion process. It will be recalled that the data of Tables 3.2-3 through 3.2-5 derive from analyses of coal ashes. To look for effects of extrusion upon the inorganic balance of unashed coals, we have examined several extrudates by X-ray fluorescence. These data, shown in Table 3.2-6, can be directly compared with the data of Tables 3.2-1 and 3.2-2.

Among the more strongly fluorescing elements, all except sulfur exhibit a fairly consistent increase in signal intensities as compared with the intensities observed in the parent coals. This is evident for aluminum, silicon, potassium, calcium, titanum, and iron. For example, the calcium Kα intensity increases in Pittsburgh #8 from 45 to 50 cps, in Ohio #9 from 96 to 153 cps, and in Kentucky #11 from 12 to 14 cps. This is a reasonable trend for nonvolatile mineral elements, since the extrusion process necessarily involves loss of moisture and some organic matter as gas and vapor.

The sulfur signal, on the other hand, is systematically less in the extrudates than in the parent coals: down from 166 to 159 cps for Pittsburgh #8, from 205 to 176 cps for Ohio #9, and from 200 to 189 and 173 cps for Kentucky #11 extrudates. This observation is not supported by the classical Eschka sulfur analysis data of Tables 3.1-1 and 3.1-3.

Table 3.2-6

X-Ray Fluorescence Analyses of Four Coal Extrudates

Fluorescent Intensities in Counts per second

Element	Method	Extrudate 1A from Pgh #8	Extrudate 2A from Ohio #9	Extrudate 4A from Ky #11	Extrudate 4B from Ky #11
Al	A	3.6	5.8	3.2	3.3
Si	A	22.6	40.2	32.7	28.2
P	A	0.5	0.3	0.7	0.2
S	A	159.3	175.8	188.5	172.8
K	A	11.	35.8	26.2	24.8
Ca	A	50.1	153.3	13.8	13.6
Ti	A	24.7	29.9	25.4	25.1
Cr	A	1.5	5.7	ND	ND
Mn	A	ND	103.	ND	ND
Fe	A	436.	741.	878.	740.
Cu	B	0.3	0.1	0.4	0.3
Zn	B	0.2	0.3	0.3	0.4
As/Pb	B	ND	0.4	0.3	0.2
Br	B	1.4	0.7	0.8	0.9
Sr	B	15.	9.9	1.4	1.9
Zr	B	6.8	7.4	2.8	3.3

---

* Method A conditions are described in the footnote to Table 3.2-1;
Method B conditions are described in the footnote to Table 3.2-2.

3.3 Plastic Properties

(Work done by Morgan R. Yewell, Jr., Katherine L. Roberts and William G. Lloyd)

The most widely used method of measuring and characterizing the plastic properties of coal was developed by Gieseler in 1937, (7) and in a modified form has become a standard American procedure. (8) The use of this method and its relationship to other approaches to the study of the plastic properties of coal is well described by Loison, Peytavy, Boyer and Grillot. (9).

The modified Gieseler plastometric analysis is a method which measures the resistance of a mass of powdered coal to the rotation of a stirrer connected to a constant-speed motor through a torque clutch; in effect what is measured is the resistance of the coal mass to a weak constant torque of about 100 g-cm (40 "gram-inches" in the standard method). The coal/stirrer/crucible assembly is heated at a controlled rate of 3°C/min, usually from 330° until coking occurs in the 450-500°C range. The stirrer shaft is fitted with a dial which is divided into 100 dial divisions. The minimum deformation which is read is that occurring when the stirrer shaft makes one hundredth of a revolution per minute, i.e., one dial division per minute (ddpm). The driving motor always operates at 300 rpm; consequently, the highest possible reading for an extremely fluid coal is 30,000 ddpm. All measurements of plastic or fluid properties obtained in Gieseler plastometry are given by numbers between 1 and 30,000 ddpm. [A newly available plastometer manufactured by Standard Instrumentation Co. replaces the optical dial with a digital output on paper tape.] In this laboratory we have found that Gieseler fluidities exceeding 25,000 ddpm are erratic and non-reproducible.

In a typical Gieseler plastometric run the 5.0-g charge of powdered coal is packed into the crucible under controlled and highly uniform conditions, the assembly placed in a solder pot furnace at 330°C, and the pot temperature maintained at 330° for about ten minutes. Bath temperature is then increased at a rate of 3.0°/min. Initially the coal is completely non-fluid; no shaft rotation occurs. For those coals exhibiting plastic

properties, however, shaft rotation will commence, often in the range 370-420°. Once it has commenced, it accelerates rapidly, goes through a "maximum fluidity", and then slows and eventually stops. For nonplastic coals no shaft rotation occurs at all. For extremely plastic coals there may be a zone in which shaft rotation exceeds 25,000 ddpm, i.e., a zone in which the coal is so fluid that its plasticity cannot be effectively measured by this method.

Temperature is normally tracked by means of a thermocouple immersed in the solder bath; this provides assurance in the course of a run that the bath temperature is at or near the proper temperature. In a preliminary experiment, the stirrer shaft going into the crucible containing the powdered coal was replaced by a second thermocouple lead, placed so that the thermocouple tip was embedded in the approximate center of the mass of packed coal within the crucible. The crucible was then immersed in the solder bath and the system run through a standard temperature ramp in a dummy run, in which temperatures of both the solder bath and the central portion of the coal were recorded. Results are shown in Figure 3.3-1. The observed bath temperature was found to remain quite close to the nominal temperature, the average deviation $| T_{bath} - T_{nominal} |$ slightly less than 1.0°C. During the initial warmup period the crucible contents reach 330° before the ramp is commenced. During the 3°C/min ramp the temperature near the middle of the crucible lags the solder bath temperature by an average of about 7°C (6.9° $\pm$ 1.4° in this test).

In reporting Gieseler data we will follow the standard practice of reporting nominal temperatures. For ASTM Gieseler runs this appears to entail a small systematic error as noted above; this error is believed to be inherent in the method.

During periods of substantial fluidity the plastic coal is believed to be quite heterogeneous. There are three definable solid phases: a meltable (but not-yet-molten) phase, a nonmelting phase, and a coked phase. There is, almost certainly, a liquid phase. There are, furthermore, gaseous and vaporized products of a series of pyrolytic processes which themselves are still

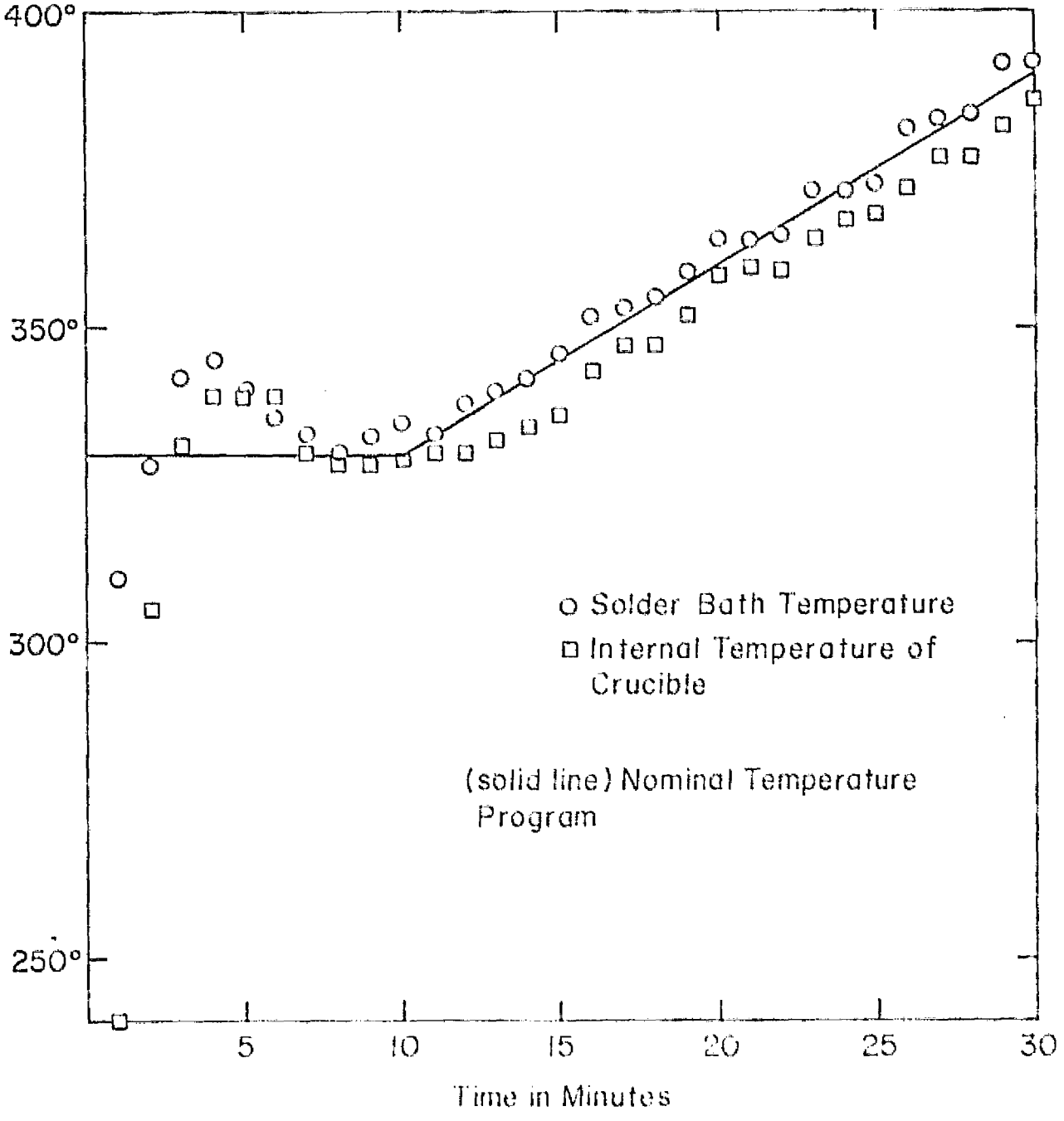

Figure 3.3-1 Nominal and Actual Temperatures in an ASTM Gieseler Plastometer Run

poorly understood. Given this high and changing order of heterogeneity, we are unlikely to be able to convert Gieseler fluidity to absolute units of viscosity. Furthermore, even if the plastic coal could be treated as a homogeneous fluid, it is most unlikely to be Newtonian fluid; and by the very nature of the Gieseler method the fluidity data are obtained over a wide range of shear rates. Nevertheless, and with these serious reservations kept in mind, it may be useful to relate Gieseler fluidity to apparent viscosity.

A viscosity calibration has been carried out, using two standard fluids supplied by Cannon Instrument Co., State College, PA. The calibration curve is shown in Figure 3.3-2. These data (cf. Table 6.3-0) show a highly linear relationship:

$$\ln[\eta \text{ in poise}] = 16.2789 - 0.96787 \cdot [\ln(\text{ddpm})]$$
$$\text{correlation coefficient} = -.9997$$

From this relationship it can be seen that Gieseler fluidities between 1 and 25,000 ddpm correspond to apparent viscosities in the range 12,000,000 to about 700 poise.

ASTM plastometry runs have been carried out by making at least three determinations for each sample, since even experienced operators experience occasional runs which are not reproducible. Data for these runs are then averaged geometrically:

$$\overline{x} = \sqrt[3]{x_1 \cdot x_2 \cdot x_3}$$

Table 3.3-1 shows a typical set of raw and averaged data. Other sets of raw data are shown in Section 6.3.

The seven coals comprising the present study have been examined in this manner. A condensed summary of the observed fluidities is shown in Table 3.3-2. It is clear that these coals exhibit a wide variation in plasti-

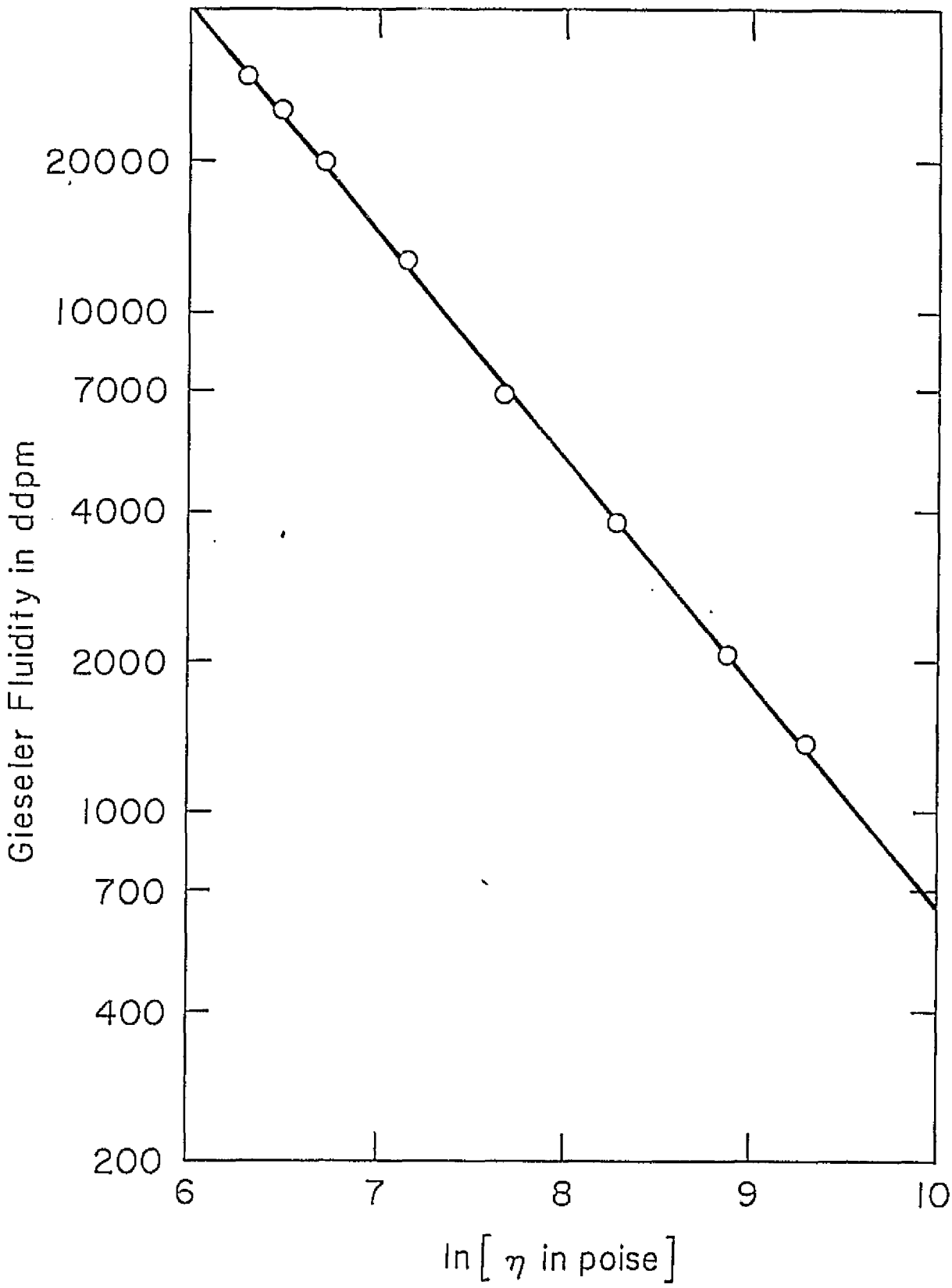

Figure 3.3-2 Fluidity - Viscosity Calibration of an ASTM Gieseler Plastometer

Table 3.3-1

Raw and Averaged ASTM Plastometric Data:

Triplicate Plastometric Runs with Pittsburgh #8 Seam Coal

time	temp	run 1	run 2	run 3	ln(run 1)	ln(run 2)	ln(run 3)	avg ln(ddpm)	Avg. ddpm
13 m	369°C	1.0	0.75	0.5	0.00	-0.29	-0.69	-0.327	0.72
14	372	1.0	1.0	1.0	0.00	0.00	0.00	0.000	1.0
15	375	1.25	1.1	1.0	0.22	0.10	0.00	0.106	1.1
16	378	1.75	1.2	1.0	0.56	0.18	0.00	.247	1.3
17	381	2.0	1.5	1.25	0.69	0.41	0.22	.441	1.6
18	384	2.25	2.0	1.5	0.81	0.69	0.41	.637	1.9
19	387	3.75	2.5	2.0	1.32	0.92	0.69	.977	2.7
20	390	6.25	3.75	3.0	1.83	1.32	1.10	1.418	4.1
21	393	9.0	6.0	5.5	2.20	1.79	1.70	1.898	6.7
22	396	19.	12.	8.5	2.94	2.48	2.14	2.523	12.5
23	399	49.	27.	18.	3.89	3.30	2.89	3.359	28.8
24	402	110.	68.	53.	4.70	4.22	3.97	4.297	73.5
25	405	560.	184.	160.	6.33	5.21	5.08	5.539	255.
26	408	3100.	645.	640.	8.04	6.47	6.46	6.990	1086.
27	411	10600.	3740.	4200.	9.27	8.23	8.34	8.613	5501.
28	414	>25000.	>25000.	>25000.	>10.	>10.	>10.	>10.	>25,000
29	417	" "	" "	" "	" "	" "	" "	" "	" "
30	420	" "	" "	" "	" "	" "	" "	" "	" "
⋮									⋮
43	459	" "	" "	" "	" "	" "	" "	" "	" "
44	462	15500.	29000.	26700.	9.65	10.28	10.19	10.039	22900.
45	465	5300.	11500.	25000.	8.58	9.35	10.13	9.351	11510.
46	468	1300.	2900.	4100.	7.17	7.97	8.32	7.820	2491.
47	471	247.	1015.	2400.	5.51	6.92	7.78	6.738	844.
48	474	57.	215.	180.	4.04	5.37	5.19	4.869	130.
49	477	15.	35.	42.	2.71	3.56	3.74	3.334	28.
50	489	5.	9.	10.	1.61	2.20	2.30	2.036	7.7
51	483	1.25	2.5	2.0	0.22	0.92	0.69	0.611	1.8
52	486	0.5	0.5	0.75	-0.69	-0.69	-0.29	-0.588	0.57

Table 3.3-2

Fluidities (by ASTM Plastometry) of Several Coals

Coal Seam	Softening Curve			Maximum Fluidity			Coking Curve		
	1 ddpm	5 ddpm	50 ddpm	T(max)	max ddpm	n(min)[1]	50 ddpm	5 ddpm	1 ddpm
Pittsburgh #8	372°	391°	401°	414-459°	>25,000.	<650	476°	481°	485°
Ohio #9	398°	412°	425°	435°	114.	1.2E+5	445°	456°	462°
L Kittanning	421°	438°	451°	465°	185.	7.5E+4	481°	489°	494°
Kentucky #11	392°	406°	414°	435°	6238.	2.5E+3	463°	470°	474°
Pocahontas #3	468°	NA[2]	NA[2]	480-483°	1.8	6.6E+6	NA[2]	NA[2]	494°
Elkhorn #1	420°	435°	NA[2]	450°	15.4	8.3E+5	NA[2]	460	467
Amax Wyoming	NA[2]	NA[2]	NA[2]	...	<0.5	>2E+7	NA[2]	NA[2]	NA[2]
Amax Blend	393°	414°	431°	438°	68.	2.0E+5	442°	455°	462°
Extrudate 1A from Pgh #8	347°	363°	385°	432°	21,770.	7.4E+2	475°	481°	486°
Extrudate 2A from Ohio #9	453°[3]	456°	458°	[4]	[4]	[4]	[4]	[4]	[4]

[1] Estimated effective viscosity in poise, from data of Figure 3.3-2.

[2] Indicated level of fluidity is never attained.

[3] Extrapolated value

[4] Unable to measure; see footnote 2 to Table 3.3-3

city, their maximum fluidities varying over a range of at least 10^5. The interval over which the fluidity exceeds 1 ddpm (sometimes referred to as the 'plastic range') varies from 113° for Pittsburgh #8 to 26° for Pocahontas #3, and is never attained by the Amax Coal.

Two extrudates have similarly been pulverized and loaded into the plastometer crucible, treated exactly as if they were ordinary coal samples. The extrudate of Pittsburgh #8 seam retains considerable plasticity, although its maximum fluidity is clearly much less than that of the parent coal. Unexpectedly, this extrudate enters the softening curve at considerably lower temperatures than the raw coal, although its coking curve temperatures are virtually identical. Consequently its plastic range is extremely large. It has not been possible to obtain a complete ASTM plastometry curve for the extrudate of Ohio #9 seam coal, owing to the melting curve behavior of this extrudate: at about 100 ddpm the sample plug breaks free from the walls of the crucible and spins on the rabble-arm stirrer. This is the only one of ten samples examined to exhibit this behavior.

Table 3.3-3 provides a full summary of the ASTM plastometric data for these samples. Several comparative features are easily seen in this table. The three most plastic coals are Pittsburgh #8, Kentucky #11, and Ohio #9, and each of thse reaches maximum fluidity in the 430-440°C range, as does also the Pittsburgh #8 extrudate. The Amax Wyoming coal shows no detectable plastic properties; its blend with Kentucky #11 closely follows the Kentucky curve, also peaking in the 435° range. Lower Kittanning develops a maximum plasticity greater than that of Ohio #9, and has a plastic range greater than that of Ohio #9, but its maximum fluidity is offset about 30° higher. The sparingly fluid Elkhorn #1 develops its maximum at an intermediate temperature; the very slightly plastic Pocahontas #3 develops its fluidity at a still higher temperature.

It is often useful to study phenomena of interest under isothermal conditions. Gieseler plastometry readily lends itself to isothermal studies, since the sample warmup time (two to three minutes) is generally short in comparison with the time scale of the overall melting/coking process. This technique has been used by Fitzgerald (10,11) and by van Krevelen and his coworkers. (12,13)

Table 3.3-3

Summary of ASTM Plastometric Data*

Temp.	Pgh #8	Ohio #9	Lower Kitt.	Ky#11	Poca #3	Elk #1	Amax Blend[1]	Extrudate Pgh #8	Extrudate Ohio #9
345°C	...	...	...	...	...	...	...	0.8	...
348	...	...	...	...	...	...	...	1.1	...
351	...	...	...	...	...	...	...	1.5	...
354	...	...	...	...	...	...	...	2.2	...
357	...	...	...	...	...	...	...	2.9	...
360	...	...	...	...	...	...	...	2.6	...
363	...	...	...	...	...	...	...	4.9	...
366	...	...	...	...	...	...	...	6.8	...
369	0.7	...	...	...	...	...	...	9.8	...
372	1.0	...	...	...	...	...	...	13.2	...
375	1.1	...	...	...	...	...	...	18.2	...
378	1.3	...	...	...	...	...	...	25.	...
381	1.6	...	...	...	...	...	...	31.	...
384	1.9	...	...	...	...	...	...	44.	...
387	2.7	...	...	...	...	...	...	60.	...
390	4.1	...	...	0.8	...	...	0.9	78.	...
393	6.7	...	...	1.1	...	...	1.0	105	...
396	12.4	0.8	...	1.5	...	...	1.2	135	...
399	29.	1.2	...	2.1	...	...	1.4	178	...
402	74.	1.7	...	2.8	...	...	1.7	246	...
405	255	2.3	...	4.0	...	...	2.0	356	...
408	1086	3.1	...	7.3	...	...	1.6	516	...
411	5490	4.4	...	16.0	...	...	3.7	770	...
414	>25000	7.0	...	43.	...	...	5.0	1599	...
417	" "	11.7	...	109	...	0.8	7.2	3684	...
420	" "	17.8	0.9	288	...	1.0	7.2	5386	...
423	" "	33.	1.3	770	...	1.3	8.3	9582	...
426	" "	64.	1.6	1947	...	1.7	13.8	14940	...
429	" "	91.	1.8[5]	3661	...	2.7	37.	20330	...
432	" "	111	2.6	5569	...	3.3	54.	21770	...
435	" "	114	3.6	6238	...	5.1	64.	14570	...

(c o n t i n u e d)

Table 3.3-3, Continued

Temp	Pgh #8	Ohio #9	Lower Kitt.	Ky #11	Poca #3	Elk #1	Amax Blend[1]	Extrudate Pgh #8	Extrudate Ohio #9
438°C	>25000	99.	4.8	6125	...	8.5	68.	12210	...
441	" "	81.	7.1	5970	...	12.0	54.	13910	...
444	" "	59.	12.4	5099	...	12.2	43.	14460	...
447	" "	35.	18.8	3955	...	14.4	29.	13120	...
450	" "	19.5	39.	2484	...	15.4	17.2	13260	...
453	" "	10.3	71.	1205	...	12.3	9.5	10280	...
456	" "	4.8	106	476	...	9.0	4.0	12050	6.6
459	" "	1.9	129	190	0.5	5.6	1.9	10940	41.
462	22900	1.0	161	78.	0.7	3.5_5	0.9	5410	61.
465	11500	0.5	185	29.	0.8	1.6^5	...	2016	96.
468	2490	...	170	9.3	1.0	0.7	...	757	[2]
471	846	...	159	3.0	1.3	...	...	239	...
474	130	...	123	1.1	1.4	...	...	78.	...
477	28.	...	85.	0.5	1.5	...	...	22.	...
480	7.7	...	58.	...	1.8	...	...	7.0	...
483	1.8	...	26.	...	1.8	...	...	2.2	...
486	0.6	...	10.7	...	1.7	...	...	0.8	...
489	...	...	5.1	...	1.6	...	...	...	...
492	...	...	1.6	...	1.3	...	...	...	...
495	...	...	0.7	...	0.9	...	...	...	...
498	...	...	...	...	...	...	...	...	...

* Data reported are Gieseler fluidities in dial divisions per minute (ddpm), and are geometric averages of three or more replicate runs. Apparatus and method are described in ASTM method D 2639-74. For an approximate conversion to standard viscosity units, see Figure 3.3-2 or Table 6.3-0.

[1] The Amax Wyoming seam coal shows no measurable fluidity under these conditions. The blend reported here is 25% Amax Wyoming, 75% Kentucky #11.

[2] Shaft 'breaks free' and spins freely, indicating separation of coal mass from crucible walls.

When fluidity is plotted on a logarithmic scale the fluidity-time curve typically shows a rapid softening curve, a well-defined peak of maximum fluidity, and a slower and substantially linear resolidification (coking) region. We have had no difficulty in duplicating this phenomenon. A typical isothermal curve, for Kentucky #11 seam coal at 410°, is shown in Figure 3.3-3 (open circles).

In the present study we have examined each coal isothermally at three temperatures, 410°, 425° and 450°. Several coals have been examined at additional temperatures. The isothermal fluidities are shown in Tables 3.3-4 through 3.3-6.

If isothermal plastometry is a predictor for coal pumpability, these data should lead to the prediction that two of these seven coals, Pocahontas #3 and Amax, will prove to be non-pumpable. Furthermore, if these data provide at least a semiquantitative correlating measure of pumpability, then extrusions of these seven coals at controlled temperatures may be useful for establishing minimum required fluidities. For example at 410° only one of these seven coals develops a fluidity greater than 1000 ddpm, only two coals greater than 100 ddpm, and only three coals greater than 10 ddpm. At 450° three coals develop fluidity greater than 1000 ddpm, four greater than 100 ddpm, and five greater than 10 ddpm.

The data in these tables illustrate some of the complexities of the temperature-time-fluidity relationships for different coals. Suppose, for example, that coals with fluidities greater than 5 ddpm (apparent viscosities below about 2.5×10^6 poise) can be efficiently pumped. At 410°C three of these seven coals are "good" (Pittsburgh #8 for 110 minutes, Kentucky #11 for 42 minutes, Ohio #9 for 19 minutes). At 425°C a fourth coal becomes marginally "good" (Elkhorn #1), while the pumpable times for the other three coals are all reduced. At 450°C a fifth coal (Lower Kittanning) becomes "good". This coal, with its high-temperature plastic range (as seen in Tables 3.3-2 and 3.3-3) has the longest fluidity time (22 minutes) at this temperature. And at 450° Elkhorn #1, marginally usable at 425°, is now "better" than Ohio #9.

Kentucky #11 seam coal, like Pittsburgh #8, shows considerable plasticity even at 410°C. To develop sufficient data to examine the temperature dependency of fluidity, three additional isothermal runs were made with this coal,

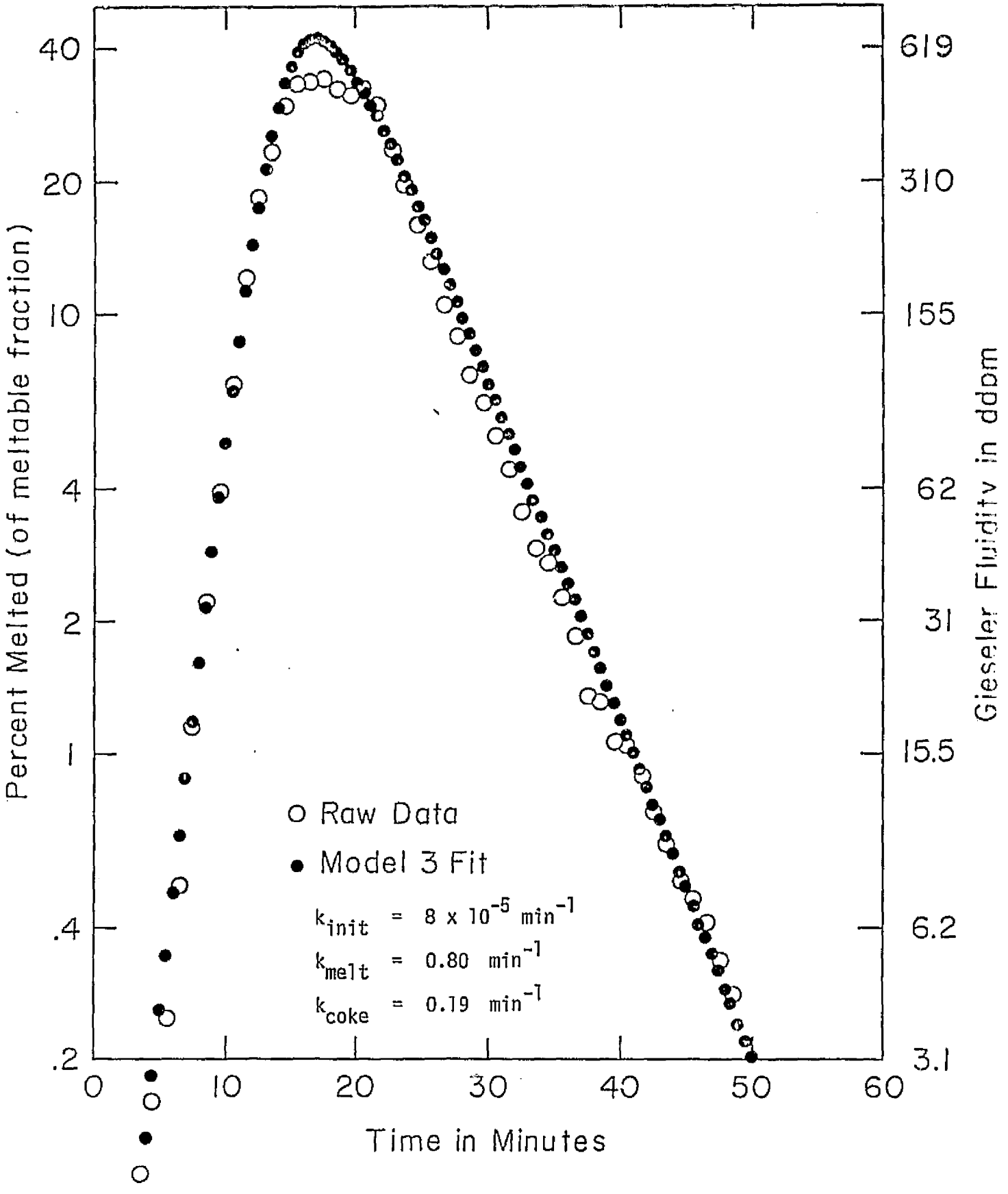

Figure 3.3-3 Approximate Fit to an Isothermal Plastometry Curve-Western Kentucky #11 at 410°C

Table 3.3-4

Isothermal Gieseler Plastometry of Several Coals at 410°C*

Coal Seam	Temp	Softening Curve			Maximum Fluidity			Coking Curve		
		1 ddpm	5 ddpm	50ddpm	t(max)	max ddpm	n(min)	50 ddpm	5 ddpm	1 ddpm
Pittsburgh #8	412°	3.0 min	4.5 min	6.7 min	(11-34)	>25,000	<650.	94.8 min	114.[1]min	127.[1]min
Ohio #9	411°	4.5	7.7	NA[2]	15.	46	2.9E+5	NA[2]	26.9	35.
Lower Kittanning	411°	NA[2]	NA[2]	NA[2]	9.	0.6	1.9E+7	NA[2]	NA[2]	NA[2]
Kentucky #11	410°	4.3	7.4	10.7	19.	522.	2.8E+4	34.5	49.2	61.3
Pocahontas #3	410°	NA[2]	NA[2]	NA[2]	...	...	...	NA[2]	NA[2]	NA[2]
Elkhorn #1	410°	20.	NA[2]	NA[2]	26	1.2	9.8E+6	NA[2]	NA[2]	31

---

* Runs conducted with the Gieseler apparatus under ASTM conditions except for the isothermal bath temperature

[1] Extrapolated values.

[2] Indicated level of fluidity is never attained.

Table 3.3-5

Isothermal Gieseler Plastometry of Several Coals at 425°C*

Coal Seam	Temp	Softening Curve			Maximum Fluidity			Coking Curve		
		1 ddpm	5 ddpm	50 ddpm	t(max)	max ddpm	n(min)	50 ddpm	5 ddpm	1 ddpm
Pittsburgh #8	426°	2.1[1]	3.0	4.2	(8-22)	>25,000	< 650	56.1	66.4	71.8[1]
Ohio #9	426°	3.9	5.1	8.1	11.	433	3.3E+4	16.4	21.2	25.2
Lower Kittanning	425.5°	4.8	NA[2]	NA[2]	(14-23)	2	6.0E+6	NA[2]	NA[2]	33.9[1]
Kentucky #11	425.5°	3.7[1]	5.0	6.1	(11-12)	> 25,000	< 650	29.4	37.2	44.0
Pocahontas #3	425°	NA[2]	NA[2]	NA[2]	...	...	...	NA[2]	NA[2]	NA[2]
Elkhorn #1	425°	6.8	12.8	NA[2]	14.	5.8	2.2E+6	NA[2]	16.4	25.2

[1] Extrapolated value.

[2] Indicated level of fluidity is never attained.

* As in preceding table.

Table 3.3-6

Isothermal Gieseler Plastometry at 450°C*

Coal Seam	Temp	Softening Curve			Maximum Fluidity			Coking Curve		
		1 ddpm	5 ddpm	50 ddpm	t(max)	max ddpm	n(min)	50 ddpm	5 ddpm	1 ddpm
Pittsburgh #8	452°	0.9 [1]	1.4	2.1	(5-10)	>25,000	< 650	18.2	21.0	23.7
Ohio #9	451°	0.8 [1]	1.2	1.8	(4- 5)	>25,000	< 650	8.6	10.6	11.7
Lower Kittanning	450°	3.8	5.2	9.7	(11-13)	77	1.8E+5	16.1	27.0	34.0
Kentucky #11	450°	2.0	2.5	3.2	7.	>25,000	< 650	12.9	15.2	16.9
Pocahontas #3	450°	NA[2]	NA[2]	NA[2]	...	...	...	NA[2]	NA[2]	NA[2]
Elkhorn #1	450°	4.4	5.3	7.5	10.	246	5.7E+4	12.9	15.5	17.5

---

* As in preceding tables.

[1] Extrapolated value.

[2] Indicated level of fluidity is never attained.

at 400°, 440° and 460°C. The six isothermal data sets for this coal are shown in Table 3.3-7. The overall temperature trends are clearly seen: both melting and coking rates increase, maximum fluidity increases sharply, and the time interval during which any given fluidity is exceeded tends to be reduced, as temperature is increased. The time-ranges for several fluidities are shown as a function of temperature in Table 3.3-8. A graphic representation of three "fluidity envelopes", based upon these data, is shown in Figure 3.3-4. These envelopes have closed bottom regions, but open tops.

The failure of the envelopes to converge more closely at the high-temperature end is very likely due, in part at least, to the time-temperature lag noted earlier (Figure 3.3-1). Crudely, if it requires about three minutes for a sample of coal in the central region of the Gieseler crucible to come up to an external temperature of about 450°C, then any time interval measurements which are in the range of small multiples of three minutes (say, any intervals as small as about 10 minutes) are likely to be badly perturbed by this lag. This consideration imposes a practical upper temperature ceiling upon the usefulness of isothermal Gieseler data.

Raw Gieseler data are tabulated in Section 6.3.

Table 3.3-7

Isothermal Plastometry of Kentucky #11 Seam Coal*

time	400.0°C	410.0°C	425.5°C	440.0°C	449.9°C	460.0°C
1 min	...	...	...	...	...	0.3
2	...	...	...	0.4	1.	6.2
3	...	...	...	7.4	28.	11760.
4	0.5	0.8	1.4	66.	340.	>29000.
5	0.9	1.7	4.8	242.	2257.	21060.
6	1.3	2.5	44.	955.	19580.	20840.
7	1.8	3.9	125.	5661.	>25000.	[24500.]
8	2.1	7.6	265.	21950.	17010.	6665.
9	2.4	17.8	1330.	27380.	8773.	1165.
10	2.7	34.	10680.	18940.	2008.	224.
11	3.6	60.	>25000.	7744.	484.	42.
12	4.5	106.	" "	3628.	118.	7.3
13	5.2	187.	20830.	1411.	43.	2.0
14	6.3	281.	17070.	615.	14.6	[0.7]
15	6.2	360.	10700.	278.	5.9	...
16	7.5	453.	5844.	137.	2.4	...
17	9.3	508.	5838.	65.	0.9	...
18	16.0	517.	3894.	33.8	0.6	...
19	25.4	522.	2655.	17.1	...	...
20	35.3	499.	1941.	8.5	...	...
21	27.5	483.	1181.	5.0	...	...
22	27.9	500.	758.	2.6	...	...
23	43.2	456.	554.	1.7	...	...
24	42.4	363.	358.	1.0	...	...
25	36.4	303.	228.	...	...	...
26	44.7	244.	176.	...	...	...
27	43.8	204.	123.	...	...	...
28	42.2	163.	83.	...	...	...
29	37.4	137.	56.5	...	...	...
30	41.9	113.	41.	...	...	...
31	42.4	97.	32.4			
32	28.6	82.	22.1			
33	32.9	68.	16.9			
34	36.6	55.	11.8			
35	33.1	45.	9.0			
36	23.2	41.9	7.2			
37	23.9	35.2	5.2			
38	26.5	28.8	4.0			
39	26.1	21.1	3.1			
40	22.8	20.2	2.2			

(continued)

*As in preceding tables.

Table 3.3-7 Con't.

time	400.0°C	410.0°C	425.5°C
41 min	17.4	16.7	1.9
42	13.4	16.0	1.6
43	16.1	13.7	1.3
44	15.5	11.2	1.0
45	15.4	9.6	0.8
46	14.7	7.9	...
47	14.2	7.2	...
48	13.2	6.4	...
49	10.5	5.2	...
50	9.4	4.2	...
51	7.6	4.2	...
52	6.6	3.0	...
53	5.9	3.1	...
54	5.5	2.7	...
55	5.2	2.3	...
56	4.9	1.9	...
57	5.0	1.7	...
58	4.7	1.55	...
59	4.7	1.3	...
60	4.4	1.2	...
61	3.9	1.0_6	...
62	3.8	0.8_4	...
63	3.7	0.7_9	...
64	3.5	...	...
65	3.0	...	...
66	2.7	...	...
67	2.6	...	...
68	2.3	...	...
69	2.2	...	...
70	1.9	...	...

Table 3.3-8

Isothermal Fluidity Ranges for Kentucky #11 Seam Coal*

Fluidity, ddpm	1	5	12.7	138	1485	16030
Viscosity, poise	10^7	2.5×10^6	10^6	10^5	10^4	10^3
400.0°	5.3-76.5	12.8-55.7	17.6-48.2	.....	.....	.....
	71	42.9	30.6			
410.0°	4.3-61.3	7.4-49.2	8.6-43.4	12.5-29.0	.....	.....
	57	41.8	34.8	16.5		
424.5°	3.7-44.0	5.0-37.1	5.4-33.8	7.1-26.7	9.0-29.5	10.2-14.1
	40.3	32.1	28.4	19.6	11.5	3.9
440.0°	2.3-24.0	2.9-21.0	3.2-19.4	4.6-16.0	6.3-13.0	7.7-10.2
	21.7	18.1	16.2	11.4	6.7	2.5
449.9°	2.0-16.9	2.5-15.2	2.8-14.2	3.65-11.9	4.8-10.2	5.9-8.1
	14.9	12.7	11.4	8.25	5.4	2.2
460.0°	1.4-13.5	1.9-12.3	2.25-11.7	2.4-10.3	2.7-8.8	3.0-7.5
	12.2	10.4	9.4	7.9	6.1†	4.5†

---

* Summary table of isothermal Gieseler fluidity data. In each column and at each temperature the small numbers give the time in minutes at which the softening and coking curves attain the indicated fluidity; the large underscored numbers show the net period of time in minutes for which the indicated fluidity is exceeded.

† Data exceed expected values.

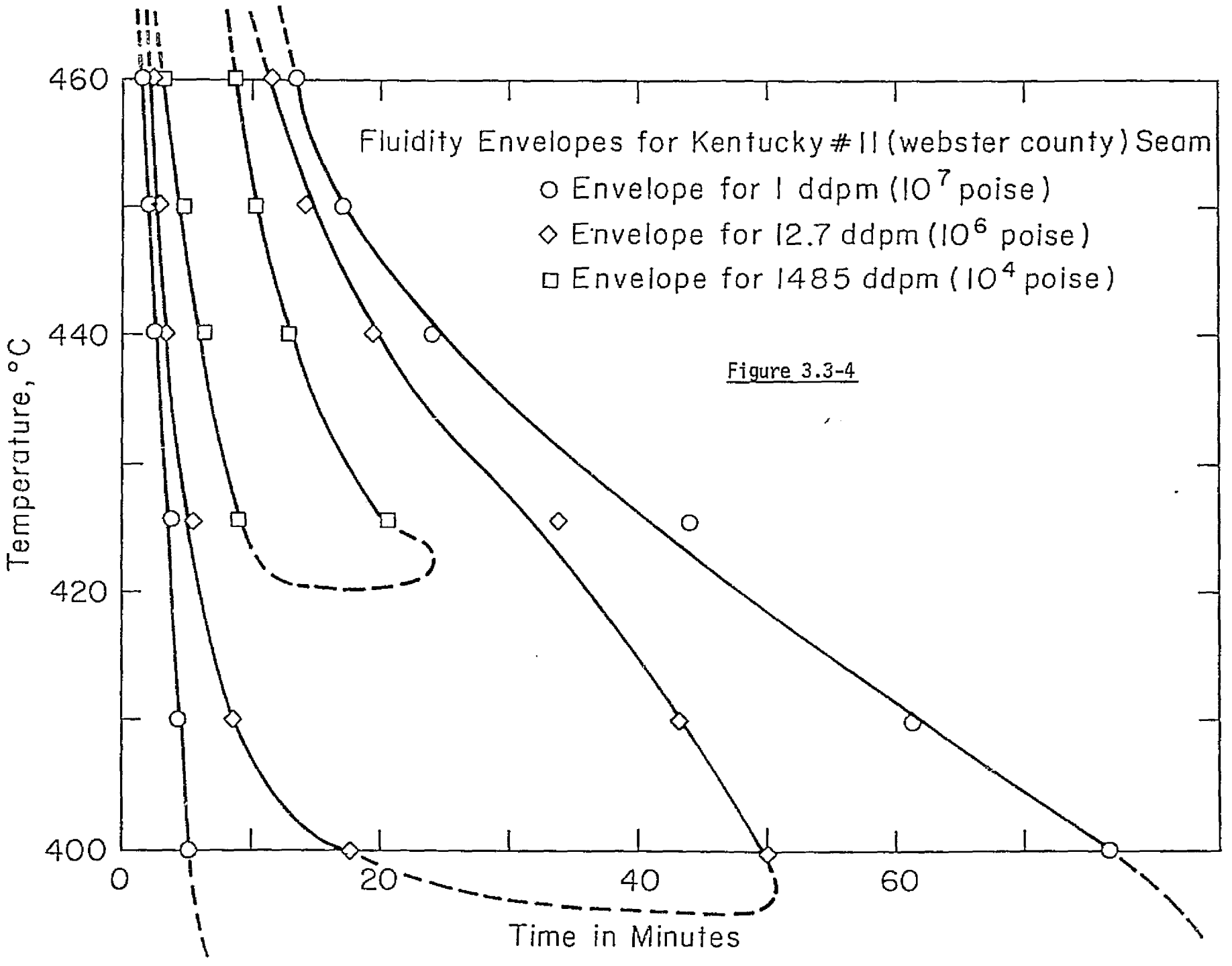
Fluidity Envelopes for Kentucky #11 (webster county) Seam
○ Envelope for 1 ddpm (10^7 poise)
◇ Envelope for 12.7 ddpm (10^6 poise)
□ Envelope for 1485 ddpm (10^4 poise)
Temperature, °C
460
440
420
400
0
20
40
60
Time in Minutes

Figure 3.3-4

3.4 Microstructure

3.4.1 Extractable Fractions.

(work performed by Clara T. Magura and Arthur W. Fort)

It has been known for decades that significant portions of the organic content of pulverized bituminous coals can be extracted by appropriate organic solvents (14). A structural view of this phenomenon, suggested by the insights of polymer science, is that bituminous coals may be considered to consist of lightly crosslinked macromolecular networks containing a substantial fraction of small "sol fraction" molecules distributed interstitially.

Coal may be effectively extracted by fairly polar protic solvents such as phenols, but not by highly polar protic solvents such as light alcohols, glycols or carboxylic acids. Coal may be effectively extracted by polar aprotic solvents such as pyridine and the quinolines, but not by less polar solvents such as dioxanes, dioxolanes or tetralins. One of the better solvents in this laboratory's experience is the neutral polar aprotic solvent N,N-dimethyl formamide (DMF). At its reflux temperature of 153°C DMF extracts as much as 30% of the total moisture-free mass of coal.

Under the conditions of DMF extraction it seems unlikely that the coal structure is undergoing chemical modification. The existence of so large an extractable fraction suggests that the covalent crosslink density is fairly low (a demonstrable requirement for vinyl network polymers). At the same time the high extraction efficiency of solvents such as DMF and the poor extractive efficiencies of such "coal-like" solvents as tetralin and benzofuran suggests that intrastructural hydrogen bonding may provide a relatively high <u>effective</u> crosslink density.

In seeking microstructural features relevant to the plastic properties of coals, we have therefore included an examination of the DMF-extractable fractions of the seven coals included in the present study.

Extractions were conducted at atmospheric reflux using Soxhlet extractors and were conducted in duplicate. A 10-gram sample of pulverized coal is weighed into a tared cellulose Soxhlet thimble, the assembly charged with 150 ml of fresh DMF, and (except as noted otherwise) the system reflux-extracted for 24 hours at a rate of 1 to 2 ml/min. The extracted coal was then subjected to a six-hour extractive reflux with reagent methanol, for the purpose of thoroughly removing residual DMF. The thimble containing the extracted coal was then removed, air-dried, vacuum-oven dried, and weighed to determine weight loss. Extractable organics were then calculated, correcting for the moisture contents of the coals. These data are given in Table 3.4-1.

The last five entries in Table 3.4-1 explore the effect of extraction time upon extraction efficiency. These data indicate that extraction is essentially complete in four hours, so that the 24-hour period may be considered to result in complete extraction.

The agreement between replicate pairs of data indicates a standard deviation of ±1.0% absolute. Consequently, the differences among the coals is considerably larger than the analytical errors. The most serious internal discrepancy is between the two sets of Pittsburgh #8 extractions, conducted at different times on different subsamples. These imply a serious homogeneity problem among these subsamples.

DMF extractables appear to correlate generally with plastometric data. Among the six bituminous coals, for example, the percent extractable conforms with the 425° isothermal plastometry behavior (Table 3.3-5). The subbituminous coal, which has significant extractability but no plastic properties, does not fit this generalization, however.

Three coal extrudates have also been subjected to extraction and are listed in Table 3.4-1. The extrudates are those of the three most plastic coals in this study. In the course of extrusion a significant loss of volatile organic material occurs. If this were the only material change occurring, the percent extractables for the extrudates would be consistently less than for the parent coals. These data do not support this view; for the two most plastic coals the

Table 3.4-1

Extractions of Several Coals with Hot N,N-Dimethylformamide

Coal Seam	Percent DMF-Extractable (Moisture-corrected)				Average
Pittsburgh #8	26.7	26.7	26.8	26.2	26.6%
Pittsburgh #8[1]		33.1	31.2		32.2%
Ohio #9		19.3	18.6		19.0%
Lower Kittanning	0.4	0.2	1.5	1.0	0.8%
Kentucky #11		25.5	28.5		27.0%
Pocahontas #3	0.0	0.0	0.0		0.0%
Amax Wyoming		13.5	14.9		14.2%
Elkhorn #1		15.7	13.6		14.7%
Extrudate 1A from Pittsburgh #8		45.5	43.8		44.7%
Extrudate 2A+2B from Ohio #9		14.0	16.5		15.3%
Extrudate 4A+4B from Kentucky #11		33.7	36.7		35.2%
Pittsburgh #8 (24 hrs)[2]		33.1	31.2		32.2%
Pittsburgh #8 (8 hrs)[2]		29.8	29.7		29.8%
Pittsburgh #8 (4 hrs)[2]		31.0	29.1		30.1%
Pittsburgh #8 (2 hrs)[2]		29.0	26.9		28.0%
Pittsburgh #8 (1 hr)[2]		26.0	17.0		ca 22 %

---

[1] This extraction was performed two months later than others in this set, using a different sub sample.

[2] All extractions are for 24 hours as described in the text, except this series, which were extracted at various schedules as indicated.

extrusion process has clearly resulted in a net increase in DMF-extractables, by about 50% in the case of the most plastic coal (Pittsburgh #8) and about 30% in the case of the next most plastic coal (Kentucky #11). On the other hand, extractables in a pooled sample of Ohio #9 extrudates (2A and 2B) are down by about 20% from that found in the raw coal. These data suggest countervailing effects in the extrusion process, perhaps a loss of volatile extractables and at the same time a chemical degradation of the network structure.

One of the classical measurements of coal properties, and one which might be related to extractable fraction, is the ASTM volatile matter determination (ASTM D3175). In this determination a sample of pulverized coal, with air excluded, is heated under a specified regimen to 950°C, and the weight loss (corrected for moisture) is reported as volatile matter. Volatile matter measurements are included and discussed in Section 3.1 of this report. Portions of the seven DMF-extracted coals in this study have been subjected to the standard volatile matter determination. Results for these extracted coals, and for their parent coals are shown in Table 3.4-2. (All data are corrected for moisture but not for ash content.) The change in percent volatile matter, as a result of extraction, at first appears random. Again these data tend to correlate with plastometric data. The three most plastic coals all show losses in volatiles of 5.2-7.5%; the moderately plastic Elkhorn #1 shows a smaller loss; the less plastic Kittanning shows a still smaller loss, and the slightly plastic Pocahontas and the completely nonplastic Amax show increases.

The effect of extrusion upon DMF-extractables of Pittsburgh #8 seam coal, noted in Table 3.4-1, has suggested the desirability of carrying out DMF extractions of the five extrudate samples provided by JPL with known thermal histories. These samples are all from a single extrusion run using Pittsburgh #8 coal, with the nominal extrusion die temperature varied from 425° to 650°C. Results of these extractions are given in Table 3.4-3.

The data of Table 3.4-3 show two significant characteristics: out-of-line values for 900°F, and a marked uniformity of values for all other temperatures.

Table 3.4-2

Effect of DMF Extraction upon Volatile Matter Determination*

Coal Seam	Volatile Matter Raw Coal	Volatile Matter Extractate	Change
Pittsburgh #8	41.18%	33.64%	- 7.5%
Ohio #9	40.27	34.42	- 5.9
Lower Kittanning	27.10	26.02	- 1.1
Kentucky #11	42.02	36.84	- 5.2
Pocahontas #3	17.48	19.18	+ 1.7
Amax Wyoming	46.66	64.62	+18.
Elkhorn #1	36.42	33.86	- 2.6

* ASTM volatile matter determination, corrected for moisture only.

Table 3.4-3

Effect of Die Temperature upon DMF-Extractables*

Die Temperature		Percent DMF-Extractable (moisture-corrected)				Average
800°F	427°C	30.4%	14.3%	34.4%	31.5%	32.1%[1]
900°F	482°C		20.1	19.3		19.7
1000°F	538°C		33.8	31.2		32.5
1100°F	593°C		32.2	31.6		31.9
1200°F	649°C		35.1	32.7		33.9

---

[1] Best three of four data

* Extrudate samples from Pittsburgh #8 seam coal.

The 900°F data probably reflect aberrant character of that particular sample rather than analytical error. This is suggested first by the internal consistency of the duplicate data, and even more forcefully by examination of other analyses of this series of extrudates, e.g., volatile matter in Table 3.1-2, and percent hydrogen in Table 3.1-3. This extrudate sample appears to be different from the other samples taken during the same extrusion run.

The marked uniformity of values for the other four die temperatures implies that die temperature does not have an important effect upon this compositional parameter under these extrusion conditions. This coal extrudate has spent approximately one minute in the screw extruder, maintained at a temperature of about 800°F (427°C), followed by about two seconds at the die temperature indicated in Table 3.4-3. (27) The portion of the fluid coal mass that is heated sensibly above 800°F during this short contact period may be rather small. In any event, these data, like the data of Tables 3.1-2 and 3.1-3, suggest that there is no significant compositional difference among the 800°, 1000°, 1100° and 1200°F extrudates.

The average extractable fraction for these four extrudates is 32.5%, as compared with 26.6-32.2% for the parent coal (Table 3.4-1). Although these extrudates have lost about 5% of their volatile matter in the course of extrusion, the total extractables remain as high as, or higher than, that found for the parent coal.

3.4.2 Micrography and Mapping

(work performed by C. T. Nightingale, Structure Probe Inc., West Chester, PA)

Another aspect of structure is seen by scanning electron microscopy, here used with particular emphasis upon mineral matter distrubution. Figure 3.4-1A shows a portion of a single pulverized particle of Pittsburgh #8 seam coal, at 500X. The mineral components show up as white to light grey particles embedded in the darker grey organic matrix. The mineral particles seen here are mainly in the range 1 to 10 μm. The electron beam itself excites x-ray fluorescence; by "reading" the fluoresced x-rays within a narrow energy window -- i.e., the x-rays associated with one particular element -- it is possible to map the distribution of the selected element for any given specimen. Figure 3.4-1B is the x-ray map for silicon for the particle shown in Figure 3.4-1A. The concentrations of white dots correspond to concentrations of silicon-rich material. Silicon itself, and aluminum (not illustrated), appear to be concentrated strongly in a few particles.

Figure 3.4-2 illustrates the appearance of pulverized coals at 50X, where the individual particles are clearly seen. In both 3.4-2A (Pittsburgh #8) and 3.4-2 (Ohio #9) the coal particles are seen to be mainly in the range 0.1 - 1.0 mm, and to contain clearly discernible particles of mineral matter.

Elemental mapping at 50X provides a considerable greater area of coverage than that of 3.4-1B. In Figure 3.4-3 are seen the elemental maps of sulfur (A) and iron (B) in the Pittsburgh #8 specimen photographed in Figure 3.4-2A. The white areas of both maps indicate high concentrations of the respective elements, and it is evident that these areas substantially coincide, identifying zones of pyritic (FeS_2) intrusions. The pyrite particles appear to be mainly in the range 40-100 μm. Figure 3.4-3A shows the rough outlines of the coal particles seen in Figure 3.4-2A; this is an artifact of the method for low-energy x-rays, and has no chemical significance. Also, the light random background dot distribution seen in the elemental maps is due partly or entirely to the method used and does not necessarily signify fine distribution. In the case of sulfur, however, we know from chemical analysis (e.g., Table 3.1-4) that pyritic sulfur is only about 40% of the total sulfur present.

Figure 3.4-1

Scanning Electron Micrography of Pittsburgh #8 Coal

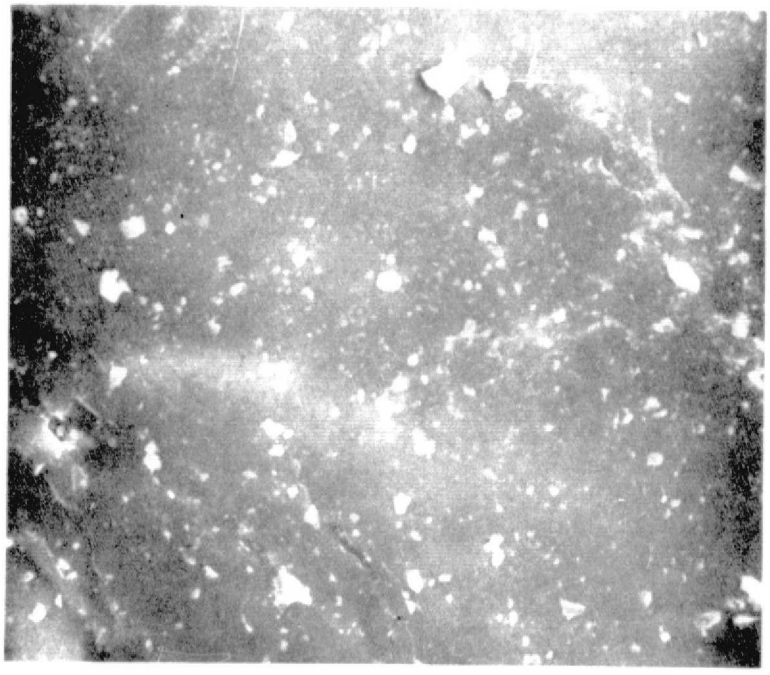

A. Micrograph at 500X

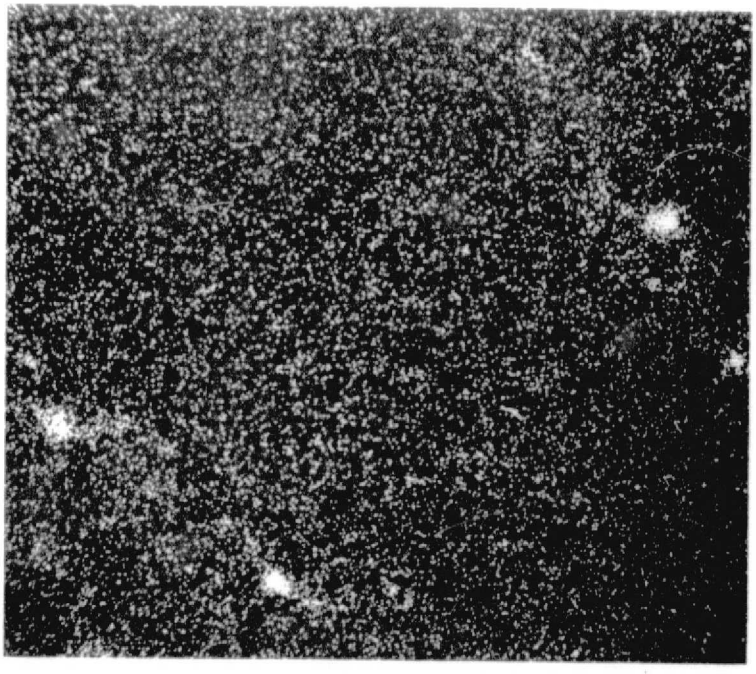

B. Elemental Map of Silicon (same field of view)

Figure 3.4-2

Two Pulverized Coals at 50X

A. Pittsburgh #8 seam coal

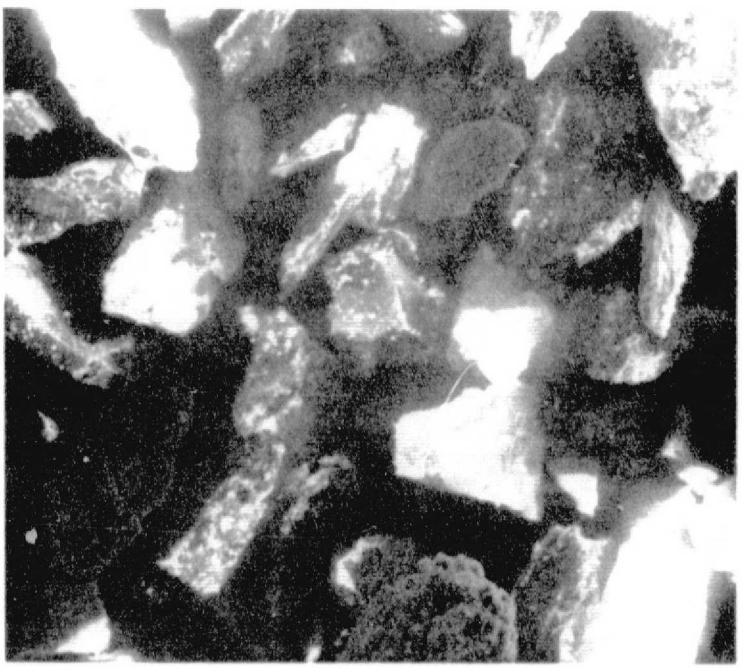

B. Ohio #9 seam coal

Figure 3.4-3

Elemental Maps of Pittsburgh #8 seam coal at 50X

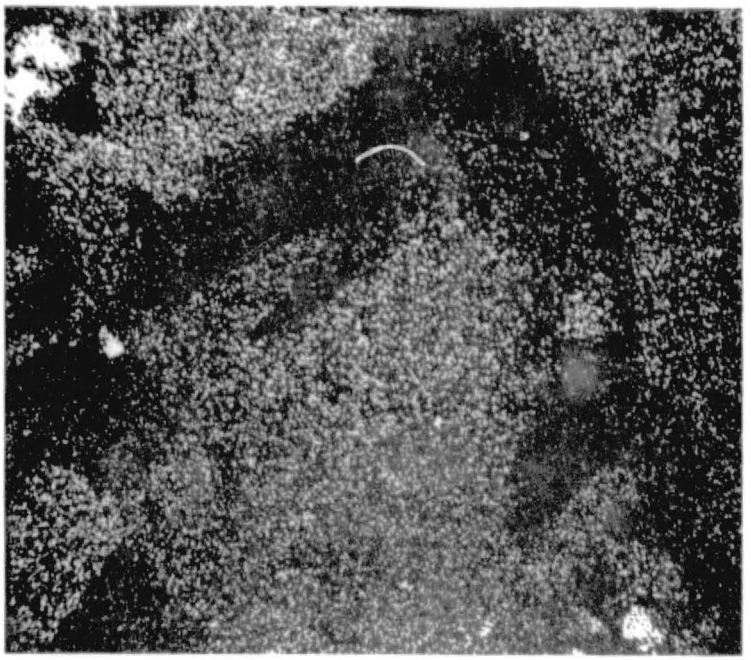

A. Sulfur

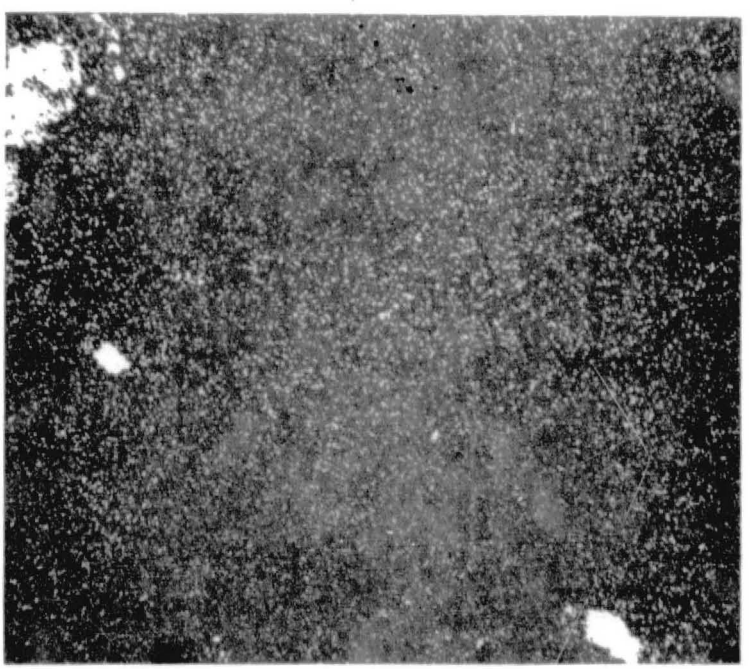

B. Iron

Maps of other elements in these two coals show clustering of aluminum, silicon and calcium, though not in the same locations as seen for iron and sulfur. Chlorine, potassium and titanium show no clustering at 50X or at 500X, and thus appear to be distributed in very fine particles throughout the coals.

Two extrudates of these coals are shown at 50X in Figure 3.4-4. The extrudate material has been similarly ground for analysis, and the particles are of the same general size as those of the parent coals. These extrudates show at least three distinct structural features of interest. They are smoother than the parent coals, and show clear signs on their fracture surfaces of being resolidified melts. They also show a number of blowholes and cavities, mainly in the 20 - 100 μm range, showing that gases or vapors were formed in the viscous melts, in some cases escaping the semisolid mass and leaving congealed bubble rings. Furthermore, these micrographs show the random distribution of mineral matter in the organic matrix, with no apparent significant aggregation or dispersion as a consequence of the extrusion process. The extruded particles appear to be substantially isotropic, while raw coal is an obviously anisotropic substance.

The elemental maps (not shown) of these two extrudates are substantially similar to those of the parent coals. Sulfur and iron are aggregated in the same particles, suggesting the survival of pyrite and/or marcasite, as would be expected. Aluminum, silicon and calcium also show aggregation, although not in the same particles as iron and sulfur. Potassium, chlorine and titanium, all present in sufficient concentrations to afford clear Kα peaks, appear to distributed throughout the extrudates, just as was observed for the corresponding raw coals. An unusual feature of the Ohio #9 extrudate is a well-defined manganese map showing a strong concentration of maganese in a few particles. We have previously noted (Table 3.2-1) the unexpectedly high concentration of manganese in this particular coal.

The principal significance of this examination is that it clearly shows on a microtopological scale that the organic matrix of these coals has truly melted and then congealed, in the course of the extrusion process; but that this extrusion process does not appear to have materially altered the gross form and distribution of mineral matter.

Figure 3.4-4

Two Coal Extrudates at 50X

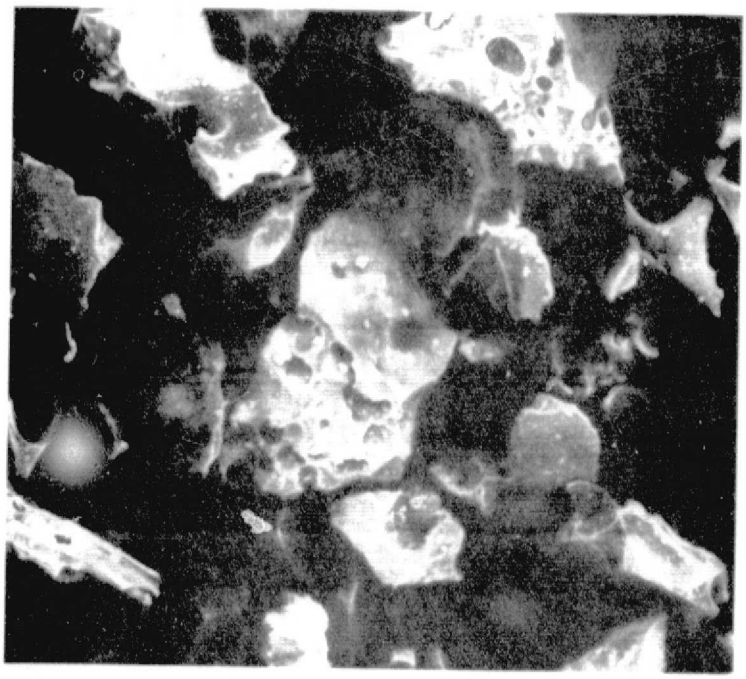

A. Extrudate 1A from Pittsburgh #8

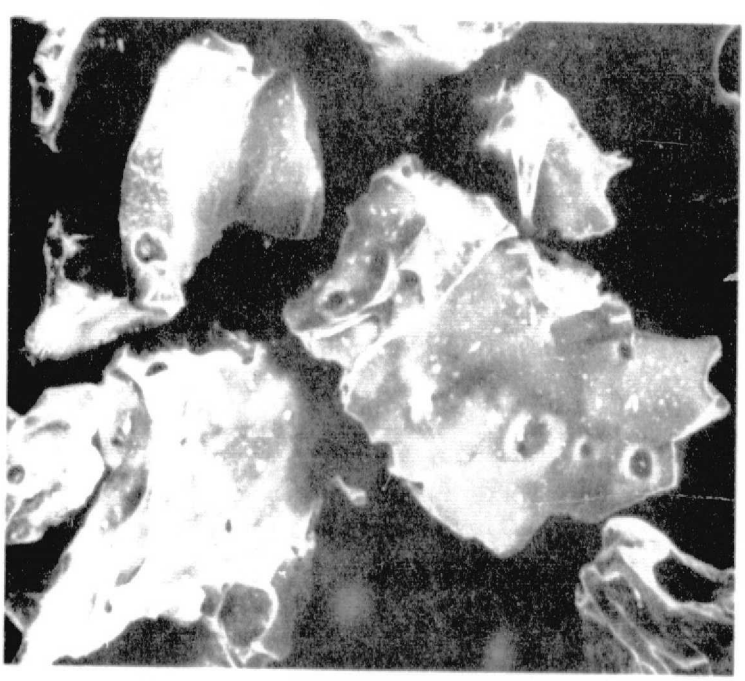

B. Extrudate 2A from Ohio #9

3.4.3 Surface Area

(work performed by Sayra N. Russell, Karen C. Moore and Burtron H. Davis)

Surface areas are estimated by measuring the amount of gas or vapor required to afford an adsorbant monolayer over a known mass of material. The amount of adsorbate is measured in various ways; in the present work we have used pressure drop (for nitrogen), a calibrated thermal conductivity detector (for carbon dioxide), and micrograviметry (for methanol).

The standard nitrogen adsorption measurement was conducted on several samples of raw, extracted and extruded coals, using an automated commercial surface area apparatus (Micrometritics Model 2500). Results are shown in Table 3.4-4.

The indicated surface areas are low (mostly in the range 1 to 5 m^2/g). Although nitrogen adsorption is extremely useful for many metallic and metal oxide surfaces, it has not proven of great value for organic substrates such as coal. In general coal, coke and char surface areas are estimated by the adsorption of more polar molecules (which also give substantially higher estimates of surface area.)

Carbon dioxide was adsorbed at dry ice-isopropyl alcohol temperature (-78°C) from a helium - carbon dioxide mixture (P/P_o = 0.10). P_o was taken to be 1.86 atm at -78°C. A sample of 50-80 mg of coal was placed in a glass gas chromatography column and secured with glasswool, degassed at 120-140° for five minutes, and the mixed-gas stream passed over the sample for 16-20 hours at -78° . The sample was then allowed to warm to ambient temperature, while the gas stream continuously passed over the sample and through a thermal conductivity detector. Desorption under these conditions is extremely rapid, and is complete in less than five minutes. Detector response was calibrated by injecting known volumes of CO_2 into the mixed-gas stream in the absence of adsorbing sample. Surface area was calculated using the standard BET one-point equation, using 20.5 $\AA^2$ as the cross-sectional area of the adsorbate. Results are shown in Table 3.4-5.

Table 3.4-4

BET Surface Areas by Nitrogen Adsorption

Coal or Coal Product	Area, m^2/g
Pittsburgh #8 (raw)	5.92
Pittsburgh #8 extracted	1.87
Pittsburgh #8 extrudate 1A	1.28
Ohio #9 (raw)	2.54
Ohio #9 extracted	4.80
Ohio #9 extrudate 2A	1.37
Lower Kittanning (raw)	6.16
Lower Kittanning extracted	1.18
Kentucky #11 (raw)	3.20
Kentucky #11 extracted	2.50
Kentucky #11 extrudate 4A	1.34
Kentucky #11 extrudate 4B	0.78
Pocahontas #3 (raw)	1.10
Pocahontas #3 extracted	1.93
Amax Wyoming extracted	4.16
Elkhorn #1 extracted	2.28

Table 3.4-5

BET Surface Areas by Carbon Dioxide Adsorption

Coal Seam	Area (raw coal)	Area (DMF-extracted)
Pittsburgh #8	56. m^2/g	>141. m^2/g[1]
Ohio #9	65.	
Lower Kittanning	67.	
Kentucky #11	23.	154.
Pocahontas #3	50.[2]	67.[2]
Amax	190.[3]	186.
Elkhorn #1	81.	
Extrudate 2A (from) Ohio #9)	30.	

[1] Greater than 141 m^2/g; peak area exceeded integrator capacity.

[2] Sharp desorption peak is followed by slow desorption. The slow desorption was neglected in calculating adsorption area.

[3] Duplicate determinations yield 192 and 188 m^2/g.

These results indicate considerably higher surface areas than were implied by nitrogen adsorption. DMF-extracted coals show consistently higher surface areas, often higher by severalfold, than their parent coals. Extruded coals, on the other hand, show surface areas which are similar to or less than those of their parent coals.

Another method of estimating adsorption area is that of methanol vapor adsorption, recently shown to be useful for hard and soft coals, and to afford estimates similar to those obtained by CO_2 at -78°. (15) In this method a few mg of coal is placed on the microbalance of a thermogravimetric analyzer and, after outgassing, is returned to 25° and the helium pad is replaced by a stream of helium saturated with methanol at 25°C. The weight gain curve is completed within two hours. Weight gain is used to calculate surface area by the BET one-point equation, taking $P/P_o = 0.27$ and a cross-sectional area for methanol of 18.4 $\AA^2$. Results are shown in Table 3.4-6.

These results are generally similar to those obtained with CO_2 (Table 3.4-5). Surface areas of the raw bituminous coals (excluding Amax subbituminous) are 40-70 m^2/g; extracted coals are noticeably higher, and extruded coals are about the same as or a little lower than their parent coals.

None of these figures is high in comparison with those of chars, typically in the order of 500 m^2/g. The data of Tables 3.4-5 and 3.4-6 indicate that the surface areas of raw bituminous coals do not differ greatly from coal to coal, notwithstanding substantial differences in rank, volatile matter, FSI and other measurements.

These data show that DMF-extracted coals exhibit considerably higher surface areas. It may be suggested that pores which in the parent coals are plugged by extractable small molecules become opened up by extraction. In support of this view, it may be noted that the coal showing the smallest increase in area as a result of extraction (Pocahontas #3) also shows an immeasurably small weight loss upon extraction. Also, the only raw coal to show a high surface area (the Amax subbituminous) has a very high moisture content and undergoes a substantial loss of interstitial small molecules upon being warmed, a loss which can open up pores analagously to the extractive removal of small organic molecules.

Table 3.4-6

BET Surface Areas by Methanol Adsorption

Coal Seam	Area (raw coal) m^2/g	Area (extracted) m^2/g
Pittsburgh #8	65.	216.
Ohio #9	44.	174.
Lower Kittanning	67.	198.
Kentucky #11	47.	163.
Pocahontas #3	48.	63.
Amax Wyoming	327.	346.
Elkhorn #1	48.	92.
Pittsburgh #8 extrudate 1A	43.	
Ohio #9 extrudate 2A	48.	
Kentucky #11 extrudate 4A	52.	
Kentucky #11 extrudate 4B	49.	

Microphotographs of the extrudates (Figure 3.4-4) show two structural changes which have opposing effects upon surface area: in extrusion (at least for these two coals) the organic matter melts and flows together, destroying fine structure and tending to reduce overall surface area; and at the same time the viscous melt is outgassing and forming vapor pockets and surface blowholes, creating new fine structure and tending to increase surface area. Based upon the surface area estimates of four extrudates of the three most plastic coals in this study, it appears that the extrusion process has a levelling effect: all four extrudates, notwithstanding other differences noted elsewhere, show methanol-adsorbate surface areas in the narrow range of 43-52 m^2/g.

3.4.4 Petrographic Analysis
(work performed by G. J. Jansen, Rocky Mountain Coal Petrography, Golden, CO)

The technological properties of coal may be estimated in terms of its degree of metamorphism (or rank). Its composition can be conveniently expressed in terms of the microscopically distinguishable organic constituents (macerals). The degree of metamorphism can be measured by determining the reflectance of the vitrinoid group, which is the principal maceral component of coals.

The coals in this study have been subjected to reflectance and maceral analysis. Vitrinoid reflectance for each coal is based upon 100 reflectance measurements of vitrinoid domains. Maceral analysis for each coal is based upon species tabulation for 1,000 grid intersections. On the basis of this count, the overall coal composition is defined in terms of reactive constituents (chiefly vitrinoids, and also including exinoids, resinoids, and reactive semifusinoids) and inert constitutents (micrinoids, fusinoids, inert semifusinoids, and mineral matter). From this information two derived terms can be calculated. The Composition-Balance Index expresses the balance of heat-reactive and heat-inert coal. The Strength Index is an indicator of the coking power of the reactive constituents: a high index indicates strong coking power. The detailed basis for calculating these derived terms has been described elsewhere. (16,17)

Results of the petrographic analysis of the seven coals in this study, and of two extrudates, are given in Table 3.4-7. The Amax subbituminous coal gives a very low reflectance which is not comparable with those of the bituminous coals; CBI and SI are not calculated for this specimen. The extrudates were subjected to maceral analysis only. Reflectances for these specimens appears to be slightly higher than that of the parent ccals, an observation which is to be expected in view of the thermal history of these samples.(18) Pore structure was evident in almost every grain (cf. Figure 3.4-4). Both extrudates show the presence of oxidation rims (extrudate 2A more strongly than extrudate 1A). These rims are specifically characteristic of coal materials

Table 3.4-7

Petrographic Analysis of Several Coals

Coal Seam	Rank[1]	Mean Maximum Reflectance	Composition-Balance Index	Strength Index	Reactive Constituents	Inert Macerals[2]
Pittsburgh #8	hvAb	0.84	0.70	3.06	80.2%	13.7%
Ohio #9	hvBb	0.66	1.2	2.58	74.1%	12.9%
Lower Kittanning	mvb	1.18	0.74	4.58	79.4%	13.8%
Kentucky #11	hvAb	0.72	0.68	2.82	82.6%	11.0%
Pocahontas #3	lvb	1.60	4.0	7.0	66.8%	27.7%
Amax	subC	ca 0.27	...	...	83.7%[3]	12.0%[3]
Elkhorn #1	hvAb	0.83	0.9	3.11	76.0%	15.6%
Extrudate 1A (from Pgh #8)	[hvAb][4]	...	...	...	78.1%	15.6%
Extrudate 2A (from Ohio #9)	[hvAb][4]	...	...	...	73.9%	9.9%

[1] from proximate analysis data according to ASTM D 388

[2] sum of micrinoids, fusinoids and inert semifusinoids

[3] using brown coal classifiations: reactive = huminite and liptinite suites; inert = inertinite suite

[4] treating extrudate as a coal, as in footnote 1

which have been heated in oxidizing atmospheres; their presence implies that neither of these extrusions was conducted with total oxygen exclusion.

The data in Table 3.4-7 show a tendency to correlate with the plastic properties of the coals. The more plastic coals tend to have reflectances in the 0.7-0.8% range; they have composition-balance indices less than unity; they have strength indices in the range 2.5-3.1.

Details of the maceral analyses are given in Table 3.4-8. The maceral classification used here is as follows:

> Vitrinoids, the major maceral type present, characteristically swell and fuse when heated.
>
> Exinoids are fossil spores, pollen grains and leaf cuticle matter, and are also considered reactive constituents, as are resinoids (minor components in these coals).
>
> Semifusinoids are thought to be burnt plant remains. These are intermediate in reactivity; reactive semifusinoids (so classed on the basis of reflectance) are counted as reactive constituents, and inert semifusinoids are, as the name suggests, inert.
>
> Fusinoids are cellular materials derived from burnt plant remains and are inert to heat.
>
> Micrinoids are thought to be formed from organic debris in early coalification, and are also inert to heat.

There are substantial differences in the character (as indicated by reflectance measurements) of the vitrinoids found in different coals. Vitrinoid types are based upon reflectance measurements: type 5 exhibits a standard reflectance in the range 0.50-0.59%; type 6 is found in the range 0.60-0.69%, and so forth. The six bituminous coals in Table 3.4-8 are arranged in order of increasing mean reflectances. These differences are substantial, and correlate well with ASTM rank (preceding table). For the plasticity temperature range 410-450°C, Ohio #9 and Elkhorn #1 vitrinoid reflectances do not accurately predict fluidity;

Table 3.4-8

Maceral Analysis of Several Coals

Coal Seam	Vitrinoids by type:													
	5	6	7	8	9	10	11	12	13	14	15	16	17	Total
Ohio #9	5.6%	56.1%	8.4%	...	...	...	...	...	...	...	...	...	...	70.1%
Kentucky #11	...	19.1	57.2	...	...	...	...	...	...	...	...	...	...	76.3
Elkhorn #1	...	...	22.9	32.3%	12.1%	...	...	...	...	...	...	...	...	67.3
Pittsburgh #8	...	...	14.3	47.4	13.6	...	...	...	...	...	...	...	...	75.3
Lower Kittanning	...	...	...	...	...	11.0%	36.9%	28.3%	2.4%	...	...	...	...	78.6
Pocahontas #3	...	...	...	...	...	...	...	...	...	5.2%	23.5%	34.1%	2.6%	65.4

	Vitrinoids	Exinoids	Resinoids	Reactive Semifusinoids	Micrinoids	Fusinoids	Inert Semifusinoids	Mineral Matter
Ohio #9	70.1%	2.1%	0.4%	1.5%	4.9%	5.0%	3.0%	13.0%
Kentucky #11	76.3	5.1	0.2	1.0	6.0	2.9	2.1	6.4
Elkhorn #1	67.3	7.1	nil	1.6	8.6	3.7	3.3	8.4
Pittsburgh #8	75.3	4.0	0.2	0.7	8.7	3.7	1.3	6.1
Lower Kittanning	78.6	nil	nil	0.8	7.3	4.9	1.6	6.8
Pocahontas #3	65.4	nil	nil	1.4	14.1	10.8	2.8	5.5
Extrudate 1A from Pgh #8	74.7	2.4	nil	1.0	11.4	2.2	2.0	6.3
Extrudate 2A from Ohio #9	70.8	1.7	nil	1.4	4.9	2.2	2.8	16.2

but the Elkhorn plasticity increases with temperature, so that reflectance might prove to be a good predictor for isothermal plastometry at, say, 480°C.

The detailed maceral compositions, based upon 1,000-point surveys of each coal, are also given in Table 3.4-8. Mineral matter, as measured petrographically, is based upon the statistical incidence of mineral regions on a polished surface; it is obviously related to, but not identical with, percent ash.

Semifusinoids make up typically 2-5% of bituminous coals. Following common U.S. practice, reflectances have been obtained on a small group of semifusinoid particles for each coal examined. The reflectance distribution observed is shown in Table 3.4-9. It is evident that the trend in reflectance distributions among these six coals parallels that for vitrinoid reflectance.

Some specific petrographic observations follow.

In the Pittsburgh #8 specimens the exinoids are well developed although not exceptionally abundant. Pyrite occurs as fine individual grains and as stringers in all maceral associations.

In the Ohio #9 specimens the calculated mineral matter percentage is unusually high (13.0%). Petrographic stability predictions are considered doubtful for coals with mineral matter contents greater than 12%.

In the Lower Kittanning specimens the inert and transitional maceral material occurs in complex intergrowths. Pyrite distribution varies from grain size of 5 to 200 μm, and varies from liberated particles to locked grains.

In the Kentucky #11 specimens fine cuticular material (exinoids) is well developed. Very minor petrographic evidence of oxidative weathering is seen.

In the Pocahontas #3 specimens there are unusually high percentages of fusinoids, semifusinoids and micrinoids. These account for the high CBI value.

In the Elkhorn #1 specimens exinoids are moderately abundant. The high ash and mineral content contributes to the rather high CBI.

Table 3.4-9

Semifusinoid Reflectance Analysis of Several Coals

Coal Seam	Semifusinoid % Reflectance[1]														
	0.8	0.9	1.0	1.1	1.2	1.3	1.4	1.5	1.6	1.7	1.8	1.9	2.0	2.1	Average value
Ohio #9	5%	25%	...	15%	10%	10%	...	20%	5%	10%	...	...	...	...	1.23%
Elkhorn #1	...	...	...	...	20%	10%	5%	10%	10%	25%	15%	...	5%	...	1.45%
Kentucky #11	...	...	...	10%	15%	5%	15%	15%	5%	15%	5%	...	5%	...	1.46%
Pittsburgh #8	...	...	...	...	...	10%	20%	35%	10%	20%	...	5%	...	...	1.53%
Lower Kittanning	...	...	...	...	...	...	...	15%	20%	20%	15%	10%	5%	15%	1.76%
Pocahontas #3	...	...	...	...	..	...	....	...	...	...	10%	30%	25%	35%	1.99%

[1]Reflectance measurements are grouped in increments of 0.1% reflectance in oil. An entry of 15% under 1.8 signifies that about 15% (3 out of 20) semifusinoid particles exhibited reflectance in the range 1.80 to 1.89%. The average value is calculated using the rounded-off data, and should be systematically low by about 0.05%.

In the Amax specimens a trial measurement of reflectances gave an average of 0.27%. This is in practical terms non-coking. Maceral analysis uses an entirely different framework based upon brown coal technology (17). Reactive maceral constituents are 76.1% huminite suite and 7.6% liptinite suite. Inert constituents are 12.0% inertinite suite and 4.3% mineral matter.

Of all of the foregoing petrographic information, the most widely used measurements are those of vitrinoid reflectance and measurement of reactive and inert macerals. These data are summarized in Table 3.4-7 and detailed in Table 3.4-8. Of all of the foregoing measurements, those of vitrinoid reflectance and of strength index appear to correlate most closely with the plastic properties of these six bituminous coals.

It is of interest that, after screw extrusion with a temperature profile including approximately 800°F for one minute, the two extrudates retain distinct maceral structures and fail to show any substantial shift in maceral composition from that of the parent coals.

3.5 Thermal Analysis

(work performed by Karen C. Moore and Henry E. Francis)

Thermogravimetric analyses under nitrogen atmospheres have been carried out on all coals, at three temperature ramps, 40°C, 80°C and 160°C per minute. Determinations were made with a Perkin-Elmer Model TGS-2 analyzer, using the following procedure.

Samples of pulverized coal weighing 9-15 mg were charged to the microbalance and the system purged with nitrogen at 50 ml min^{-1} for five minutes prior to weighing. The sample was then heated rapidly (320°/min) to 330°C and maintained at that temperature until the derivative pen indicated no further weight loss. (This initial loss of moisture and labile volatiles typically requires one to two minutes.) The weight pen was then zeroed, and an appropriate scale expansion selected (typically 30% loss = full scale) to provide maximum information. The appropriate temperature ramp was selected and the thermogravimetric analysis (TGA) commenced.

A series of TGA determinations was carried out with Pittsburgh #8 seam coal, at ramps from 2.5°C/min (close to Gieseler conditions) to 160°C/min, the highest heating rate for which we believe the instrument to be reasonably accurate. The family of TGA curves is shown in Figure 3.5-1. If the 2.5°/min curve is ignored, the general pattern observed is that of a family of sigmoid curves which at progressively higher heating rates are progressively offset to the right. The weight loss observed at any given temperature is greatest at low heating rates. This offset is largely an artifact of the method, however. When corrections are made for temperature lag, this family of curves becomes very close indeed.

The seven coals under study have been subjected to TGA determinations at three ramps, 40°, 80°, and 160°C/min. Their behavior at each temperature ramp reflects the substantial differences among these coals. The series of curves at 80°C/min are shown in Figure 3.5-2. The curves in this figure are coded as follows:

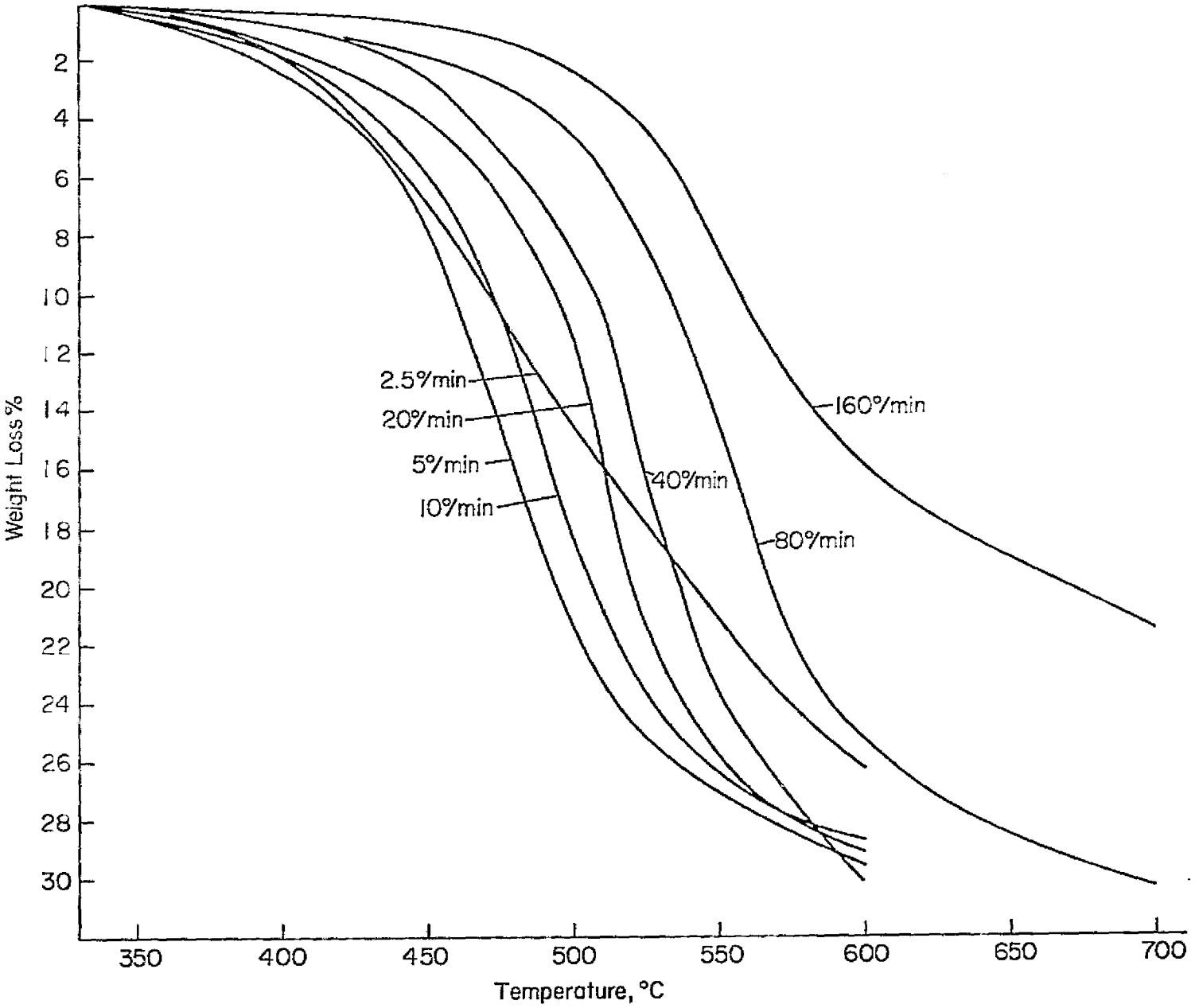

Figure 3.5-1 Thermogravimetric Curves for Pittsburgh #8 Seam Coal at Various Heating Rates

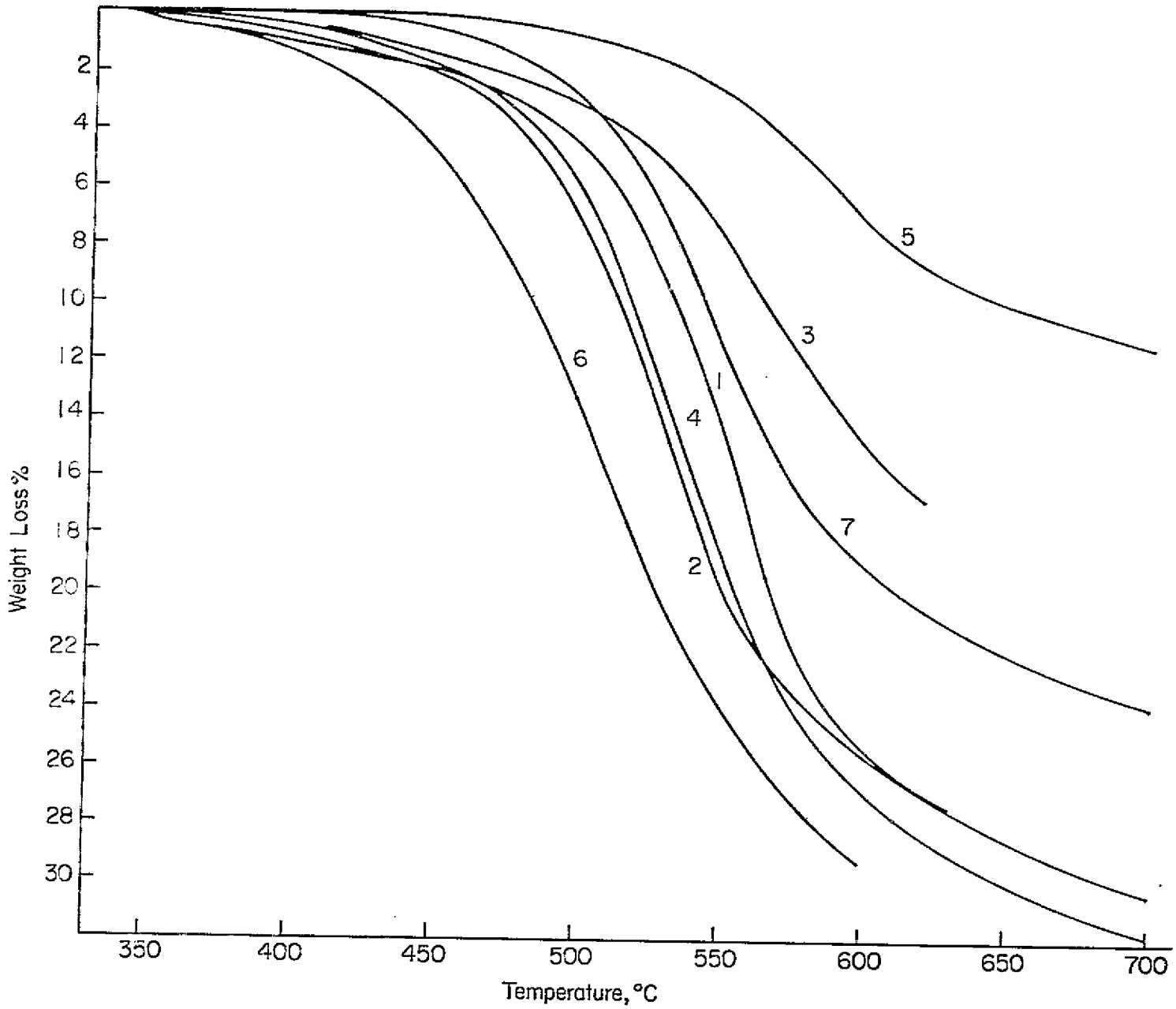

Figure 3.5-2 Thermogravimetric Curves for Seven Coals Heated at 80°C/min

1 - Pittsburgh #8
2 - Ohio #9
3 - Lower Kittanning
4 - Kentucky #11
5 - Pocahontas #3
6 - Amax
7 - Elkhorn #1

The general expectation is that the curves of Figure 3.5-2 may be expected roughly to conform to the volatile matter contents of these coals; indeed, thermogravimetric analysis under somewhat different conditions has been proposed as an equivalent method to measure volatile matter. (19) Notwithstanding the differences in heating ramp and in final temperature (950°C in ASTM D 3175), we are nevertheless comparing two methods of measuring the weight loss of coals when they are pyrolyzed in substantially inert atmospheres.

This expectation is realized here, as can be seen by comparing the family of curves in Figure 3.5-2 with the maf volatile matter for these coals (Table 3.1-1). Ranking them by decreasing maf volatile matter the order is: Amax > Ohio #9 > Kentucky #11 > Pittsburgh #8 > Elkhorn #1 >> Lower Kittanning >> Pocahontas #3. Over the large central portions of these curves (4-20% weight loss) this is exactly the order found. This same order -- with minor perturbations among the near neighbors, Ohio, Pittsburgh and Kentucky #11 -- is found at the 40°/min and 160°/min ramps.

One way of making numeric comparisons among a number of TGA curves is to measure weight loss at arbitrary benchmark temperatures. Four temperatures have been selected (450-600°C = 842-1112°F) for this comparison. The weight losses for the seven coals at these temperatures are shown in Table 3.5-1.

An important inference from these data (for which all temperatures have been corrected for thermal lag) is that, over the range 40-160°/min, there is in most cases no important temperature ramp effect. At all ramps the main weight loss zone is 500-600°C, excepting only Amax (450-550°C).

Table 3.5-1

Weight Losses of Seven Coals at Various Temperatures*

Coal Seam	Temp.,°C	Temp.,°F	Heating Rate, degrees min^{-1}		
			40°/m	80°/m	160°/m
Pittsburgh #8	450°	842°	3.7%	2.8%	2.4%
	500°	932°	11.0	8.2	8.2
	550°	1022°	25.6	21.7	15.8
	600°	1112°	31.0[1]	27.2	18.9
Ohio #9	450°	842°	3.8	3.7	1.8
	500°	932°	13.7	12.7	6.5
	550°	1022°	23.1	23.3	17.8
	600°	1112°	26.6	25.0	24.5
Lower Kittanning	450°	842°	1.9	2.1	1.8
	500°	932°	4.8	4.7	3.7
	550°	1022°	11.7	11.4	9.2
	600°	1112°	15.1[1]	16.4[1]	14.9
Kentucky #11	450°	842°	4.0	3.1	1.9
	500°	932°	15.3	11.5	10.5
	550°	1022°	25.0	23.7	24.1
	600°	1112°	28.5	28.5	27.9
Pocahontas #3	450°	842°	0.2	0.4	0.5
	500°	932°	1.3	1.4	1.3
	550°	1022°	3.5	4.5	3.8
	600°	1112°	6.4	8.8	8.1
Amax	450°	842°	9.0	8.3	7.4
	500°	932°	18.6	19.1	18.0
	550°	1022°	25.0	26.9	26.3
	600°	1112°	28.7	30.6	30.5
Elkhorn #1	450°	842°	1.2	1.3	1.3
	500°	932°	6.9	6.0	5.4
	550°	1022°	15.9	16.1	15.4
	600°	1112°	23.6	20.8	21.6

* Thermogravimetric analyses under nitrogen, temperatures corrected for thermal lag, weight losses calculated on a moisture-free basis.

[1] Extrapolated value.

Another way of making numeric comparisons is to determine the temperatures at which arbitrary benchmark weight losses are found to occur. Table 3.5-2 tabulates data for 10%, 15% and 20% (moisture-free) weight losses. These data are incomplete for Pocahontas #3, which by 700°C has lost only about 12% of its mf weight. The Lower Kittanning data are based upon extrapolations in some cases, for a similar reason.

These data support the observations noted above, namely, that these coals tend to array themselves in accordance with maf volatile matter determinations (and should be expected to correlate better with mf volatile matter data), and that -- with the possible exception of Pittsburgh #8 -- these coals do not show an important weight loss dependency upon heating ramp in the 40-160°C/min range.

Dilatometric measurements record the displacement of a piston in contact with a shaped, pulverized or pelletized coal sample in a closed cylinder, as a function of temperature. In this study dilatometric characterization was obtained using 100-mg samples of pulverized coal in the thermomechanical module of a Dupont Model 990 Thermal Analysis system.

Typical curves for Kentucky #11 coal at three heating ramps are shown in Figure 3.5-3. For this and many other coals there is no pronounced dimensional change until the system reaches a temperature in the vicinity of 400°C, whereupon a sharply defined expansion takes place. The swelling temperature is the intersection of the baseline and the steep swelling slope. The maximum expansion temperature is the temperature at which the curve peaks. The maximum expansion itself is measured by the height of the peak above baseline.

Figure 3.5-3 illustrates two general effects of increasing temperature ramp. At higher ramps the characteristic temperatures are shifted to higher values, and the maximum expansion is also generally increased.(9)

Some coals undergo a contraction or shrinkage prior to swelling. Figure 3.5-4 illustrates curves (in this case carried from ambient temp-

Table 3.5-2

Temperatures for Standard Weight Losses of Seven Coals*

Coal Seam	Weight Loss	Heating Rate, degrees min^{-1} 40°/m	80°/m	160°/m
Pittsburgh #8	10%	497°C	509°C	509°C
	15%	510°	528°	542°
	20%	525°	544°	622°
Ohio #9	10%	485°C	489°C	519°C
	15%	505°	509°	538°
	20%	530°	551°	561°
Lower Kittanning	10%	544°C	541°C	555°C
	15%	600°[1]	601°[1]	614°
	20%	648°[1]	666°[1]	...
Kentucky #11	10%	484°C	494°C	498°C
	15%	499°	513°	515°
	20%	512°	531°	532°
Pocahontas #3	10%	...	628°C	635°C
	15%	...	...	...
	20%	...	...	...
Amax	10%	456°C	459°C	465°C
	15%	481°	483°	487°
	20%	508°	504°	509°
Elkhorn #1	10%	524°C	519°C	527°C
	15%	546°	543°	549°
	20%	568°	586°	580°

* Thermogravimetric analyses under nitrogen, temperatures corrected for thermal lag, weight losses calculated on a moisture-free basis.

[1] Extrapolated value.

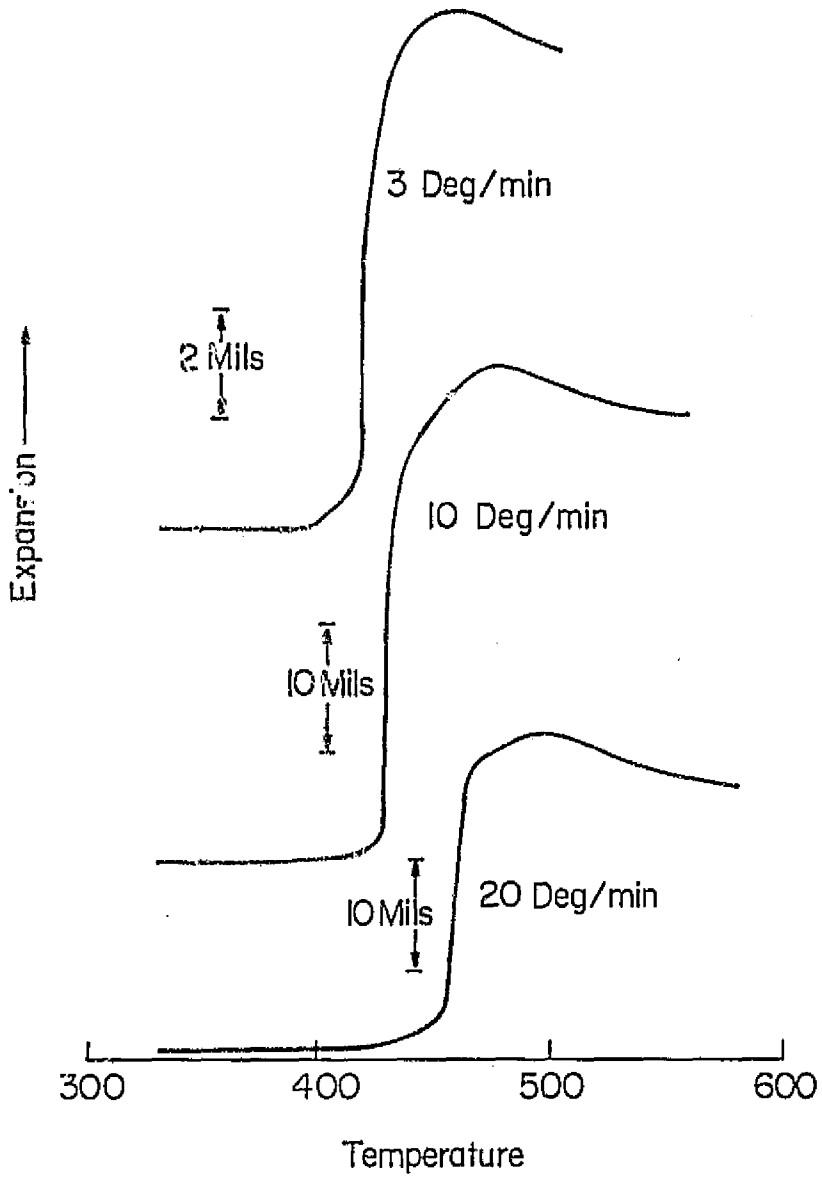

Figure 3.5-3 Thermomechanical (Dilatometric) Curves for Kentucky #11 Seam Coal at Three Heating Rates

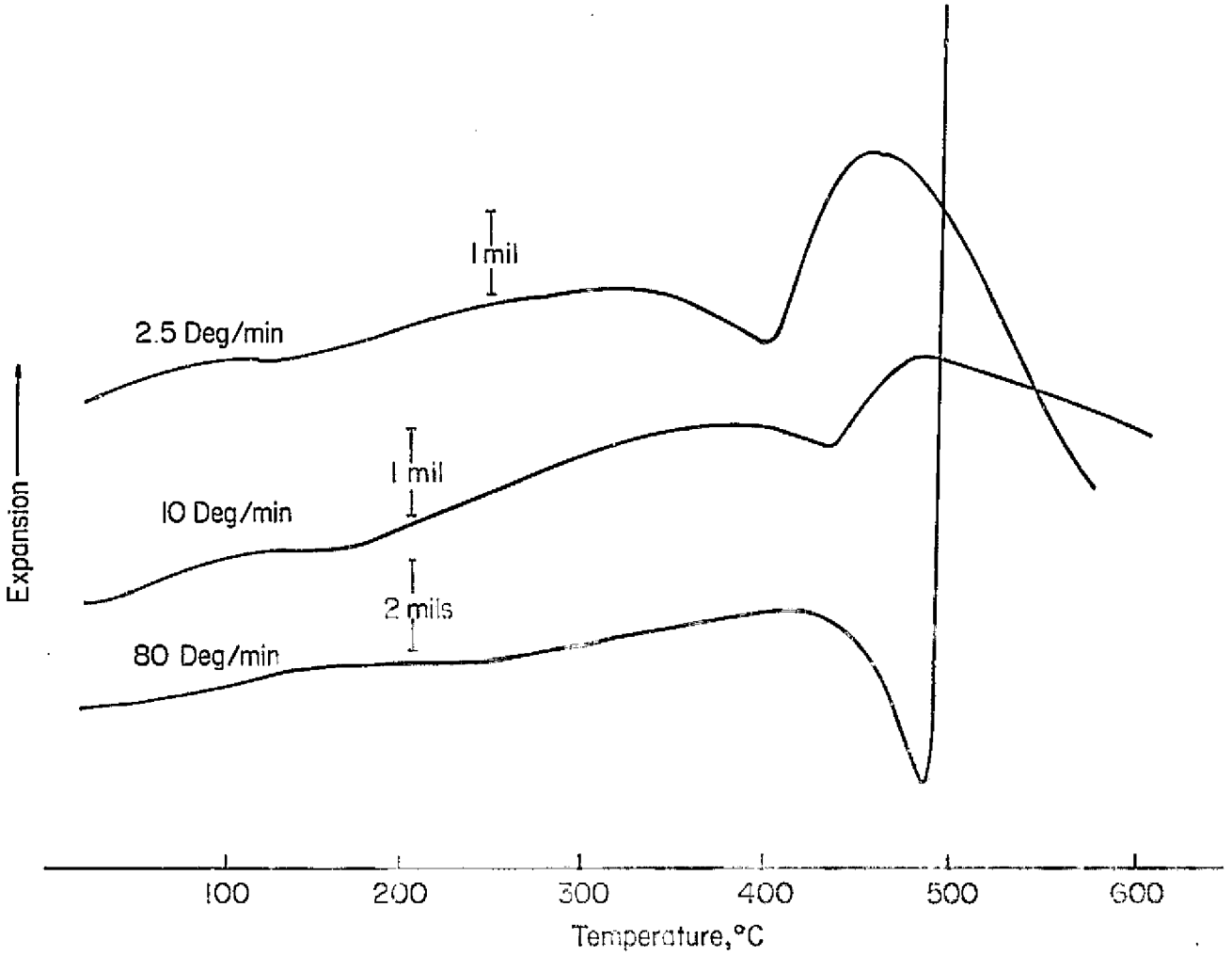

Figure 3.5-4 Thermomechanical (Dilatometric) Curves for Elkhorn #1 Seam Coal at Three Heating Rates

erature) of a coal which shows this shrinkage very clearly. For these curves the initial softening temperature marks the onset of compression. The initial swelling temperature in this case, is also the maximum compression temperature.

Coals in the present study were examined by warming to 330°C, holding at this temperature for 10 min., to permit release of moisture and light volatiles, then heating at a rate of 3.0°C/min. This temperature profile is identical with that of the ASTM Gieseler procedure, with which the data may be compared. The results of these runs are shown in Table 3.5-3.

All coals in this study except Amax give well-defined expansions in the 400-500°C range. Based upon replicate runs it is apparent that the characteristic temperatures obtained by this method are fairly well defined and reproducible within ± 5°C. The expansion itself, however, is erratic and, for highly expanding coals, appears to be of very limited value.

Extrudate 1A is seen to behave similarly to its parent coal. This was also found to be the case with respect to plastometric behavior.

When Kentucky #11 is examined at a 10°C/min ramp, the initial swelling temperature is 404° ± 4 (up about 10°C), the maximum expansion temperature is 475° ± 5 (up by 15-20°), and the expansion itself is 45-50 mils, sharply up, when compared with the 3°/min data of Table 3.5-3.

When Elkhorn #1 is examined at a 10°/min ramp and at a 80°/min ramp, the initial swelling temperatures are 400° ± 7 and 447° ± 6, respectively; the maximum compression temperature is increased from 402° to 435° ± 2 and 496° ± 2, respectively; and the maximum expansion temperature is increased from 465° to 475° ± ? and >520°, respectively. This coal, with its low volatile matter content, is low swelling at 3°C/min, but is high swelling (expansion >90 mils and off-scale) at 80°C/min.

The source of the large uncertainty/error in measuring maximum expansion is, we believe, associated with the lack of a highly uniform

Table 3.5-3

THERMOMECHANICAL (DILATOMETRIC) BEHAVIOR OF SEVERAL COALS*

Coal Seam	Initial Softening Temp, C	Initial Swelling Temp, C[3]	Maximum Expansion Temp, C	Expansion at Maximum, mils	Degrees of Freedom
Pittsburgh #8	ND	410° ± 8	466° ± 1	ca 16.	2
Ohio #9	361° ± 3	393° ± 4	468° ± 4	4.6 ± 1.0	5
Lower Kittanning	395°	430°	485°	3.3	0
Kentucky #11	ND	393° ± 3	458° ± 5	15. ± 10.	3
Pocahontas #3	407°	468°	495°,510°	0.5	0
Amax	[1]	[1]	[1]	[1]	
Elkhorn #1[2]	398°	402°	465°	1.6	0
Extrudate 1A from Pittsburgh #8	ND	413°	472°	10.	0

* Using thermomechanical module of DuPont Instrument Products Divn. Model 990 Thermal Analysis System. Coals (100 mg samples) are heated rapidly to 330°C, held isothermally for 10 min, then warmed at 3.0°C per min.

[1] Amax coal exhibits no thermal expansion under these conditions.

[2] Warmed from ambient temperature at 2.5°C/min.

[3] Where initial softening is evident, this is also the maximum compression temperature.

means of packing the coal into the quartz cell used in this apparatus. Several experimental runs were made with Kentucky #11 coal samples which had been pelletized using a Parr pellet press. These pellets are slightly smaller than the internal diameter of the quartz cell. Data with pelletized coals were still less reproducible, with standard deviations of temperature of ± 20°C.

van Krevelen (20) has reported that the maximum expansion temperature for a given coal exhibiting plastic and dilation properties will occur at essentially the temperature of maximum fluidity as determined by Gieseler plastometry. This is easily checked for the present study by comparing the data of Tables 3.3-2 and 3.5-3. Our data do not conform to this generalization. For all coals in this study (and for extrudate 1A too) the maximum expansion temperature at 3°C/min occurs well beyond the temperature of maximum fluidity. The temperature spreads are considerably greater than the analytical precisions (ΔT is 26°,.s.d. ± 9° for the set of Ohio #9, Lower Kittanning, Kentucky #11, Elkhorn #1, and extrudate 1A, for which well-defined maxima are available by both methods).

Additional thermal data has been sought by differential scanning calorimetry (DSC), using a Perkin-Elmer DSC-2 instrument. In this technique a coal sample in a stainless steel holder is heated along with an inert reference sample (in this case, alumina in a similar stainless steel holder); the instrument circuitry is designed to maintain the sample and reference holders at identical temperatures throughout the heating ramp by supplying small electric currents as required to maintain thermal balance. When a transition occurs in the sample, the power required to maintain thermal parity between sample and reference holders is a direct measure of the heat of transition. Endothermic transitions and increases in C_p are shown as upward departures from the baseline in strip chart output; exothermic reactions and decreases in C_p appear as downward departures.

This method is especially attractive in principle, in that it provides a direct measurement of enthalpy change, ΔH. When applied to the thermal reactions of coal under inert gas, even a systematic and careful worker finds it difficult to obtain meaningful information. (21)

In the present study stainless steel pans (Perkin-Elmer high volume) with loosely fitting lids were used. Oxidation was prevented by maintaining a dry nitrogen purge over the cell compartment. The loose-fitting pan lid provides a second insurance barrier against adventitious oxygen, as the sample is heated in the atmosphere of its own vapors.

The general forms of DSC curves generated are illustrated in Figure 3.5-5. All three curves are of Pittsburgh #8 seam coal, at different heating rates. The actual temperatures at various points along each curve are shown. Several generalizations may be made:

(1) Most dramatically, at some temperature (about 470°C for the slowest heating rate, and about 555°C for the highest) there is a precipitous swing offscale in an "exothermic" direction.

(2) Up until this very large swing, at moderate ramps (curves a and b) the most striking feature may be that there are no pronounced thermal occurrences, even in this highly plastic coal which we know undergoes major physical transformations in the 390-490° region (cf. for example Table 3.3-1).

(3) Recognizing the basic ambiguity of any DSC curve which lacks a well-defined baseline, we believe that these curves reveal two endothermic regions: one which may associate with the softening or melting process (390-450° in curve a, 415-475° in curve b, 420-490° in curve c), and a second region which in each case occurs just prior to the offscale "exothermic" swing.

Some interpretational problems are discussed in section 4. Notwithstanding these questions, we have subjected all coals in the study to DSC thermograms, with the aim of measuring and recording the enthalpic character of these curves. Obtenance of reproducible numeric data has proven to be an intractable problem. We have concluded that the DSC "exotherm" is a method artifact (section 4.3.1).

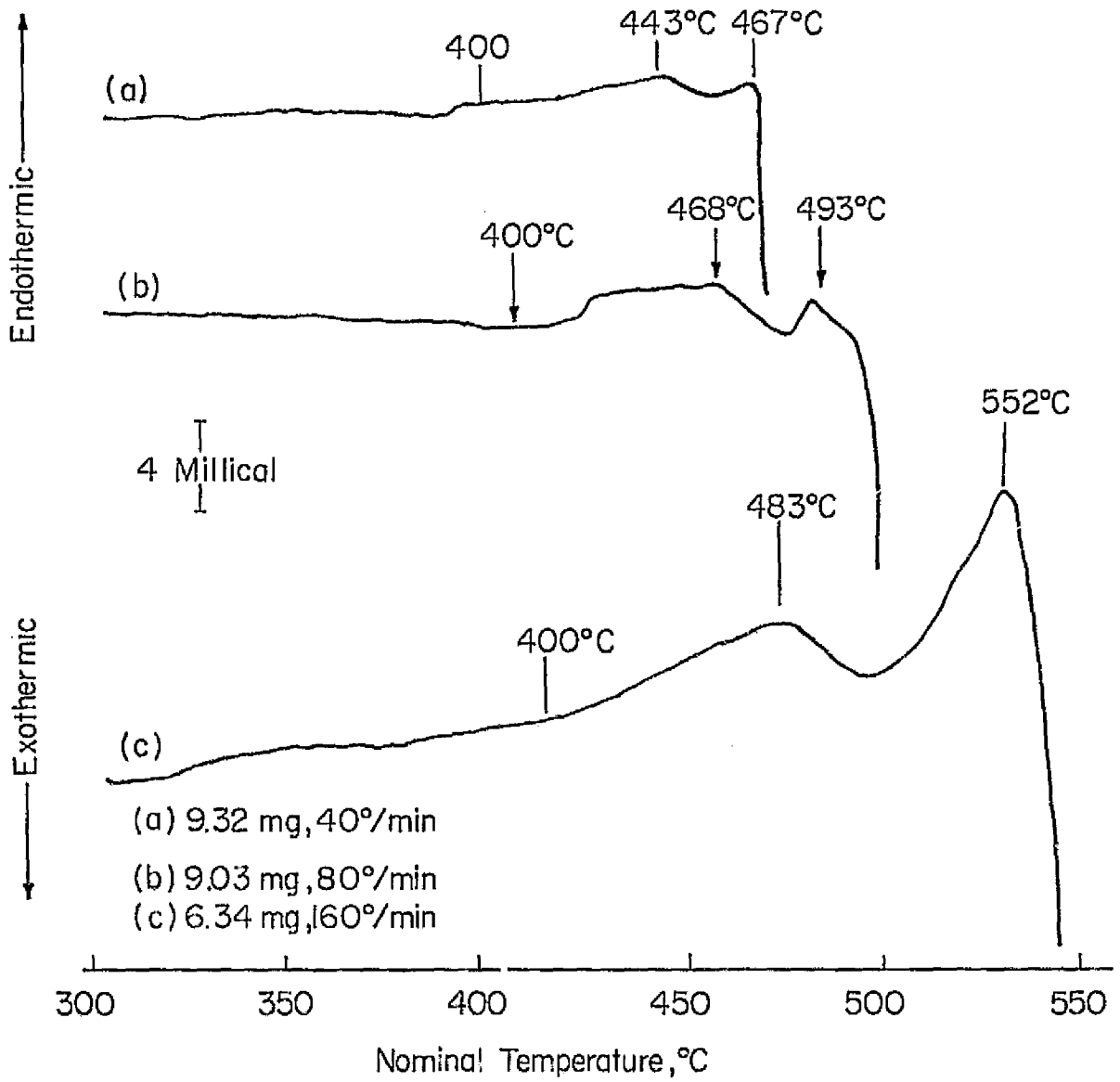

Figure 3.5-5 DSC Curves of Pittsburgh #8 Seam Coal at Three Heating Rates

4. DISCUSSION

4.1 THE ISOTHERMAL PLASTOMETRIC CURVE

Under isothermal conditions the plastometric curve of a plastic coal is characterized by an initially accelerating region of increasing fluidity, a well defined point of maximum fluidity, and finally a region of smoothly decreasing fluidity (the coking region), ending with complete resolidification in the 450-500°C region. A typical curve is shown in Figure 3.3-3.

When log(fluidity) is plotted against time, the early "softening" region is approximately linear (i.e., fluidity is increasing exponentially with time). Later the coking region is clearly linear on this semilogarithmic plot, as Fitzgerald has noted.(10.11) This first-order coking behavior has been explained in terms of a simple set of consecutive first-order reactions: (10-13)

$$C \rightarrow M \qquad k_i \quad \text{(first-order melting)}$$

$$M \rightarrow S \qquad k_c \quad \text{(first-order coking)}$$

Here C, M and S signify the meltable portion of the original coal, the fraction melted, and the fraction resolidified, respectively. The melted fraction is thus predicted to rise to a maximum value, then to decrease with further time, in accordance with the rate law:

$$d[M]/dt = k_i[C] - k_c[M] \qquad (1)$$

This kinetic analysis has been often quoted; however, it fails materially to predict plastometric curves of the type actually observed. Thus, for example, Equation 1 predicts that for all values of k_i and k_c the melting process must be progressively decelerating, while both past (10-13) and present data show the melting process to have an important autoaccelerating region.

We are not prepared to propose an mechanistic model for the softening/coking phenomenon. It may be useful, however, to introduce an assumption which permits a better mathematical modelling of the isothermal plastometric curve. The limits of an assumption of this type have been noted by Osiander: (22) "..These causes are not advanced in order to convince anyone that they are true but only in order that they may posit a correct basis for calculation."

The trial assumption we will make is that, in the presence of some amount of molten phase, a second-order melting process also occurs, the rate of which is dependent upon the concentration of molten phase as well as upon the concentration of the meltable fraction:

$$C + M \rightarrow 2\,M \qquad k_m \text{ (second-order melting)}$$

The rate law now acquires a third term:

$$d[M]/dt = k_i[C] + k_m[C]\cdot[M] - k_c[M] \qquad (2)$$

The virtue of Equation 2 is that, for most isothermal plastometric runs, it provides a framework for a fairly good fit to the raw isothermal data. In Figure 3.3-3 the solid circles show the curve generated by this equation; the open circles show the actual raw data. Even curves obtained with coals which are too fluid to permit the measurement of maximum fluidity may be fitted to this equation. Figure 4.1-1 shows the fit to the data for the extremely fluid Pittsburgh #8 seam coal at 412°C.

An empirical analysis of the isothermal curves obtained in the present study begins with the determination of the melting and coking slopes and a calculated maximum fluidity based upon the extrapolation of these two slopes to intersection. This has been done by a least-squares program, for which we have made two arbitrary assumptions: only fluidities greater than 1 ddpm are included, and only fluidities less than one fifth the highest observed fluidity are included. The data of Table 4.1-1 have been generated subject to these constraints. All numbers are in min^{-1}.

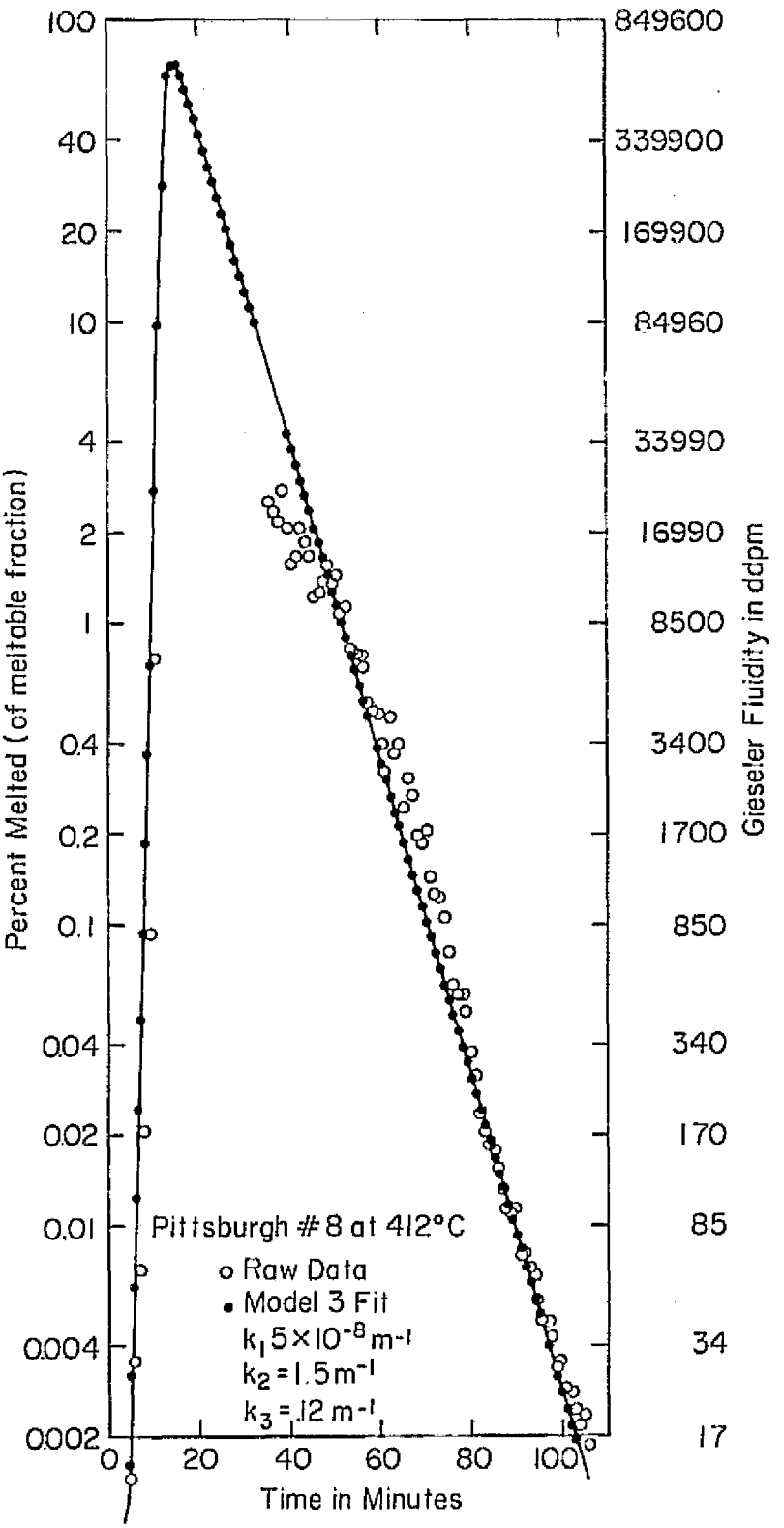

Figure 4.1-1 Approximate Fit to an Isothermal Plastometry Curve

Table 4.1-1

Slope Analysis of Isothermal Gieseler Plastometry Runs

Seam	Temp,°C	melting slope				coking slope				Max Fluidity	$t_{max\ flu}$
		slope	s.d.	int.	s.d.	slope	s.d.	int.	s.d.	(intercept)	
Pittsburgh #8	412°	1.081	0.050	-3.24	.32	-.1294	0030	16.24	.25	1.402 E+6	16.10 min
	426°	1.919	.049	-4.19	.23	-.2133	.0022	15.75	.12	9.407 E+5	9.35
	452°	3.56	.17	-3.39	.37	-.813	.017	18.84	.31	2.43 E+6	5.09
Ohio #9	411°	0.425	.019	-1.69	.14	-.2095	.0067	7.29	.20	75.2	14.16
	426°	0.871	.077	-3.04	.47	-.4452	.0087	11.17	.18	579.	10.80
	541°	3.8_7	[1]	-2.9_2	[1]	1-.455	.134	16.9	1.2	9.507 E+4	3.71
Lower Kittanning	411°	[2]				[2]				[2]	[2]
	425.5°	0.266	.083	-5.98	.34	-.0770[3]	.0034	2.646	.106	8.5[3]	6.54[3]
	450°	0.666	.124	-2.05	.70	-.2361	.0059	7.99	.17	213.	11.13
Kentucky #11	400.0°	0.1745	.0074	-0.682	.085	-.0639	.0027	5.23	.16	38.4	24.82
	410.0°	0.622	0.30	-2.79	.25	-.1504	.0017	9.987	.082	876.	15.37
	425.5°	1.353	.095	-4.91	.64	-.3204	.0062	13.62	.20	2.367 E+4	11.08
	440.0°	1.588	.146	-2.51	.68	-.679	.017	15.93	.31	3.308 E+4	8.13
	449.9°	2.57	.23	-4.76	.84	-1.110	.048	18.39	.63	8.890 E+4	6.30
	460.0°	3.0_3	[1]	-4.2_3	[1]	-1.616	.044	21.55	.48	2.910 E+5	5.55
Pocahontas #3	450.0°	[2]				[2]				[2]	[2]
Amax	450.0°	[2]				[2]				[2]	[2]
Elkhorn #1	410°	[2]				[2]				[2]	[2]
	425°	0.491	.026	-3.36	.20	-.288	.022	7.19	.54	26.8	13.54
	450°	1.505	.186	-6.55	1.04	-.842	.022	14.71	.35	1191.	9.06

[1]Slope estimated from only two data points; DF = 0. [2]Maximum plasticity less than 1 ddpm; no calculations made.

[3]Maximum plasticity less than 10 ddpm; slope and intercept accuracy is poor.

In order to make convenient use of a model, it is necessary to develop a way to apply it to actual data. Some effort in this direction is described in Section 6.4. Several generalizations can be made on the basis of model studies.

(1) The value of k_{coke} cannot be assumed to be equal to the negative of the coking slope. As Figure 4.1-2 shows, that equality is approached only for the limiting case that k_{melt} is substantially greater (about fourfold greater) than k_{coke}. The value of k_{coke} can be estimated from a more complex relationship, as shown in Figure 4.1-3. A quadratic regression analysis of the appendix data yields the empirical relationship:

$$\ln\left[\frac{-k_{coke}}{m_{coke}} - 1\right] = -8.2709 + 24.0332\left[\frac{-m_{coke}}{m_{melt}}\right] - 17.3436\left[\frac{-m_{coke}}{m_{melt}}\right]^2 \quad (3)$$

where m_{melt} and m_{coke} denote the observed slopes, d[ln(ddpm)]/dt, for the melting and coking portions of the curves.

(2) The value of k_{melt} can be roughly estimated by the simple relationship:

$$k_{melt} = m_{melt} + k_{coke} \quad (4)$$

Equation 4 is fairly good when k_{init} is relatively small and when k_{melt} is at least twice as great as k_{coke}. A quadratic regression analysis yields the more general relationship:

$$\left[\frac{k_{melt}}{m_{melt}}\right] = 1.1195 - 0.188\left[\frac{-m_{coke}}{m_{melt}}\right] + 2.9015\left[\frac{-m_{coke}}{m_{melt}}\right]^2 \quad (5)$$

This provides a fairly good fit to the data, as is seen in Figure 4.1-4.

(3) The value of k_{init} can be seen to relate closely to the value of $t_{max\ flu}$ (Table 6.4-5). For example, for the case $k_{melt} = 1.0\ min^{-1}$ and $k_{coke} = 0.4\ min^{-1}$, for $k_{init} = 10^{-8}$, 10^{-7}, 10^{-6} and $10^{-5}\ min^{-1}$, $t_{max\ flu}$ is 29.81, 25.95, 22.06, and 18.14 min (intervals 3.86, 3.89 and 3.92 min). An empirical fit can be made, using the estimates of k_{melt} and k_{coke}:

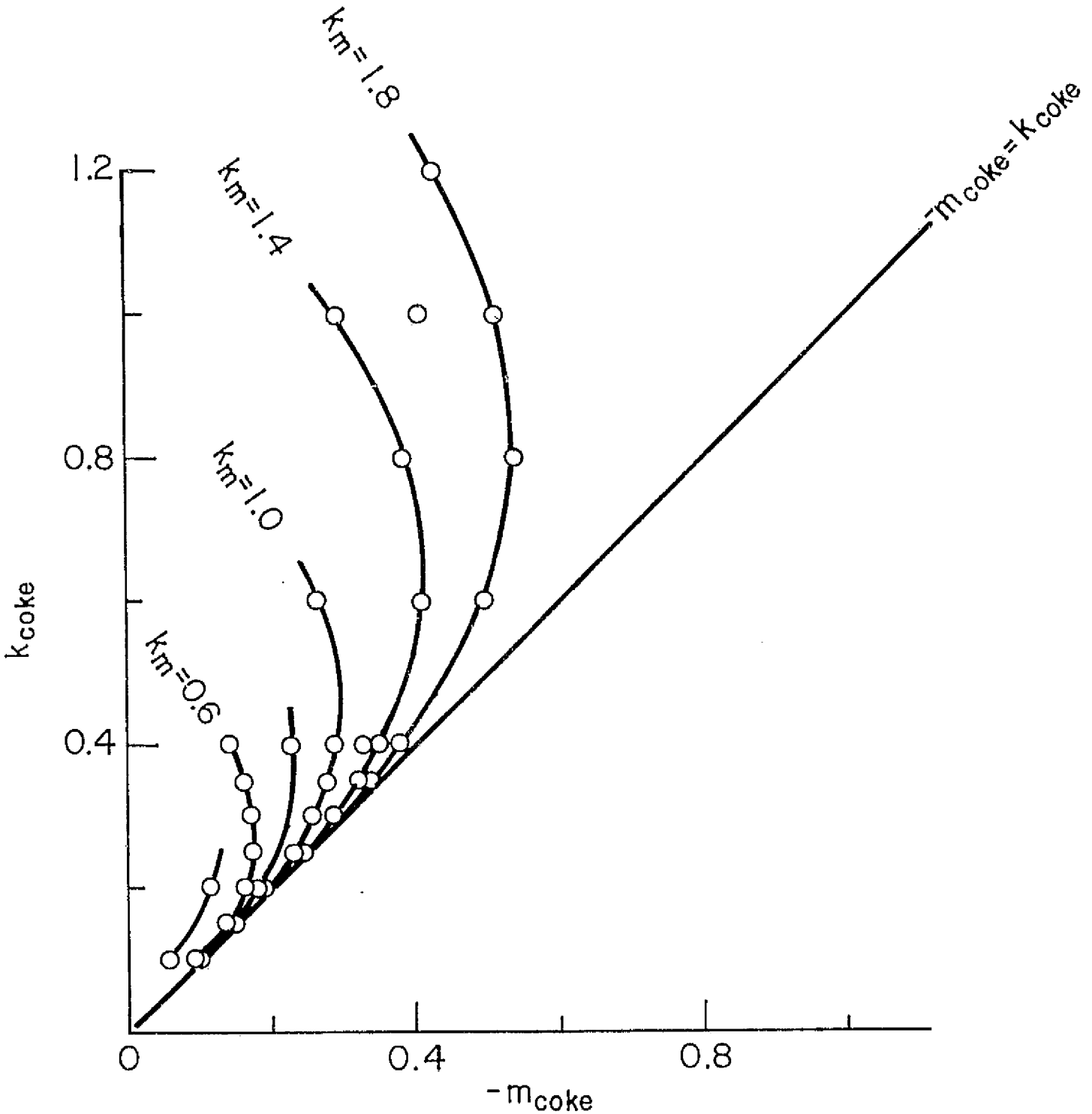

Figure 4.1-2 k_{coke} is Not Identical With $-m_{coke}$

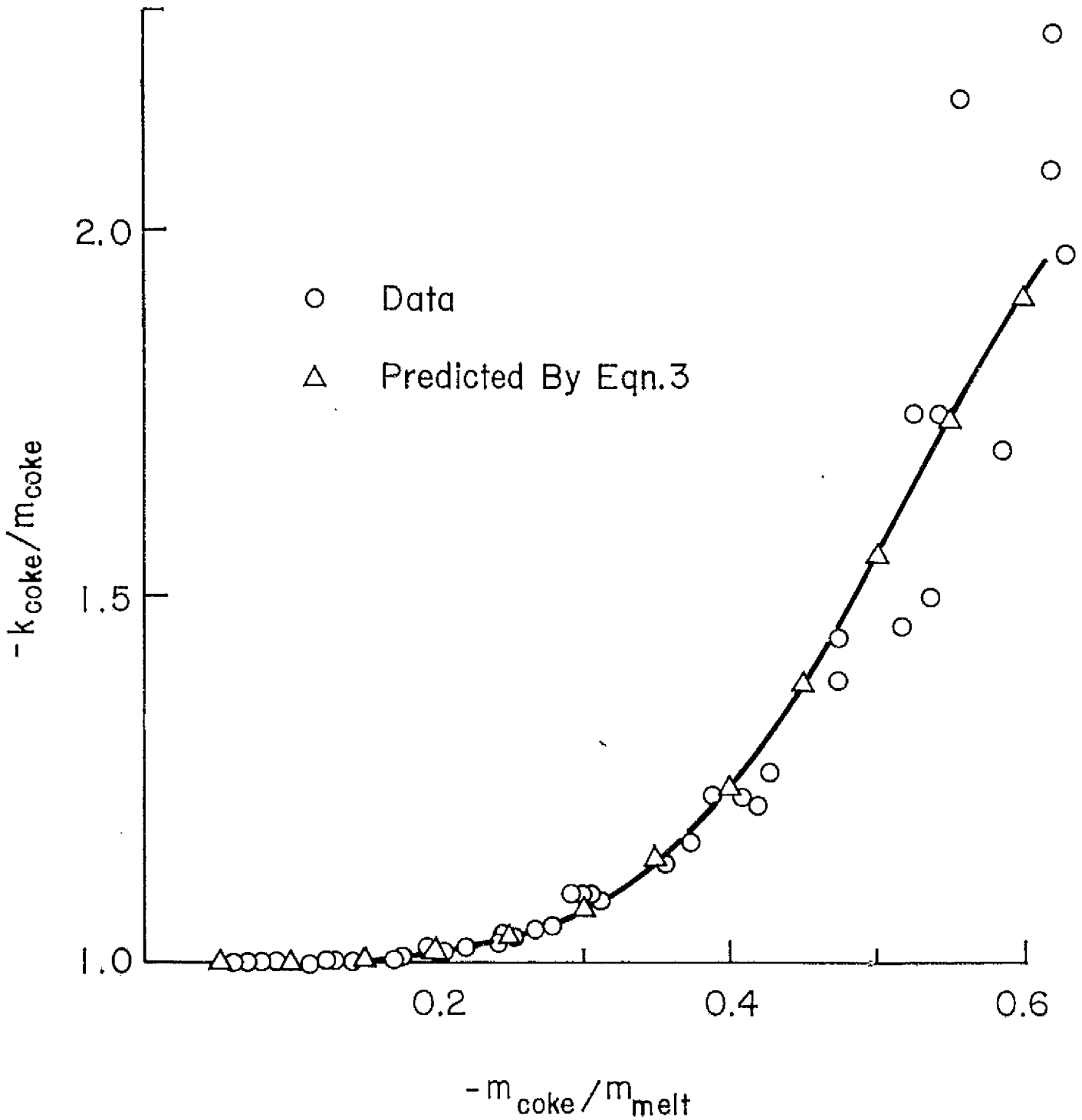

Figure 4.1-3 k_{coke} as Function of m_{coke} and m_{melt}

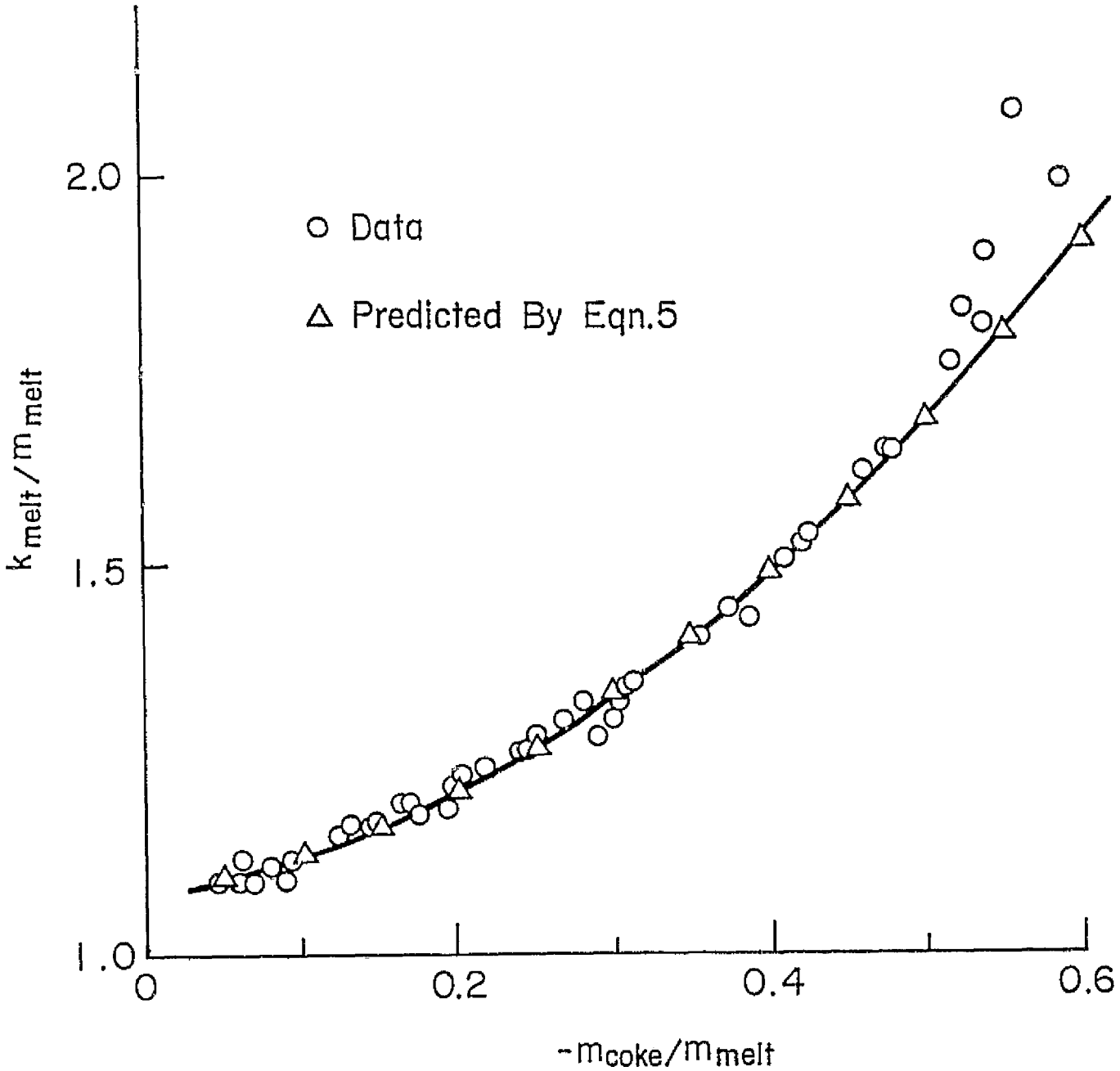

Figure 4.1-4 k_{melt} as a Function of m_{coke} and m_{melt}

$$\ln[k_{init}] = -0.649 - 0.948[t_{max\ flu}\ (k_{melt} - k_{coke})^{+0.93}] \quad (6)$$

The goodness of this fit is indicated in Figure 4.1-5.

Using these empirical equations, rough estimates can be made of k_{melt} and k_{coke}, using the slopes of the experimental curves listed in Table 4.1-1. Resulting estimates are given in Table 4.1-2. It is also possible to estimate values for k_{init}. Such estimates include errors from the estimates of the other k's. For these data k_{init} appears to fall in the range 10^{-7} - 10^{-3} min^{-1}.

For values of k_{init} less than 10^{-4} min, its impact upon k_{melt} is negligible. For this situation the melting and coking constants can be estimated from the melting and coking slopes, and k_{init} can then be estimated from $t_{max\ flu}$.

The data of Table 4.1-2. represent estimates of values of effective rate constants. These values may be expected to exhibit an Arrhenius dependency. Fitzgerald found such a dependency for raw coking slopes. (10,11) Table 4.1-3 shows the activation energy calculations based upon the generalized (Maxwell-Boltzmann, Arrhenius, Andrade) dependency:

$$k = a \exp[-\{\frac{E}{R}\}\{\frac{1}{T}\}] \quad (7)$$

Figures 4.1-6 and 4.1-7 indicate that these estimates of k_{melt} and k_{coke} appear to follow this dependency. The average E_a(coke) in Table 4.1-3 is 48.4 ± 5.7 kcal [202.5 kJ], in excellent agreement with Fitzgerald's estimate of 50 kcal for the coking slopes of a group of British coals. (10)

The present model provides, we believe, the first formulation and estimate of the second-order melting constant, k_{melt}. Values of k_{melt} also tend to follow the temperature dependency of Equation 7 (Figure 4.1-6). The average E_a (melt) from the data of Table 4.1-3 is 41.9 ± 4.5 kcal [175 kJ]. This temperature dependency, unlike that of k_{coke}, may vary significantly from coal to coal. Waters, using early softening data (0.1-1.0 ddpm) for a group of Australian coals, has estimated an 'activation energy of flow' of 73 kcal [305 kJ]. (23).

The substantial differences in the isothermal plastometric behavior of the coals in this study (summarized in Tables 3.3-4 through 3.3-6) may be explained,

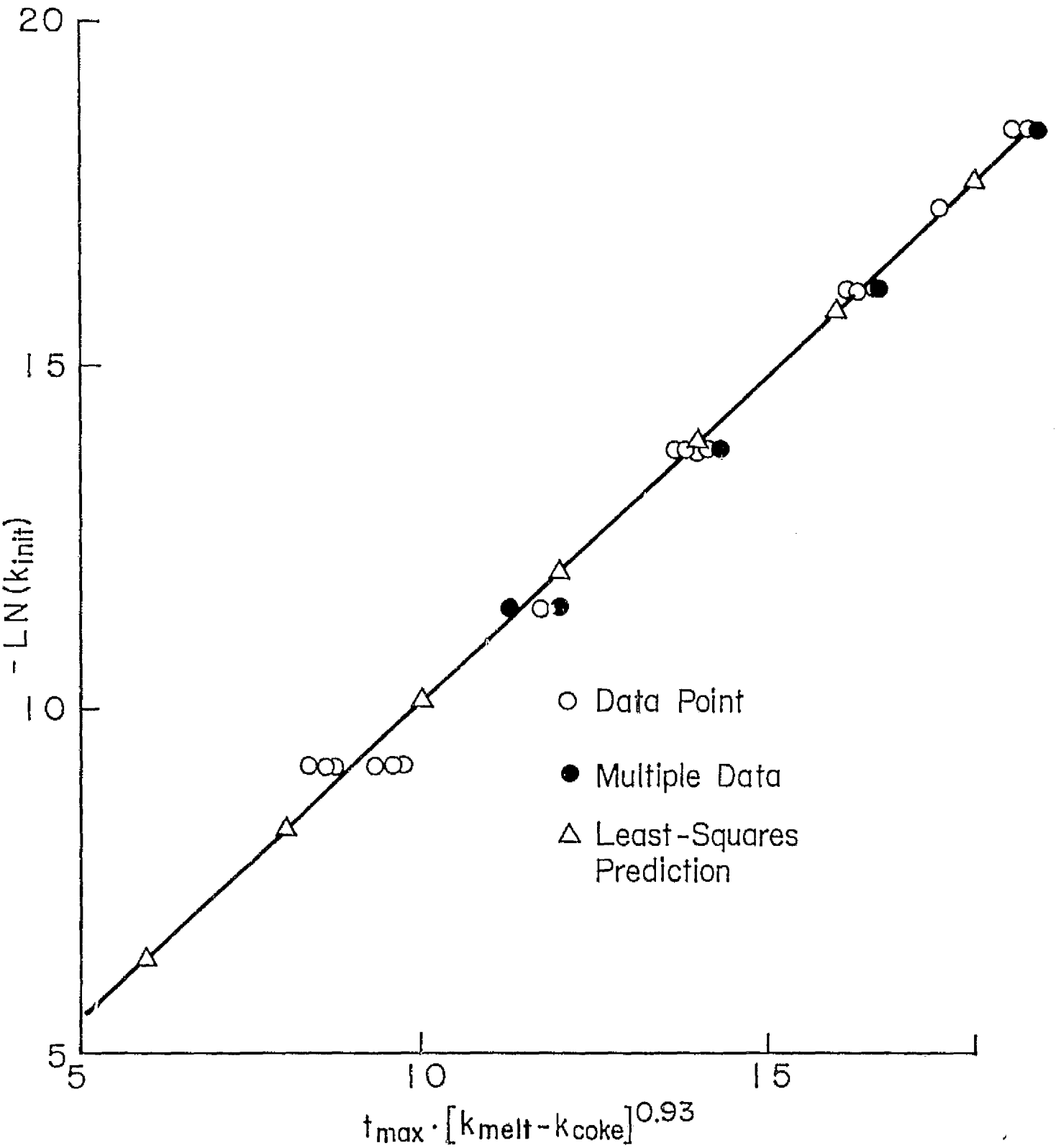

Figure 4.1-5 The Estimation of k_{init}

Table 4.1-2

Estimates of Rate Constants Controlling Plastic Behavior of Coals*

Coal Seam	Temp, °C	k(melt), min^{-1}	k(coke), min^{-1}
Pittsburgh #8	412°	0.94_2	0.13_0
	426°	2.1_8	0.21_4
	452°	4.4	0.83
Ohio #9	411°	0.74	0.32_0
	426°	1.5_5	0.71
	451°	$5._6$	$1._7$
Lower Kittanning	425.5°	0.3_5	0.0_8
	450°	0.9_4	0.2_7
Kentucky #11	400°	0.25_1	0.074_5
	410°	0.77_4	0.15_5
	425.5°	1.6_8	0.33_0
	440°	2.5	0.89
	449.9°	4.1	1.4_7
	460°	$5._6$	$2._7$
Elkhorn #1	425°	0.9_9	0.5_4
	450°	2.9	1.5

---

* calculated from the data of Table 4.1-1, using the derivations of Section 6.3 (Equations 3, 5 and 6).

Table 4.1-3

Estimates of Activation Energies for Melting and Coking Rate Constants*

Coal Seam	Melting					Coking				
	E_a	s.d.	pre-exp	n	DF	E_a	s.d.	pre-exp	n	DF
Pittsburgh #8	36.8	± 7.8	6×10^{11}	3	1	52.	...	6×10^{15}	2	0
						46.5	± 4.8	8×10^{13}	3	1
Ohio #9	50.0	1.3	7×10^{15}	3	1	50.6	...	5×10^{15}	2	0
						40.6	4.2	3×10^{12}	3	1
Lower Kittanning	41.	...	2×10^{12}	2	0	50.	...	3×10^{14}	2	0
Kentucky #11	38.9	2.0	2×10^{12}	5	3	57.9	1.4	5×10^{17}	6	4
Elkhorn #1	43.	...	3×10^{13}	2	0	41.	...	4×10^{12}	2	0

* calculated from the data of Table 4.1-2. Energies in kcal/mole [=0.239kJ/mole]. Pre-exponentials are in min^{-1}.

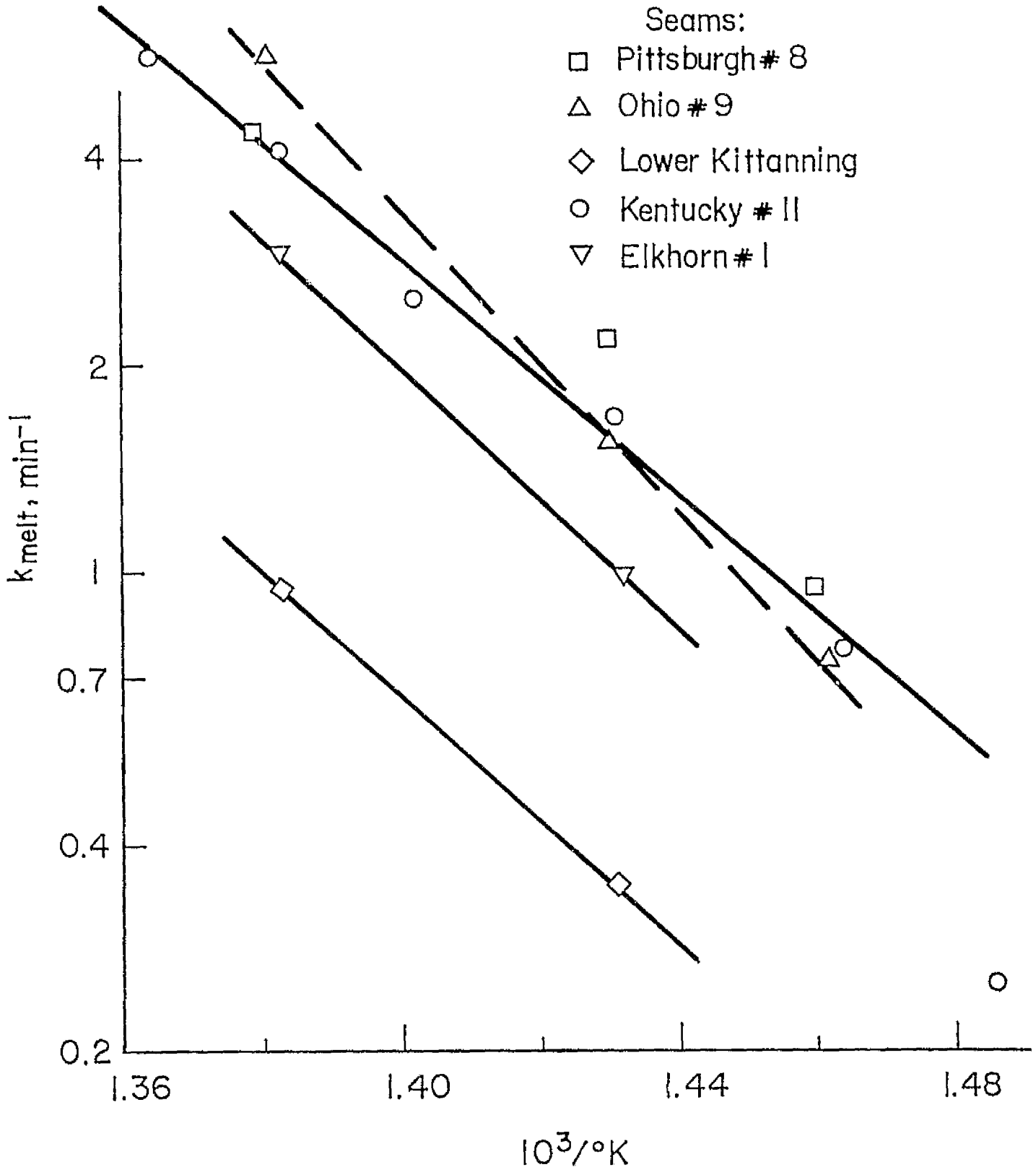

Figure 4.1-6 Arrhenius Plot of Values of k_{melt}

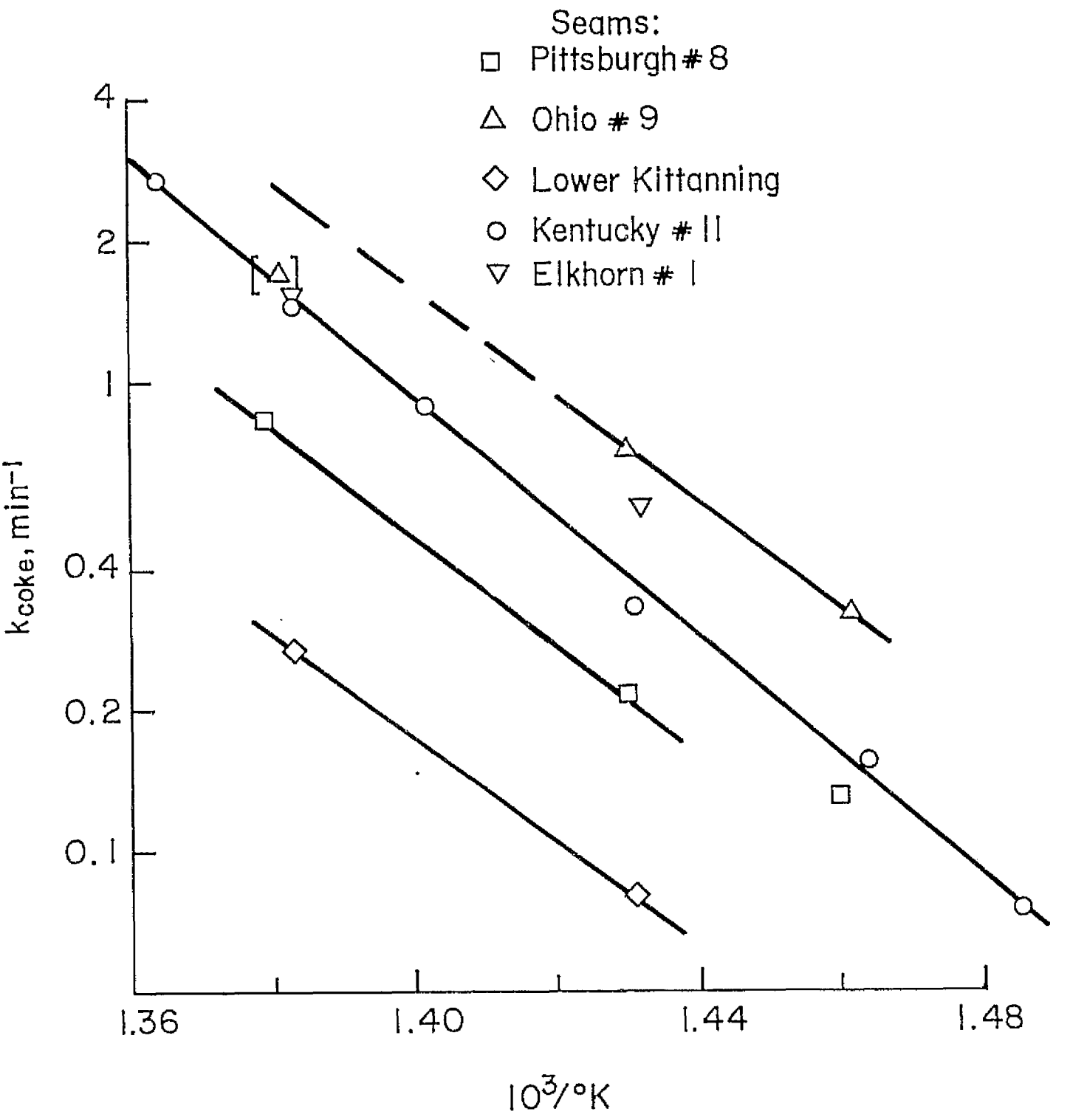

Figure 4.1-7 Arrhenius Plot of Values of k_{coke}

in terms of this model, by comparatively small differences in the values of k_{melt} and k_{coke}. For example, for three coals at 425°C,:

	k_{melt}	k_{coke}
Elkhorn #1	1.0	0.54
Ohio #9	1.6	0.7
Kentucky #11	1.7	0.33

the maximum observed fluidities are 6, 430 and >25,000 ddpm, respectively. Even the extremely fluid Pittsburgh #8 coal has melting constants only slightly higher, and coking constants only moderately lower, than those of Kentucky #11 and Ohio #9 coals.

4.2 Correlations

The major objective of this study has been to contribute to the better understanding of the plastic state of coal, with specific reference to support of the coal pump project at the Jet Propulsion Laboratory. As a first approximation, we assume that Gieseler plasticity is an indicator of pumpability. There is some support for this assumption. Screw extruders can pump fluids with viscosity in excess of 10,000 poise, (24) and have successfully extruded at least four coals with apparent viscosities up to about 100,000 poise.(25) Pocahontas #3 coal, which we estimate (Table 3.3-2) to develop a minimum viscosity of about 7×10^6 poise, jammed the 1.5-inch CPL extruder and showed no flow properties by hot capillary rheometry. (26) A good coking coal affords a viscosity minimum of about 10,000 poise. (12)

Assuming that we can relate pumpability to Gieseler plastometry, it is relevant to summarize the fluidity behavior of the seven coals studied here. This information, along with seam identification and coal rank, is given in Table 4.2-1 In order of decreasing overall plasticity, these coals are: Pittsburgh #8 > Kentucky #11 > Ohio #9 > Lower Kittanning and Elkhorn #1 >> Pocahontas #3 and Amax Wyoming. In terms of coal rank a rough grouping is evident: the high-volatile bituminous A coals (hvAb) are plastic, as is the hvBb coal, but plasticity falls off as rank drops, and also as rank increases above hvAb.

Before a consideration of correlation of plastic behavior with other measurements, some observations can be made about the effect of the hot extrusion process upon the coal material. A priori it might be expected that the hot processing with the attendant loss of organic gases and vapors might result in a significant reduction in rank. This is not found to be the case for the coal extrudates in the present study (cf. Tables 3.1-1 and 3.2-1). The seven extrudates of Pittsburgh #8 seam coal improved their maf fixed carbon contents and substantially maintained their maf calorific value. The same is true of the two extrudates of Kentucky #11 seam coal. The parent Ohio #9 coal is high hvBb; a small improvement in maf heating value attendant upon extrusion raised the apparent rank of the Ohio extrudates from hvBb to hvAb.

Table 4.2-1

Rank and Fluidity Ranges of Seven Coals

Coal Seam and Origin	Rank[1]	Time in Minutes with Apparent Viscosity Less Than:[2] 10^6 poise	10^5 poise	10^4 poise	2500 poise	
Pocahontas #3 (Wyoming Co., WV)	lvb	NA	NA	NA	NA	at 410-2°C
		NA	NA	NA	NA	at 425-7°C
		NA	NA	NA	NA	at 450-2°C
Lower Kittanning (Fayette Co., PA)	mvb	NA	NA	NA	NA	at 410-2°C
		NA	NA	NA	NA	at 425-7°C
		15.6	NA	NA	NA	at 450-2°C
Pittsburgh #8 (from MERC)	hvAb	102.	78.	61.	46.	at 410-2°C
		58.	47.	35.	25.6	at 425-7°C
		18.1	14.7	11.3	8.9	at 450-2°C
Kentucky #11 (Webster Co., KY)	hvAb	35.	16.5	NA	NA	at 410-2°C
		28.3	19.6	11.5	6.2	at 425-7°C
		11.4	8.3	5.4	3.8	at 450-2°C
Elkhorn #1 (Floyd Co., KY)	hvAb	NA	NA	NA	NA	at 410-2°C
		NA	NA	NA	NA	at 425-7°C
		8.6	2.7	NA	NA	at 450-2°C
Ohio #9 (Noble Co., OH)	hvBb	13.2	NA	NA	NA	at 410-2°C
		13.0	5.5	NA	NA	at 425-7°C
		8.4	6.0	4.4	3.3	at 450-2°C
Amax (Gillette Co., WY)	subC	NA	NA	NA	NA	at 410-2°C
		NA	NA	NA	NA	at 425-7°C
		NA	NA	NA	NA	at 450-2°C

[1] rank assigned by volatile matter and calorific value in accordance with ASTM method D 388.

[2] using calibration data of Table 6.3-0 and interpolating data of Tables 6.3-6, 6.3-7 and 6.3-8.

Volatile matter content is decreased by extrusion, but only moderately. The extrudates which we have examined by Gieseler plastometry retain significant plastic behavior, sometimes a high degree of plastic behavior in this test (Tables 3.3-2, 3.3-3). Furthermore, notwithstanding the loss of about 5% gross volatile matter, extrudates are found to have at least as large an extractable fraction as their parent coals, in some instances to have a considerably larger extractable fraction (section 3.4.1). This clearly implies that the network structure, or crosslink density, of the coal itself is significantly modified by the melting/extrusion process, even though the overall petrographic composition is substantially unchanged (section 3.4.4).

In the 1.5-inch extruder, with a residence time in the screw of about one minute, the coal is typically brought from about 200°F (93°C) to about 800°F (427°C) in about 30 sec and is then maintained at this higher temperature for perhaps another 30 sec before being extruded at 800°F or, in some cases, at a higher temperature. Contact time in the die itself is only of the order of two sec, (27) and consequently, at least for die temperatures up to 1200°F (649°C), no substantial changes in extrudate character are observed as a result of die temperature (see Table 3.4-3 and related discussion).

The following subsections address some specific correlations of plastic behavior.

4.2.1 Plasticity and Proximate/Ultimate Analysis

Plastic behavior in coals generally relates to rank, and has been related to such properties as volatile matter (maximum at 25-30%), percent carbon (maximum near 89%) and percent hydrogen maf (the higher the better). (9, 23, 28, 29)

Wu and Frederic (29) have made a statistical study of the relationship of various other coal properties to Gieseler plastometric measurement. Estimates based upon data from 77 plastic coals indicate the best single linear regression parameter for softening point, maximum fluidity temperature, and resolidification point is maf volatile matter:

$$T_{soft} = 479.96 - 2.9953(VM) \qquad r^2 = .832$$

$$T_{max\ flu} = 511.46 - 1.7817(VM) \qquad r^2 = .908$$

$$T_{resol} = 549.18 - 1.7487(VM) \qquad r^2 = .856$$

Higher correlation coefficients (0.90 and better) are obtained by using multiple linear regression on two independent variables, such as volatile matter and calorific value. (29) No good predictors were found for maximum fluidity: the best single-parameter fit was with maf percent hydrogen, but this yielded a correlation coefficient of only 0.33.

The above equations can be applied to predict the data in Table 3.3-2 from the data in Tables 3.1-1 and 3.1-2. The results indicate an underestimation of the initial softening temperature averaging more than 40°C. This almost certainly reflects a method difference, since ASTM methods D1812 and D2639 define this temperature as that at which a fluidity of 1.0 ddpm (3.6°/min in European notation) is attained, while Bureau of Mines practice (30) has been to take $T_{init\ soft}$ as the point at which a fluidity of 0.1 ddpm (0.36°/min) is attained. The predicted maximum fluidity temperature and the predicted resolidification temperature have standard errors of ± 6.8° (6 DF) and ± 7.5° (7 DF), respectively, reasonably close considering the differences in coal-handling and plastometry-measuring procedures between our laboratories.

From the small set of seven coals in this study, the following rough indicators may be seen from the ultimate analysis data. (1) The four coals with maf % carbon between 79% and 85% (Pittsburgh #8, Elkhorn #1, Kentucky #11 and Ohio #9) are all moderately plastic to highly plastic, while the three falling outside this range show little or no plastic behavior. (2) The four coals with maf % hydrogen 5.3% and 5.5% (the same four) are moderately to highly plastic, while the other three show less than 5% hydrogen. (3) The four coals with maf carbon/hydrogen ratios of 15.0-15.5 (the same four) are moderately to highly plastic, while the others, with higher C/H ratios, show little plasticity. These three parameters have also been noted by Wu and Frederic. (29) None of these parameters appears to have very fine prediction power; for example, none discriminates between Elkhorn (slightly plastic) and Pittsburgh (highly plastic).

4.2.2 Plasticity and Mineral Composition

One possible view of the mechanism of coal plasticization is that of mineral-catalyzed "depolymerization"such as the retro-Diels-Alder reaction. If this view has validity, it would be expected that the plastic behavior of any set of coals would show a systematic relationship with mineral compositional analysis such as that of Table 3.2-3.

The alumina contents of the high temperature ashes of the three most plastic coals are all within the range 19-23%; those of the sparingly plastic Elkhorn and Lower Kittanning are 26-29%, and these of the nonplastic coals are higher (32%) or lower (16%).

The iron oxide (Fe_2O_3) contents of the ashes of the three most plastic coals are in the range 16-20.5%; those of the sparingly plastic Elkhorn and Lower Kittanning are in the range 8-12%, and those of the nonplastic coals are 5% and 3%.

The iron oxide/aluminum oxide ratio, as expected in light of the above rankings, is another good indicator, with values for the three most plastic coals 0.7-1.0, for the two sparingly plastic coals 0.3-0.4, and for the two nonplastic coals 0.1-0.3. The use of this ratio is of practical importance for another reason: the ratio can be estimated, comparatively, by x-ray fluorescence analysis of whole coals; and hence it can be determined for any given coal in a matter of minutes, without ashing, ash dissolution, and the rigorous standardization required for quantitative atomic absorption analysis.

The application of XRF signal ratios can be seen with reference to the data of Table 3.2-1. The Fe/Al XRF ratios are numerically quite different from those calculated from atomic absorption data: the fluorescent efficiency of Fe is much greater than that of Al under these conditions; the measurements are upon whole coal rather than ash; and no matrix or interelement corrections are made. The rankings, however, are similar: the three most plastic coals show intensity ratios greater than 125; the two sparingly plastic coals have ratios of 107 and 73; and the nonplastic Pocahontas #3 has a ratio of 46. This test does not do as well for the one subbituminous coal in the group: Amax

has an intensity ratio of 99, implying more plasticity than that coal has.

The possibility of predicting plasticities by such a rapid nondestructive test warrants further investigation. We have conducted a single experiment which has failed to support the hypothesis of mineral-catalyzed plasticization. A five-g sample of Pocahontas #3 coal was mixed with the low-temperature ash obtained by plasma-ashing five g of the highly plastic Pittsburgh #8 coal. This mixture was subjected to a Gieseler run, and showed only slight plasticity, consistent with that of the Pocahontas coal. This test could have failed for various reasons, such as inadequate mixing, mineralogical conversions during ashing, and the like. Its failure, however, serves as a cautionary flag with regard to the use of mineralogical analysis as a predictor of coal plasticity.

4.2.3 Plasticity and Thermal Analysis

Our thermogravimetric data, obtained at 40-160°C/min, indicate that the weight loss - temperature curves, after correction for instrumental thermal lag (important at the higher heating ramps), are substantially ramp-independent. Brown(31) has made a similar observation in his study of Australian coals. It is convenient to make uncorrected TGA plots, as in Figure 3.5-1. However, it would be mistaken to conclude that volatilization is suppressed or delayed at high heating rates. In fact, Brown has suggested that the maximum rate of weight loss per degree be considered as a standard parameter to characterize a coal, since it is so independent of heating rate. This maximum weight loss occurs close to the resolidification temperature, i.e., well beyond the maximum fluidity temperature.(31)

The TGA data of Tables 3.5-1 and 3.5-2 can be used as rough predictors of fluidity. For example, the weight loss data at 500°C and 80°/min can be grouped as follows: those coals undergoing 8-13% weight loss are the three highly plastic coals; those undergoint 4-6% loss are the two slightly plastic coals; while the two nonplastic coals are well outside of these ranges (Amax at 1% and Pocahontas at 1.4%). For another example, the temperatures at which 10% weight loss is obtained at 80°/min can be used: for the three most plastic coals this temperature is in the range 489-509°C; for the two moderately plastic coals 519-541°C, and again the two nonplastic coals fall well outside of these ranges (Amax at 459°C and Pocahontas #3 at 628°C).

The dilatation data (Table 3.5-3) appear to be less useful as predictors. The best dilatation measure seems to be that which is least accurately obtained, namely, maximum expansion. The maximum expansion temperature, according to van Krevelen,(17) is expected to coincide with the maximum fluidity temperature by Gieseler plastometry. As we have noted, our data indicate the maximum expansion temperature to occur typically 20-30°C above the maximum fluidity temperature. Brown(31) has observed that the maximum weight loss occurs on an average 24° above the maximum fluidity. Our data and Brown's suggest the generalization that T(maximum weight loss rate) and T(maximum expansion) occur at approximately the same point, and that this point is close to T(resolidification).

Using the maximum expansion data of Table 3.5-3, the three highly plastic coals yield the largest expansions (ca. 5 to ca. 16 mils), the two moderately plastic coals yield smaller expansions (ca. 1.5 to ca. 3 mils), and the substantially nonplastic coals yield 0.5 and 0.0 mils. This is a good ordering of these seven coals. However, TGA data are equally good predictors and are easier to obtain and more reproducible.

Differential scanning calorimetry (DSC) presents some special problems which are considered in a subsequent section. In general, the heat capacities of coals increase fairly steadily through the plastic range, from about 0.3 cal/g-°C at 300°F (149°C) to about 0.7 cal/g-°C at 1000°F (538°C). (24) This conforms well with other recent estimates, e.g., of a group of Russian coals with effective C_p's of about 0.35 cal/g-°C at 300°C, all increasing smoothly to about 0.65-0.75 cal/g-°C at 600°C,(32) and a study of a Synthane process char from an Illinois #6 seam showing C_p to increase from 0.50 cal/g-°C at 327°C to 0.58 cal/g-°C at 527°C. (33) In all cases the observed C_p, whether or not corrected for volatilization, shows a fairly smooth increase over the coking range. The baseline DSC curve, when referenced against a material of substantially constant C_p, therefore will be a smooth concave-upwards curve, i.e., showing a steady endothermic drift.

There is abundant evidence, from earlier DSC data obtained by JPL, (24) from Gold's study, (21) and from our own data (e.g., Figure 3.5-5) that DSC runs of bituminous coals commonly produce apparent exotherms of some magnitude, typically in the 450-500°C range. However, several other careful studies using different instrumentation have failed to detect any exotherm below 600°C. Furthermore we are hard pressed to imagine a chemical/physical event productive of a sizeable exotherm in the 450-500°C range which is consistent with what we think we know about the structure and composition of coals. The possibility must be considered, therefore, that this exotherm is a method artifact. This problem is considered in more detail in section 4.3.1. At this point DSC data provide no basis for the prediction of plastic properties.

4.2.4 Plasticity and Microstructure

The correlation of plastic behavior with extractable fraction has been considered by Berkowitz,(34) but has not been considered to be of general significance.(9) Our data, based upon soxhlet extraction with dimethyl formamide at atmospheric reflux, appear to have good predictive character for the small set of coals examined in this study. Extractable fractions range from 0.0% (Pocahontas #3) to 45% (extrudate 1A from Pittsburgh #8), with a duplicate precision of ± 1.0%. Excluding Amax and considering the six bituminous coals, the three most plastic coals show 19-30% extractables; the two slightly plastic coals show 1-15% extractables, and the nonplastic Pocahontas shows 0.0%. Furthermore, extraction correctly orders the three most plastic coals as Pittsburgh #8 > Kentucky #11 > Ohio #9.

The DMF extraction data also show their predictive utility with regard to the extrudates tested. Only the Ohio #9 extrudate, with 15% extractables, fails to show a value predictive of good plastometry, and that is the only extrudate in this study to give poor plastometric data. Again, in Table 3.4-3 the 900°F die extrudate has an anomalously low extractable fraction; sample size has not permitted a plastometric analysis of this extrudate, but on the basis of the anomalously low volatile matter this sample is probably only slightly plastic.

Surface area measurements are informative with regard to the effects of extrusion and extraction, but are not useful predictors of plastic properties.

Petrographic analysis yields both reflectance and maceral compositional information which are commonly used for rank characterization. Based upon the data of this small group of coals, petrography may also provide useful predictions concerning plasticity. The three most plastic coals contain 70-76% vitrinoids; the two slightly plastic coals fall outside of this range (67% and 79%), and Pocahontas #3 falls still lower (65%). The vitrinoid contents of extrudates 1A and 2A are found in the highly plastic 70-76% range; extrudate 1A is highly plastic, while extrudate 2A is less plastic (Table 3.3-3).

Prediction by the other petrographic data shown in Table 3.4-7 is less satisfactory. The slightly plastic Elkhorn #1 affords values of reflectance, CBI, Strength Index, and total reactive constituents which are indistinguishable from those of the highly plastic coals.

To summarize, there are a number of measurements which appear to have fair to good predictive value in the rough classification of coals as highly plastic ($\eta < 10^6$ poise at 410°C), slightly plastic ($\eta < 10^6$ poise at 450°C), and nonplastic ($\eta > 10^6$ poise at 450°C). These include mineral analysis data (Fe, Al, Fe/Al), thermal data (thermogravimetric and thermomechanical), DMF extraction data, and vitrinoid content. The use of C/H ratio, Fe/Al fluorescent intensity ratio, TGA curves, or DMF extractables has the general advantage of methods which are reasonably insensitive to sample size and to duplication of instrument geometry among laboratories. Before any of these measurements can be used as predictors it will be necessary to conduct validation tests with a larger group of coals of varying plastic properties.

4.3 Problem Areas

In the course of the present study two problem areas have been identified, the presence of a large although implausible exotherm in the DSC analysis of plastic coals (Figure 3.5-5), and the limitations of variable-shear viscosity measurements of highly non-Newtonian fluids. Some aspects of these problems are noted in the following subsections.

4.3.1 The DSC Exotherm

The major features of a typical fast differential scanning calorimetric (DSC) analysis of a plastic coal are shown schematically in Table 4.3-1. When char is heated through the plastic region of coal (300-500°C) the baseline curve is typically concave-upwards (curve X--X in Table 4.3-1). When a plastic bituminous coal is heated through this temperature range at 40°C/min or faster, the curves are difficult to reproduce and more difficult to explain.

These curves are dominated by two features. The first of these, found usually in the 250-450°C region, is endothermic, typically with two identifiable peak regions,(24) the later endotherm often peaking just prior to its termination. This region of the DSC curve is reasonable, if for no other reason than the melting and vaporization processes known to occur. The second major feature is the challenge: a sharp, highly variable (21, 34) but generally substantial exotherm, which characteristically tends to return close to the original baseline. This is shown schematically as curve Y--Y in Table 4.3-1, and is illustrated by the curves in Figure 4.3-1, taken from recent work in other laboratories.(21,34)

Table 4.3-1 lists the possible processes which may be conceived to account for this characteristic curve. The endothermic portion can be explained in terms of processes A-1 and A-5; the concave-upwards shape of the baseline reflects the steady increase of C_p with temperature. (24,32,33) Processes of type A-3 and A-4 are possible but are not necessary to explain these data.

The strong exotherm (region B) must, if it is real, be associated with a specific process. The possibilities are noted below.

Table 4.3-1

Possible Processes Contributing to DSC Thermograms

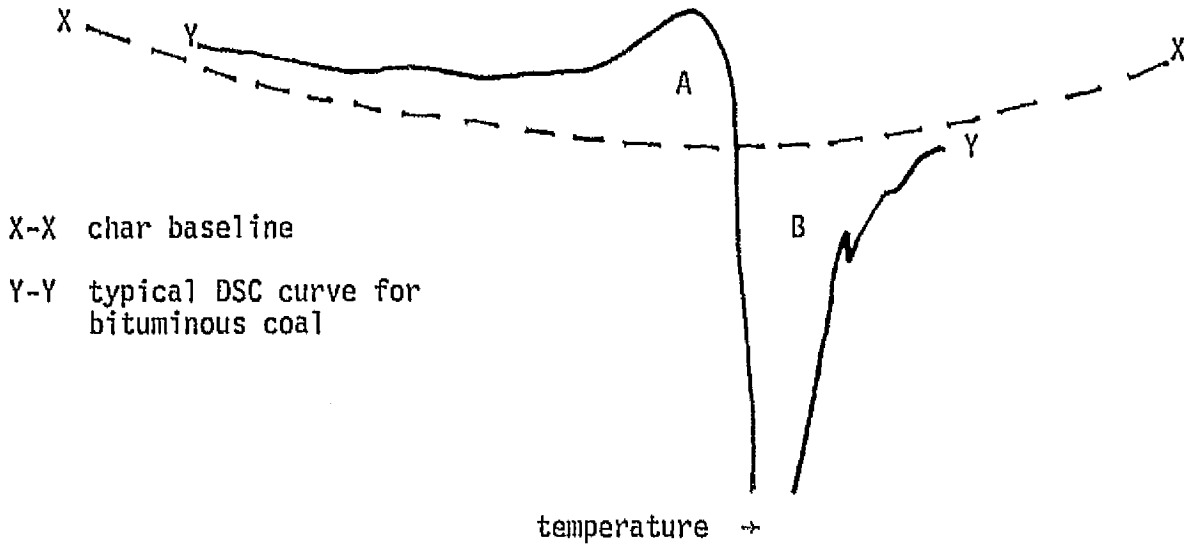

X-X char baseline

Y-Y typical DSC curve for bituminous coal

		reversibility
Endothermic (Region "A"):		
A-1	melting endotherm	partially
A-2	increase in C_p	not reversible
A-3	irreversible endothermic decomposition	not reversible
A-4	reversible endothermic reaction	reversible
A-5	vaporization endotherm	not reversible here
Exothermic (Region "B"):		
B-1	solidification exotherm	cf. A-1
B-2	decrease in C_p	opposite of A-2
B-3	irreversible exothermic decomposition	not reversible
B-4	coking by reverse of step A-4	not reversible

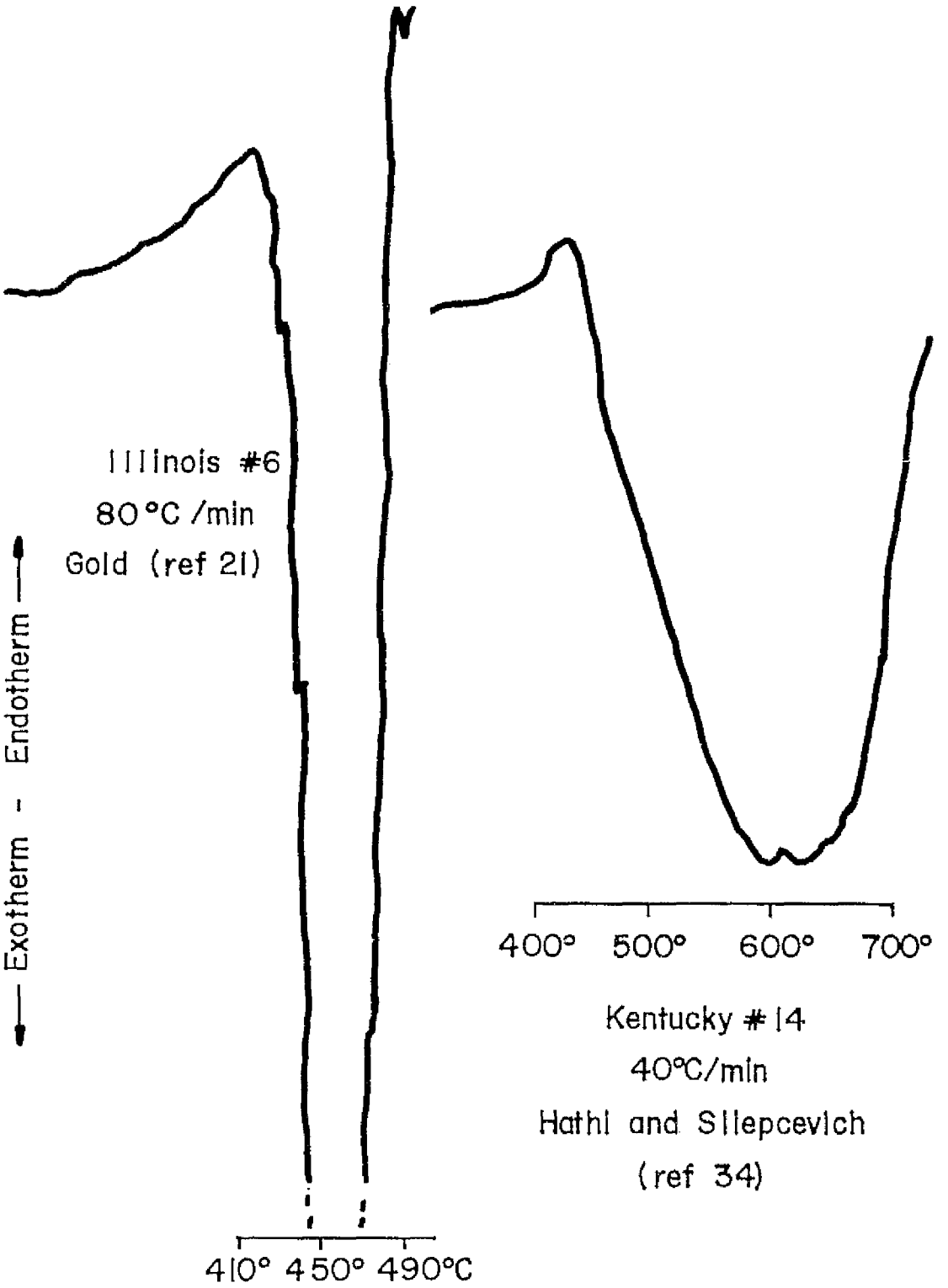

Figure 4.3-1 Typical Exothermic Signals In the DSC Analysis of Coking Coals

The resolidification (coking) process may be sensibly exothermic. This is not likely to be large for a noncrystalline solid, however; heats of fusion for compounds which do not form ordered or crystalline solids are less than 5 cal/g. Process B-1 is not important here.

A decrease in C_p would result in a downward drift, though not a downward sweep of the curve. As noted above, however, there is good evidence from several sources that C_p undergoes a steady increase with temperature in this region. Process B-2 does not occur here.

The possibility of an abrupt irreversible exothermic decomposition (process B-3) has been suggested by others and must be considered on the face of the experimental curves. This hypothesis faces at least three problems, however. First, given such a substantial exothermic reaction (such as might be caused by oxidation with adventitious oxygen), the ultimate return of the curve to the original baseline is an unlikely coincidence. Second, there are few covalent bond systems which decompose thermally with large exotherms; and these structures (peroxy, azine, nitroso- and nitro-organics) seem most unlikely to be encountered in a coking coal. Third, a substantial exotherm in a coking coal requires that the resulting coke have a suitably lower calorific value, if the First Law is to honored. But this is not found with 950°C cokes from coking coals; their values on a maf basis are about the same as those of their parent coals, sometimes slightly higher. Since the hydrogen-rich-volatile matter typically exhibits a higher calorific value than the hydrogen-impoverished coke, the overall enthalpy of the coal-coke-volatile matter system has been increased by the application of external heat. This is consistent with a predominantly endothermic DSC trace; it is inconsistent with a real exotherm which dominates the DSC curve. Process B-3 cannot occur as a dominating thermal event, and may not occur at all.

Process B-4 is coupled with Process A-4. Here a slow, steady endothermic process builds a concentration of high-energy intermediates, which are assumed to be immobilized in the network structure, until some sharply defined event occurs, perhaps a sudden melting which allows these species to react quickly and release their bound energy in one big exotherm. This has the same thermodynamic objection as Process B-3, and the additional aesthetic objection that a fairly detailed hypothetical mechanism has been elaborated solely to account for a single experimental observation. If Process B-3 or B-4 occurred as important thermal

events, there would be other evidence, e.g., a visible exotherm in Figure 3.3-1.

Tha above argument leads to the conclusion that the large, poorly reproducible exotherm, which has been observed in DSC studies in at least four different laboratories including our own, has no real existence: it is, somehow, an artifact of the method.

This "exotherm" occurs in DSC runs at medium to high ramp conditions, but not in any DTA runs, not to an extent sufficient to perturb the smooth TGA curves, and not in the dummy Gieseler runs (with embedded thermocouple). Studies directed to the measurement of heat capacity over a broad temperature range show smooth temperature dependencies (32,33) with no perturbations such as would be required if a substantial exotherm occurred.

In reviewing the incidence of the DSC exotherms, the following generalizations appear to hold:

(a) They are highly unreproducible in all laboratories.

(b) They occur at 40°/min and higher ramps, are sharply enhanced by increasing heating ramp, but they are generally not seen at 10°/min or lower ramps.

(c) They occur with coking, plastic coals, but do not occur in non-plastic or sparingly plastic coals.

(d) Mesh size of coal is a critical variable with regard to this exotherm; a coal fraction of fairly coarse mesh (-20 +30) has been found to give a very large exotherm, while finer-mesh portions of the same coal produced smaller exotherms. (21)

(e) Coal sample size in the DSC pan is an astonishingly important variable: 20-mg samples produce more than tenfold the exotherms of 10-mg samples, and at smaller sample sizes the exotherm abruptly vanishes. (21)

These observations suggest a specific method artifact which we believe may be responsible for these large "exotherms". It is suggested that when these coking coals reach the coking portion of their plastic region, and as they undergo their most rapid mass loss, the particles flow sufficiently to adhere to one another and the mass is then 'foamed' into a cellular structure which, in comparison with the unfoamed coal, makes much poorer contact with the DSC pan bottom. The sensor

beneath the pan bottom detects this change as a sudden drop in effective heat capacity: the only heat required to maintain the pan bottom on the temperature ramp is, for practical purposes, that required to keep the pan bottom itself on ramp. This registers as a strong exothermal event. However, this is only a kinetic effect, not a thermodynamic one. The coal mass, most of it, is still there; the only difference is that the fast conductive transfer of heat through the coal sample is now largely replaced by slower convective and radiative transfer. Within a short time, as soon as a new gradient is established between pan bottom and coal mass, the same total system specific heat requires the same number of millicalories as before; so the pen returns from its sharp exothermic excursion to the neighborhood of the baseline.

A consideration of generalizations (a) through (e) above suggests that each of these specific observations is consistent with this method artifact. In order to provide an experimental test of this hypothesis, the following experiment was designed.

A strongly plastic coal (Pittsburgh #8 seam) was mixed in varying proportions (75:25, 50:50, and 25:75) with 950° char derived from this same coal. Portions of these coal/char blends were then subjected to 80°/min open-cup DSC scans, using the same analytical conditions as we and others have employed. The char baseline is known. If the sharp exotherm of the plain coal is a real event, the expectation is that its magnitude will be linearly diluted by the char component. If the sharp exotherm of the plain coal is a method artifact, however, and is reliant upon the coal's undergoing the 'foaming' phenomenon, the char component will reduce or eliminate this phenomenon and will thereby forestall the observed exotherm.

The results of these tests are consistent with the method artifact explanation. With 100% coal, after the two small endotherms a sudden strong exotherm at 500°C takes the recorder pen off scale; there is an irregular return, roughly to the baseline by about 600°C. When a mixture of 75% coal - 25% char is run under identical conditions, the endotherms are slightly attenuated by dilution, and a very slight irregular exotherm is seen in the range 500-550°C; this exotherm is less than one tenth that obtained with 100% coal. When mixtures containing 50% coal - 50% char and 25% coal - 75% char are run under identical conditions, the endotherms are further attenuated by dilution, and there is no trace of exotherm up to the limit of the run (720°C).

4.3.2 Nonideal Fluid Behavior

We have frequently referred to the viscosity of a coal melt as if the property of viscosity were a fundamental characteristic at a certain point in its time-temperature history, that is, as if we were dealing with an ideal Newtonian fluid. This is, of course, not at all the case. There are at least four different kinds of departure from ideality that we can recognize.

(1) Far from being a homogeneous fluid, a coal melt is highly heterogeneous, consisting of a molten or liquid phase, a gas/vapor phase, and a complex solid phase which includes (a) reactive (meltable but not-yet-melted) maceral matter, (b) unreactive (non-meltable) maceral matter, (c) insoluble mineral matter, and (d) coked organic matter. van Krevelen has discussed this multiphase nature of the coal melt. (12,20)

(2) The viscosity of a Newtonian fluid is independent of shear rate. Such a fluid will therefore exhibit the same viscosity characteristics in various processes and in systems with differing geometries. The temperature dependency of a Newtonian fluid has been shown to follow the law: (35)

$$\frac{1}{\eta} = A \cdot \exp(-E/RT) \qquad (8)$$

which permits interpolations and extrapolations from small amounts of data. However, coal melts are not Newtonian: as shear stress (torque) increases linearly, shear rate increases more rapidly. This is pseudoplastic behavior, and is generally characteristic of coal melts.(23,24)

This can be expressed in terms of the effect of shearing rate $\dot{\gamma}$ upon viscosity η:(24)

$$\eta = k\,\dot{\gamma}^{\alpha-1} \qquad (9)$$

where for Newtonian fluids $\alpha = 1$, for common pseudoplastic fluids $\alpha \approx 0.6$, and for dilatant fluids $\alpha > 1.0$. (In this equation k is a proportionality constant.) Since coal melts are non-Newtonian, effective viscosities are dependent upon shear rates. The Gieseler plastometer, like other constant-torque devices for measuring fluidity, operates at variable shear rate, in fact for highly fluid coals operates

at shear rates which vary over about four orders of magnitude. Consequently, the apparent viscosities, deduced from instrument calibration with Newtonian fluids, are likely to be quite different from the effective viscosities. Furthermore, and of particular significance to the transfer of Gieseler plastometric data to screw extrusion problems, the range of Gieseler shear rates is well below the estimated shear rates encountered in the 1.5- and 2.5-inch coal pumps.

(3) To add a further complication, the nature of the nonideality of the coal melt (i.e., the value of α in Eqn. 9) is subject to change with time, even for a given coal at a given temperature. After the fluidity maximum has passed, during the coking portion of the fluidity curve, coal melts develop viscoelastic properties. (36) For example, Fitzgerald modified a Gieseler plastometer so that torque could be quickly removed from the stirrer shaft; when this was done during the coking portion of Gieseler runs at 435-450°C the stirrer reversed its direction (elastic recovery). This behavior conforms to Eqn. 10:

$$\ln(x_\infty - x_t) = a - b \cdot t \qquad (10)$$

where x_∞ and x_t are the extents of elastic return at infinite time and at time t. Fitzgerald notes that this behavior fits the Alfrey model for viscoelastic polymers. (37) Preliminary rheological data obtained at JPL indicate that the value of α in Eqn. 9 may vary from 0.1 to 1.3 for the same coal over a 40°C range. (24)

(4) The carbonization kinetics of coal have been examined under isothermal conditions in the range 317-524°C. From this study Berkowitz concludes that the devolatilization rate is sharply dependent upon particle size. (38) The recent DSC study by Gold (21) found that the sharp exotherm (discussed in the preceding section) is sharply dependent upon mesh size. These observations raise the question of the significance of particle size distribution in the extruder screw feed. It seems possible, at least, that the geometry and mechanics of coal feeding, to the extent that they determine particle size distribution of the compacted unmelted coal, may be an important factor in the overall performance of an extruder.

Some of the above problems can be addressed by laboratory investigations. The Andrade relationship (Eqn. 8) is roughly followed by the plastic coals

in this study, notwithstanding their obvious nonideality. The problem of the varying fraction of solids can be approached, as Fitzgerald has done,(10) by relating fluidity to the proportion of solids in the coal:

$$\Theta_r = (1 - \chi)^{\lambda} \qquad (11)$$

where Θ_r, χ, and λ are relative fluidity, solid fraction, and an exponential constant, theoretically 2.5(39,40)

If we rewrite Θ_r as β/η (where η is viscosity and β a proportionality constant), Eqn. 11 may be rearranged as:

$$\eta = \beta \ (1-\chi)^{-\lambda} \qquad (12)$$

Empirically, the right hand side of Eqn. 12 may be taken to represent in more detail the χ-sensitive proportionality constant of Eqn. 9. Combining these, the viscosity of a coal melt may be represented as:

$$\eta = \beta \ (1-\chi)^{-\lambda} \ \dot{\gamma}^{(\alpha-1)} \qquad (13)$$

The viscosity of coal melts is conveniently treated in terms of an ideal fluid, for example, as in Eqn. 8. This treatment (which we have implicitly followed in the bulk of this report) may prove to be sufficient for the design needs of coal pump development, especially since screw pumps are normally overdesigned and since the largest single error in the Newtonian assumption may be in the pseudoplasticity of the melt, an error tending to overestimate resistance to high-shear screw pumping. It may still be useful, however, for those working in this area to keep in mind that our convenient assumption (that $\eta_1 = k$) is indeed a considerable simplification. The reality is more closely approached by an expression such as Eqn. 13; and even here, even under isothermal conditions, χ and α are time-dependent.

4.4 Future Work

Several areas may be suggested for future laboratory work to be conducted in support of the coal pump development program at JPL. These are briefly noted below.

1. A quantitative study of the non-Newtonian character of coal in its fluid state. A careful study by isothermal Gieseler plastometry with varying coal-char compositions may permit the evaluation of λ and the close estimation of χ for several model coals (Eqn. 13), at various stages in their fluidity curves. The exponential term α can be evaluated by another series of runs with varying torque at constant composition. Such a study may provide a better basis for predicting the rheological behavior of coals at various stages in their plastic states and under varying conditions of T, P, and mechanical forces.

2. In the present study we have advanced the hypothesis (section 4.3.1) that the large exotherm often observed in differential scanning calorimetry is purely a system artifact. This can be proven or disproven by further experiments using DSC and calibrated differential thermal analysis. The systematic use of multiple reference compounds for calibration, as shown by Heilpern (41), permits quantitative thermal calculations of coal endotherms from DTA data. [Heilpern observes no exotherm below about 600°C.]

3. Several possible means of correlating/predicting plastic behavior of coals with various analytical data have been noted (section 4.2). A laboratory study of at least two dozen bituminous coals can provide a sufficient data set to determine which of these analytical measurements may be of general use in predicting and explaining the plastic behavior of bituminous coals. This understanding may provide a basis for the development of techniques for controlling and modifying the plastic properties of coals.

5. REFERENCES

1. P. R. Ryason and C. England, Fuel, 57, 241 (1978)

2. H. J. Gluskoter, ibid., 44, 285 (1965)

3. C. E. Gleit and W. D. Holland, Anal. Chem., 34, 1454 (1962)

4. J. S. Webb and M. Thompson, Pure Appl. Chem., 49, 1507 (1976)

5. J. K. Kuhn, W. F. Harfst and N. F. Shimp, in S. Babu, ed., "Trace Elements in Fuel", Advances in Chem., 144, pp66ff (1975)

6. W. G. Lloyd and H. E. Francis, Proc. ERDA X -and Gamma-Ray Symp., Ann Arbor, MI, 1976, pp166ff; J. A. Cooper, B. D. Wheeler, G. J. Wolfe, D. M. Bartell and D. B. Schlafke, ibid., pp169ff.

7. K. Gieseler, Gluckauf, 70, 178 (1934)

8. ASTM D 2639-74, Amer. Soc. for Testing and Materials, 1916 Race St., Philadelphia, PA.

9. R. Loison, A. Peytavy, A. F. Boyer and R. Grillot, "The Plastic Properties of Coal", in H. H. Lowry, ed., "Chemistry of Coal Utilization - Supplementary Volume", John Wiley & Sons, New York, 1963.

10. D. Fitzgerald, Trans. Faraday Soc., 52, 362 (1956)

11. D. Fitzgerald, Fuel, 35, 178 (1956)

12. D. W. van Krevelen, F. J. Huntjens and H. N. M. Dormans, ibid., 462 (1956).

13. H. A. G. Chermin and D. W. van Krevelen, ibid , 36, 85 (1957).

14. W. S. Wise, "Solvent Treatment of Coal", Mills & Boon, Ltd., London, 1971.

15. Z. Spitzer and L. Ulicky, Fuel, 55, 21 (1976).

16. J. A. Harrison, et al., Illinois State Geological Survey Circular 366 (1964).

17. E. Stach, M. -Th. Mackowsky, M. Teichmuller, G. H. Taylor, D. Chandra and R. Teichmuller, "Stach's Handbook of Coal Petrology", 2nd ed. Gebruder Borntraeger, Berlin, 1975.

18. G. J. Jansen, private communication.

19. R. L. Fyans, "Rapid Characterization of Coal by Thermogravimetric and Scanning Calorimetric Analysis", 28th Annual Pittsburgh Conference on Analytical Chemistry and Spectroscopy, Cleveland, March, 1977.

20. D. W. van Krevelen, "Coal", Elsevier Publishing Co., Amsterdam, 1961, Chap. XIV.

21. P. I. Gold, "Differential Scanning Calorimetry of Coal", final rept., National Aeronautics and Space Administration Contract No. NSG-7263 (April, 1978)

22. Osiander, introduction to Canon N. Koppernijk (Copernicus), "De Revolutionibus Orbium Coelestium", Petreius, Nuremberg (1543).

23. P. L. Waters, Fuel, 41, 3 (1962).

24. A. Murphy, R. Phen and W. Schatz, "Coal Pump Development and Technical Support Quarterly Project Report", Jet Propulsion Laboratory, California Institute of Technology, #5030-144 (October 1977).

25. A. Murphy, R. Phen and W. Schatz, ibid., #5030-208 (April 1978).

26. A. Murphy, R. Phen and W. Schatz, "Coal Pump Development and Technical Support Monthly Project Report", Jet Propulsion Laboratory, California Institute of Technology #5030-221 (May 1978).

27. C. England (Jet Propulsion Laboratory), private communication.

28. J. G. King, Fuel, 23, 61 (1944).

29. W. R. K. Wu and W. H. Frederic, "Coal Composition, Coal Plasticity, and Coke Strength", USBM Bulletin 661 (1973).

30. J. G. Walters, W. H. Ode and L. Spinetti, "Plastic, Agglutinating, and Free-Swelling Properties of American Coals", USBM Bulletin 610 (1963).

31. H. R. Brown, J. Inst. Fuel, 30, 137 (1957).

32. A. A. Agroskin, E. I. Goncharov, L. A. Makeev and V. P. Yakunin, Coke and Chemistry, 5, 7 (1970).

33. L. L. Isaacs, Amer. Chem. Soc., Divn. of Fuel Chem. Preprints, 23, No. 4, 215 (1978).

34. V. V. Hathi and C. M. Sliepcevich, "Thermal and Kinetic Analysis of the Pyrolysis of Coals", EPRI AF-528 final report, August, 1977.

35. E. N. daC. Andrade, Nature, 125, 309 (1930).

36. D. Fitzgerald, Fuel, 36, 389 (1957).

37. T. Alfrey, Jr., "Mechanical Properties of High Polymers", Interscience, New York, 1948.

38. N. Berkowitz, Fuel, 39, 47 (1960).

39. R. Roscoe, Brit. J. Appl. Physics, 3, 267 (1952).

40. H. C. Brinkman, J. Chem. Phys., 20, 571 (1952).

41. S. Heilpern, in I. Buzas, ed., "Thermal Analysis", Heyden & Son, Ltd., London, Vol. 3, 1974, pp 283ff.

6. APPENDIX

This section consists mainly of tabulations of raw analytical data, the averages of which appear in the tabular data of Section 3. Tables of proximate and ultimate analysis (pp 124-6), mineral analysis (pp 127-33), and ASTM and isothermal Gieseler plastometric data (pp 134-54) are included.

In addition, Section 6.4 (pp 155-63) presents some of the detailed discussion and data used in the development of the isothermal plastometric model described in Section 4.1.

Mineral analysis, as this term is used in this report, refers to the compositional (elemental) analysis of the mineral fraction, not to mineralogical identifications.

Table 6.1-1

Raw Values of Proximate and Ultimate Analysis of Seven Coals*

	Proximate Analysis, Percent				Ultimate Analysis, Percent					
Seam	Moisture	Ash	Volatile Matter	Fixed Carbon	Carbon	Hydrogen	Nitrogen	Sulfur	Calorific Value	FSI
Pittsburgh #8	0.82	8.62	40.60	49.96	76.82	5.05	1.31	2.64	13,849	7½
	0.76	8.68	41.09	49.47	77.13	5.07	1.29	2.65	13,841	
					76.52	5.07	1.29			
Ohio #9	2.11	18.81	39.50	39.58	62.76	4.45	0.89	4.22	11,072	3
	2.18	18.93	39.29	39.60	62.70	4.42	0.89	4.28	11,059	
					62.71	4.42	0.90			
Lower Kittanning	1.96	10.67	26.41	60.96	76.56	4.62	1.11	1.67	13,175	8
	1.93	10.84	26.72	60.51	76.30	4.41	1.22	1.67	13,126	
					76.76	4.50	1.25			
Kentucky #11	1.95	8.37	41.12	48.45	73.77	5.01	1.21	3.15	13,234	7
	1.99	8.30	41.26	48.56	73.87	5.11	1.22	3.17	13,239	
					73.57	5.14	1.24			
Pocahontas #3	0.48	9.67	17.41	72.44	80.84	3.73	0.90	0.64	13,939	4½
								0.62		
	0.46	9.68	17.39	72.47	81.07	3.79	0.92	0.69	13,932	
					80.94	3.78	0.93	0.66		
Amax Wyoming	29.03	5.23	34.66	33.08	50.44	3.93	0.60	0.46	8,606	0
	29.20	5.45	33.49	33.86	50.41	3.88	0.54	0.44	8,557	
					50.72	3.88	0.50		8,580	
Elkhorn #1	2.47	14.81	35.43	47.29	69.45	4.76	1.27	0.78	12,075	3½
	2.43	14.80	35.62	47.15	68.99	4.71	1.27	0.78	12,065	
					69.40	4.74	1.27	0.79		

* Oxygen by Difference.

Table 6.1-2

Raw Values of Proximate, FSI and Calorific Values of Coal Extrudates

Extrudate Source	Moisture	Ash	Volatile Matter	Fixed Carbon	Calorific Value	FSI
Pittsburgh #8 1/78 (1A)	0.00 0.00	8.92 8.86	36.35 36.17	54.73 54.97	13,947 13,947	8
Pittsburgh #8 1/78 (2A)	0.10 0.10	8.55 8.54	34.45 34.91	56.90 56.45	13,857 13,802	7½
Ohio #9 1/78 (2A)	0.25 0.28	24.97 25.07	28.99 29.20	44.79 45.45	10,895 10,858	2½
Ohio #9 1/78 (2B)	0.27 0.34	25.47 25.68	28.71 28.79	45.55 45.19	10,737 10,711	1½
Kentucky #11 4/78	0.0 .	15.48 15.72	32.76 32.78	51.76 51.50	12,405 12,389	6.5 6.5
Kentucky #11 5/78	0.0	11.96 11.90	35.44 35.40	52.60 52.70	13,138 13,148	4.0 4.0
Pittsburgh #8 4/78 - 800 F	0.0 0.03	7.82 7.85	35.96 36.45	56.22 55.70	13,910 13,951	8 8
Pittsburgh #8 4/78 - 900 F	0.20 0.15	8.27 8.26	31.31 31.40	60.22 60.19	13,649 13,644	6 6
Pittsburgh #8 4/78 - 1000 F	0.0 0.0	8.21 8.30	34.95 34.54	56.84 57.16	13,775 13,752	7.5 7.5
Pittsburgh #8 4/78 - 1100 F	0.12 0.0	8.12 8.14	35.67 35.59	56.21 56.27	13,948 13,941	8 8
Pittsburgh #8 4/78 - 1200 F	0.10 0.0	8.33 8.39	36.86 36.97	54.81 54.64	13,845 13,868	7.5 7.5

Table 6.1-3

Raw Values of Ultimate Analyses of Coal Extrudates*

Extrudate source	% C	% H	% N	% S	% O
Pittsburgh #8	77.22	4.94	1.61	2.84	4.56
1/78 (1A)				2.73	
Pittsburgh #8				2.73	
1/78 (2B)	76.98	4.87	1.58	2.82	5.26
Ohio #9				4.23	
1/78 (2A)	62.51	3.89	1.10	4.49	3.12
Ohio #9					
1/78 (2B)	61.52	3.73	1.22	4.47	3.49
Kentucky #11	68.64	4.27	1.31	4.49	5.81
4/78	68.74	4.31	1.27	4.53	5.43
Kentucky #11	73.02	4.84	1.29	3.44	5.45
5/78	72.86	4.86	1.26	3.40	5.72
Pittsburgh #8	77.97	4.95	1.28	2.25	5.84
7/78 - 800 F	77.83	4.94	1.28	2.29	
	77.74	4.96	1.22		
Pittsburgh #8	77.72	4.55	1.32	2.15	6.00
4/78 - 900 F	77.64	4.51	1.32	2.16	
	77.67	4.60	1.39		
Pittsburgh #8	77.57	4.77	1.27	2.36	5.68
4/78 - 1000 F	77.72	4.76	1.24	2.42	
	77.63	4.82	1.28		
Pittsburgh #8	77.44	4.94	1.25	2.05	6.16
4/78 - 1100 F	77.38	4.88	1.24	2.18	
	77.54	4.89	1.26		
Pittsburgh #8	77.58	4.97	1.30	2.28	5.48
4/78 - 1200 F	77.82	4.93	1.22	2.15	
	77.82	4.94	1.27		

* Oxygen by difference, using ash values of Table 6.1-2.

Table 6.2-1

Individual Analyses by X-Ray Fluorescence at 14 KeV of Whole Coals

Coal Seam	Al	Si	P	S	K	Ca	Ti	Cr	Mn	Fe
Pittsburgh #8	3.118	20.123		165.633	10.836	45.169	23.749	1.469		405.146
	3.098	21.303		164.468	11.401	44.909	23.473	2.098		407.235
	3.405	20.868		167.491	10.863	44.840	24.272	1.765		408.682
	3.212	21.511		165.616	11.382	45.838	24.796	1.533		410.065
	3.102	20.911		168.958	10.595	45.556	24.371	1.926		409.243
	3.187	20.943		166.433	11.015	45.262	24.312	1.758		408.074
Pittsburgh #8 Extrudate	3.454	22.187	.381	159.802	11.303	51.117	24.855	1.640		435.112
	3.801	23.180	.727	159.730	11.164	50.864	24.935	.875		436.796
	3.782	22.949	.426	158.665	11.267	49.560	24.275	.750		434.234
	3.685	22.889	.522	159.032	10.768	49.281	24.274	1.943		434.098
	3.656	22.358	.770	159.174	10.716	50.275	25.130	1.611		437.482
	3.587	21.934	.225	159.641	10.912	49.421	24.955	2.388		436.724
	3.660	22.582	.508	159.340	11.021	50.086	24.737	1.534		435.741
Ohio #9	5.277	36.587		205.445	31.367	94.950	26.549	1.700	39.041	720.097
	5.525	36.897		207.694	31.964	95.317	26.189	2.243	37.902	720.784
	5.269	37.101		203.777	31.908	95.811	26.063	2.028	37.326	724.770
	4.853	37.200		204.327	31.510	96.855	26.304	2.410	37.819	722.159
	4.937	36.502		206.130	31.562	95.898	26.992	2.416	37.665	724.679
	5.172	36.857		205.274	31.662	95.766	26.419	2.159	37.950	722.497
Ohio #9 Extrudate	6.098	40.801	.518	177.607	35.613	153.362	29.563	6.160	103.811	801.571
	5.870	40.483	.426	176.089	35.845	153.952	29.994	5.119	103.619	802.259
	5.619	40.234	.124	174.771	35.987	153.571	29.607	5.190	102.891	801.321
	5.709	39.686	.197	175.207	35.955	152.078	29.896	5.869	102.756	800.333
	5.711	39.819	.232	175.118	35.887	153.417	30.701	6.321	101.932	801.281
	5.801	40.202	.299	175.753	35.857	153.276	29.932	5.731	103.001	741.353

Con't Table 6.2-1

Coal Seam	Al	Si	P	S	K	Ca	Ti	Cr	Mn	Fe
Lower Kittanning	4.368	22.942	.539	95.377	18.460	25.514	38.481	1.458	0	501.521
	4.706	22.324	.782	96.070	18.045	24.834	37.948	2.136	0	502.691
	5.007	23.092	.996	94.742	18.459	24.389	39.391	1.317	.155	503.772
	4.737	22.321	.692	94.940	17.898	25.520	39.946	1.405	.267	505.512
	4.678	22.858	.943	95.018	18.520	25.655	39.524	.676	.222	501.886
	4.699	22.707	.790	95.229	18.276	25.182	39.058	1.398	.128	503.076
Western Kentucky #11	2.993	22.910		199.413	19.927	11.780	20.503	2.715		565.558
	2.679	23.868		198.995	19.244	11.724	19.879	2.097		565.599
	2.605	23.945		201.338	19.550	11.911	19.519	3.283		568.725
	2.205	23.516		199.546	20.174	11.953	21.218	2.233		569.161
	2.410	22.682		200.223	19.653	11.932	19.811	3.328		574.125
	2.578	23.384		199.903	19.709	11.860	20.186	2.731		568.533
Pocahontas #3	3.985	22.847		54.777	3.887	9.613	67.313	1.889		183.097
	4.197	22.758		54.831	4.472	9.060	67.760	2.026		185.241
	3.895	23.097		54.519	4.309	9.988	68.722	1.646		182.400
	3.899	22.522		54.649	3.410	9.272	67.441	.939		184.566
	3.907	23.328		54.458	3.362	9.270	67.944	1.232		185.213
	3.967	29.910		54.643	3.888	9.441	67.836	1.546		184.103
Amax Wyoming	1.986	7.918	1.953	40.440	1.799	288.049	27.874	.416	2.768	183.901
	1.803	7.885	1.761	41.489	1.160	292.772	28.078	1.092	3.678	188.309
	1.772	8.236	2.035	40.772	1.122	295.658	27.317	2.054	3.363	189.706
	2.021	7.713	1.612	40.594	1.196	296.199	28.811	.367	4.023	188.091
	1.720	8.097	1.840	42.413	1.540	295.715	27.698	1.315	2.776	191.791
	1.860	7.959	9.201	41.141	1.363	293.678	27.955	1.048	3.321	188.359

Con't Table 6.2-1

Coal Seam	Al	Si	P	S	K	Ca	Ti	Cr	Mn	Fe
Elkhorn	6.676	42.112		43.519	56.465	24.656	38.541	2.289	1.458	496.242
#1	6.778	41.442		42.732	56.818	25.552	38.362	.747	2.176	499.194
	6.941	42.339		42.705	56.811	27.092	39.028	1.713	1.805	497.371
	6.757	41.192		43.622	56.689	25.596	38.626	1.321	2.439	498.605
	6.790	41.280		42.463	57.241	26.324	39.183	1.365	1.889	497.090
	6.788	41.673		43.008	56.805	25.844	38.748	1.487	1.953	497.700

Table 6.2-2

Individual Analyses by X-Ray Fluorescence at 40 KeV of Whole Coals

Coal Seam	Cu	Zn	As/Pb	Br	Rb	Sr	Y	Zr
Pittsburgh #8	.150	.232		1.321	0	19.121		9.772
	.179	.226		1.170	.425	18.173		9.423
	.139	.177		1.727	0	17.923		9.053
	.293	.127		1.415	1.728	19.967		9.865
	.131	.168		1.379	.387	19.339		10.002
average	.178	.186		1.402	.508	18.905		9.623
Pittsburgh #8 Extrudate	.264	.111		1.307	.550	15.142		6.686
	.366	.290		1.627	0	15.214		8.146
	.100	.209		1.264	.546	14.510		6.867
	.156	.149		1.530	.308	15.125		6.115
	.372	.231		1.131	.759	15.094		6.466
average	.252	.198		1.372	.433	15.017		6.856
Ohio #9	.306	.514	.708	0	.877	5.777		6.468
	.388	.505	.656	.202	1.518	7.186		6.147
	.421	.639	.667	.105	1.706	6.078		6.041
	.415	.493	.703	6	1.164	6.572		4.741
	.162	.388	.671	47	.813	6.304		5.328
average	.328	.507	.681	.072	1.215	6.383		5.745
Ohio #9 Extrudate	.166	.367	.470	.683	1.208	9.249		7.360
	. 70	.281	.583	.774	.706	10.633		7.687
	.139	.408	.313	.756	1.385	9.766		6.462
	.160	.366	.434	.703	1.045	9.753		7.770
	.102	.217	.376	.816	1.418	10.126		7.929
average	.127	.327	.435	.746	1.152	9.925		7.441

Con't Table 6.2-2

Coal Seam	Cu	Zn	As/Pb	Br	Rb	Sr	Y	Zr
Lower Kittanning	. 45	.735	2.169	2.560		20.052		10.510
	.385	.465	2.282	2.745		21.103		10.538
	.209	.838	2.448	2.847		19.900		10.042
	.340	.978	2.016	3.063		21.002		10.329
	.348	.785	2.261	2.562		20.077		9.794
average	.265	.760	2.235	2.755		20.426		10.242
Western Kentucky #11	.329	.351		1.113	.611	1.281		5.153
	.192	. 81		1.394	1.304	1.094		3.462
	.294	.499		1.435	.807	2.055		5.721
	.217	.253		1.939	1.504	2.142		5.603
	.111	.369		1.920	1.633	2.564		5.439
average	.228	.310		1.560	1.171	1.827		5.075
Pocahontas #3	.752		.160	3.658		7.073	2.039	12.005
	.579		.520	4.972		7.232	1.861	13.795
	.878		.544	3.980		8.599	1.985	11.291
	.722		.600	3.947		6.922	2.268	13.735
	.705		.760	4.020		7.021	2.043	12.690
average	.727		.517	4.115		7.369	2.039	12.703
Amax Wyoming	.525	.319				14.022		4.923
	.572	.357				13.655		6.498
	.547	.382				14.307		4.973
	.654	.177				14.333		5.719
	.561	.244				13.428		4.107
average	.571	.295				13.949		5.244

Con't Table 6.2-2

Coal Seam	Cu	Zn	As/Pb	Br	Rb	Sr	Y	Zr
Elkhorn	.913	.218		1.959	3.020	6.357	.544	6.827
#1	.941	.428		1.124	2.346	5.842	.873	6.783
	.917	.277		1.797	1.925	5.671	.177	7.449
	.896	.437		1.439	2.346	6.172	.608	5.674
	.942	.357		1.537	1.924	7.072	.897	6.797
average	.922	.343		1.571	2.312	6.223	.620	6.706

Table 6.2-3

Individual Analyses by Atomic Absorption Spectrometry of Mineral Components in the Reignited Ashes of Seven Coals.

Coal Seam	Fe_2O_3	SiO_2	Al_2O_3	CaO	MgO	K_2O	Na_2O	TiO_2	SO_3
Pittsburgh #8	16.28	52.49	23.66	3.36	0.85	1.22	0.39	1.57	3.08
	15.42	48.45	23.02	3.12	0.81	1.20	0.75	1.48	3.16
			23.54	3.44	0.86	1.34	1.04		
			23.35	3.47	0.90	1.32	1.11		
Ohio #9	16.85	43.43	18.50	5.14	3.86	2.23	0.054	0.60	5.97
	16.87	42.90	18.54	5.50	3.81	2.23	0.071	0.92	6.03
			18.93	5.41	3.84	2.20	0.46		
			19.36	5.29	3.83	2.24	0.46		
Lower Kittanning	12.16	50.25	30.18	0.83	0.55	1.73	0.20	2.15	1.00
	12.26	46.81	30.16	0.57	0.53	1.78	0.063	1.75	1.00
			27.71	1.40	0.58	1.72	0.18		
			28.60	1.47	0.58	1.77	0.28		
Western Kentucky #11	20.28	50.11	20.22	0.80	0.68	2.34	0.61	1.57	0.64
	20.64	50.99	20.14	0.88	0.68	2.32	0.54	1.45	0.62
			20.02	0.94	0.78	2.38	0.42		
			20.19	1.08	0.75	2.41	0.34		
Pocahontas #3	2.84	59.74	32.71	0.43	0.35	0.41	0.46	4.39	0.53
	2.83	56.50	32.45	0.11	0.32	0.42	0.62	4.27	0.54
			30.51	0.87	0.40	0.46	0.76		
			30.90	0.73	0.41	0.47	0.77		
Amax Wyoming	5.49	31.70	15.74	23.46	3.30	0.18	2.05	1.93	5.28
	5.46	32.17	15.63	22.78	3.30	0.18	1.74	1.30	5.38
			16.08	22.48	3.37	0.29	1.38		
			15.91	22.50	3.45	0.31	1.59		
Elkhorn #1	8.31	70.73	26.46	0.87	1.76	4.05	0.46	1.82	0.65
	8.35	69.61	26.14	0.88	1.69	4.08	0.23	1.82	0.65
	8.45	63.22	25.73	0.88	1.69	4.13	0.22	1.82	
Pittsburgh #8 Extrudate	16.98	44.24	22.81	4.66	0.81	1.12	2.94		3.69
	17.00	46.21	22.45	4.34	0.81	1.05	0.96		3.68
Ohio #9 Extrudate	15.82	38.39	16.59	7.19	4.53	1.90	0.53		9.31
	15.97	35.82	16.84	6.86	4.56	1.89	0.23		9.39

Table 6.3-0

Viscosity Calibration of the FRICO Gieseler Plastometer[1]

Standard[2]	Temp, °C	Viscosity, poise[3]	Fluidity, ddpm
N 190000	18.55	10,807	1,391
	22.91	7,156	2,109
	29.46	3,940	3,842
	36.30	2,169	6,933
S 30,000	18.58	1,290	12,800
	23.39	828.6	19,900
	26.03	653.7	25,400
	28.06	546.5	29,530

---

[1] The Institute's Gieseler Plastometer was built in 1976 by Fuel Research and Instrument Corp., Chicago, IL, conforming to the design requirements of ASTM Method D 2639 ("Plastic Properties of Coal by the Constant-Torque Gieseler Plastometer").

[2] Supplied by Cannon Instrument Corp., State College, PA.

[3] Interpolated from the calibration data supplied by the manufacturer. These fluids exhibit Andrade linearity over this temperature range.

Table 6.3-1

Gieseler Plastometry (ASTM) of Ohio #9 seam coal (Meigs Creek)

time	temp	run 1	run 2	run 3	ln(run 1)	ln(run 2)	ln(run 3)	avg ln(ddpm)	avg. ddpm
18 m	384°C	0.2	0.5	0.5	-1.61	-0.69	-0.69	-1.00	0.4
19	387	0.5	0.5	0.5	-0.69	-0.69	-0.69	-0.69	0.5
20	390	0.5	0.7	0.5	-0.69	-0.36	-0.69	-0.58	0.6
21	393	0.7	0.7	0.8	-0.36	-0.36	-0.22	-0.31	0.7
22	396	0.8	0.6	1.1	-0.22	-0.51	0.10	-0.21	0.8
23	399	1.25	1.0	1.25	0.22	0.00	0.22	0.15	1.2
24	402	1.5	1.75	1.75	0.41	0.56	0.56	0.51	1.7
25	405	2.0	2.25	2.50	0.69	0.81	0.92	0.81	2.2
26	408	2.75	3.00	3.50	1.01	1.10	1.25	1.12	3.1
27	411	4.50	4.50	4.25	1.50	1.50	1.45	1.49	4.4
28	414	6.0	7.0	8.0	1.79	1.95	2.08	1.94	7.0
29	417	10.	14.	11.5	2.30	2.64	2.44	2.46	11.7
30	420	17.	20.	16.5	2.83	3.00	2.80	2.88	17.8
31	423	37.	27.	35.	3.61	3.30	3.56	3.49	33.
32	426	64.	70.	58.	4.16	4.25	4.06	4.16	65.
33	429	102.	90.	81.	4.62	4.50	4.39	4.51	91.
34	432	130.	102.	104.	4.87	4.62	4.64	4.71	111.
35	435	128.	111.	105.	4.85	4.71	4.65	4.74	114.
36	438	120.	92.	88.	4.79	4.52	4.48	4.60	99.
37	441	100.	65.	80.	4.61	4.17	4.38	4.39	80.
38	444	66.	47.	64.	4.19	3.85	4.16	4.07	58.
39	447	45.	29.	32.	3.81	3.37	3.47	3.55	35.
40	450	21.	13.	27.	3.04	2.56	3.30	2.97	19.5
41	453	12.	7.0	13.	2.48	1.95	2.56	2.33	10.3
42	456	6.0	4.0	4.5	1.79	1.39	1.50	1.56	4.8
43	459	2.25	1.5	2.0	0.81	0.41	0.69	0.64	1.9
44	462	1.25	0.75	1.0	0.22	-0.29	0.00	-0.02	1.0
45	465	0.5	...	...	-0.69	...	...	(-0.69)	

Table 6.3-2

Gieseler Plastometry (ASTM) of Lower Kittanning seam coal

time	temp	run 1	run 2	run 3	ln(run 1)	ln(run 2)	ln(run 3)	avg ln(ddpm)	avg ddpm
28 m	414°C	0.75	0.50	0.50	-0.29	-0.69	-0.69	-0.56	0.57
29	417	1.0	0.75	0.75	0.00	-0.29	-0.29	-0.19	0.83
30	420	1.25	0.85	0.75	0.22	-0.16	-0.29	-0.08	0.93
31	423	1.75	1.0	1.25	0.56	0.00	0.22	0.26	1.3
32	426	1.75	1.7	1.5	0.56	0.53	0.41	0.50	1.65
33	429	2.0	1.75	1.75	0.69	0.56	0.56	0.60	1.8
34	432	3.0	2.25	2.5	1.10	0.81	0.92	0.94	2.6
35	435	4.75	3.25	3.5	1.56	1.18	1.25	1.33	3.8
36	438	6.	4.	4.5	1.79	1.39	1.50	1.56	4.8
37	441	8.5	6.	7.	2.14	1.79	1.95	1.96	7.1
38	444	15.5	9.5	13.	2.74	2.25	2.56	2.52	12.4
39	447	23.5	13.5	21.	3.16	2.60	3.04	2.93	18.8
40	450	53.5	29.	38.	3.98	3.37	3.64	3.66	38.9
41	453	85.	53.5	79.	4.44	3.98	4.37	4.26	71.
42	456	118.	86.	116.	4.77	4.45	4.75	4.66	106.
43	459	130.	117.	141.	4.87	4.76	4.95	4.86	129.
44	462	165.	141.	180.	5.11	4.95	5.19	5.08	161.
45	465	195.	163.	200.	5.27	5.09	5.30	5.22	185.
46	468	180.	154.	178.	5.19	5.04	5.18	5.14	170.
47	471	165.	138.	175.	5.11	4.93	5.16	5.07	159.
48	474	130.	105.	135.	4.87	4.65	4.91	4.81	123.
49	477	87.	78.	91.	4.47	4.36	4.51	4.44	85.
50	480	65.	46.	66.	4.17	3.83	4.19	4.06	58.
51	483	25.	28.	26.	3.22	3.33	3.26	3.27	26.3
52	486	9.5	10.	13.	2.25	2.30	2.56	2.37	10.7
53	489	4.75	5.5	5.	1.56	1.70	1.61	1.62	5.1
54	492	2.0	1.6	1.25	0.69	0.47	0.22	0.46	1.6
55	495	0.75	0.65	0.75	-0.29	-0.43	-0.29	-0.34	0.7

Table 6.3-3

Gieseler Plastometry (ASTM) of Western Kentucky #11 Seam Coal

time	temp	run 1	run 2	run 3	run 4	run 5	run 6	run 7	ln(1)	ln(2)	ln(3)	ln(4)	ln(5)	ln(6)	ln(7)	avg ln	avg ddpm
19 m	387°C	1.	0.5	0.7	0.5	0.7	0.7	0.7	0.00	-0.69	-0.36	-0.69	-0.36	-0.36	-0.36	-0.40	0.7
20	390	1.2	0.7	1.0	0.7	0.5	0.8	0.8	0.18	-0.36	0.00	-0.36	-0.69	-0.22	-0.22	-0.24	0.8
21	393	1.7	1.2	1.3	0.8	0.6	1.3	1.4	0.53	0.18	0.26	-0.22	-0.51	0.26	0.34	0.12	1.1
22	396	2.	1.3	1.5	1.2	1.2	1.2	2.	0.69	0.26	0.41	0.18	0.18	0.18	0.69	0.37	1.5
23	399	3.	1.8	2.	1.5	1.8	2.3	2.5	1.10	0.59	0.69	0.41	0.59	0.83	0.92	0.73	2.1
24	402	4.	2.8	3.	2.3	2.3	2.8	3.	1.39	1.03	1.10	0.83	0.83	1.03	1.10	1.04	2.8
25	405	6.	3.8	3.8	2.5	3.	4.8	5.	1.79	1.34	1.34	0.92	1.10	1.57	1.61	1.38	4.0
26	408	12.	6.	7.	5.	4.8	9.5	9.5	2.48	1.79	1.95	1.61	1.57	2.25	2.25	1.99	7.3
27	411	30.	12.	14.	14.	9.5	20.5	19.5	3.40	2.48	2.64	2.64	2.25	3.02	2.97	2.77	16.0
28	414	88.	28.5	32.	46.	22.5	59.	55.	4.48	3.35	3.47	3.83	3.11	4.08	4.01	3.76	43.
29	417	262.	87.	83.	88.	62.	150.	119.	5.57	4.47	4.42	4.48	4.13	5.01	4.78	4.69	109.
30	420	845.	227.	193.	265.	168.	398.	248.	6.74	5.42	5.26	5.58	5.12	5.99	5.51	5.66	288.
31	423	2630	525	495	930	420	1190	505	7.87	6.26	6.20	6.84	6.04	7.08	6.22	6.65	770.
32	426	13310	1100	1280	2420	1020	2595	885	9.50	7.00	7.15	7.79	6.93	7.86	6.79	7.57	1947.
33	429	23100	1800	1880	9120	1780	4960	1400	10.05	7.50	7.54	9.12	7.48	8.51	7.24	8.21	3661.
34	432	25300	2600	2050	14000	2600	18400	1840	10.14	7.86	7.63	9.55	7.86	9.82	7.52	8.63	5569.
35	435	26200	3200	2600	19300	2500	23000	1520	10.17	8.07	7.86	9.87	7.82	10.04	7.33	8.74	6238.
36	438	21000	3200	2100	19400	2700	19800	2210	9.95	8.07	7.65	9.87	7.90	9.89	7.70	8.72	6125.
37	441	17700	2900	1900	17100	2600	16100	3870	9.78	7.97	7.55	9.75	7.86	9.69	8.26	8.69	5970.
38	444	14100	2000	1650	14400	2270	13400	4400	9.55	7.60	7.41	9.57	7.73	9.50	8.39	8.54	5099.
39	447	10400	1950	1200	9300	1670	8900	4500	9.25	7.58	7.09	9.14	7.42	9.09	8.41	8.28	3955.
40	450	4900	1500	670	6200	1115	4900	3500	8.50	7.31	6.51	8.73	7.02	8.50	8.16	7.82	2484.
41	453	1640	900	375	2940	655	2050	1685	7.40	6.80	5.93	7.99	6.48	7.63	7.43	7.09	1205.
42	456	645	410	180	900	275	730	645	6.47	6.02	5.19	6.80	5.62	6.59	6.47	6.17	476.
43	459	210	162	80	364	122	310	242	5.35	5.09	4.38	5.90	4.80	5.74	5.49	5.25	190.
44	462	83	60	50	120	48	95	134	4.42	4.09	3.91	4.79	3.87	4.55	4.90	4.36	78.
45	465	29	22	14	33	18	65	52	3.37	3.09	2.64	3.50	2.89	4.17	3.95	3.37	29.
46	468	9.	6.	4.	12.	7.5	16.	20.	2.20	1.79	1.39	2.48	2.01	2.77	3.00	2.23	9.3
47	471	3.	2.	2.	3.3	2.3	5.5	4.8	1.10	0.69	0.69	1.19	0.83	1.70	1.57	1.11	3.0
48	474	1.	1.	1.	1.3	0.8	1.8	1.3	0.00	0.00	0.00	0.26	-0.22	0.59	0.26	0.13	1.1
49	477	[0.3]	[0.4]	[0.5]	0.5	[0.3]	0.7	0.7	-1.20	-0.92	-0.69	-0.69	-1.20	-0.36	-0.36	-0.77	0.5

Table 6.3-4

Gieseler Plastometry (ASTM) of Pocahontas #3 Seam Coal

time	temp	run 1	run 2	run 3	ln(1)	ln(2)	ln(3)	avg ln	avg ddpm
43 m	459°C	0.4	0.5	0.75	-0.92	-0.69	-0.29	-0.63	0.53
44	462	0.75	0.85	0.65	-0.29	-0.16	-0.43	-0.29	0.75
45	465	0.85	0.9	0.75	-0.16	-0.11	-0.29	-0.19	0.83
46	468	1.	0.85	1.25	0.00	-0.16	0.22	0.02	1.0
47	471	1.15	1.15	1.5	0.14	0.14	0.41	0.23	1.3
48	474	1.25	1.5	1.5	0.22	0.41	0.41	0.35	1.4
49	477	1.5	1.5	1.6	0.41	0.41	0.47	0.43	1.5
50	480	1.75	1.65	1.9	0.56	0.50	0.64	0.57	1.8
51	483	1.75	1.6	2.	0.56	0.47	0.69	0.57	1.8
52	486	1.6	1.6	1.9	0.47	0.47	0.64	0.53	1.7
53	489	1.65	1.65	1.6	0.50	0.50	0.47	0.49	1.6
54	492	1.35	1.25	1.4	0.30	0.22	0.34	0.29	1.3
55	495	1.	0.75	1.	0.00	-0.29	0.00	-0.10	0.9
56	498	0.8	...	0.6	-0.22	...	-0.51	-0.37	0.7

Table 6.3-5

Gieseler Plastometry (ASTM) of Elkhorn #1 Seam Coal

time	temp	run 1	run 2	run 3	ln(1)	ln(2)	ln(3)	avg ln	avg ddpm
29 m	417°C	0.8	1.	0.7	-.223	.000	-.357	-.193	0.8
30	420	0.9	1.5	0.8	-.105	.405	-.223	.026	1.0
31	423	1.1	1.8	1.	.095	.588	.000	.228	1.3
32	426	1.3	2.8	1.3	.262	1.030	.262	.518	1.7
33	429	2.3	3.5	2.5	.833	1.253	.916	1.001	2.7
34	432	2.8	4.3	3.0	1.030	1.459	1.099	1.196	3.3
35	435	5.0	6.5	4.0	1.609	1.872	1.386	1.623	5.1
36	438	8.0	10.	7.6	2.079	2.303	2.028	2.137	8.5
37	441	12.	10.3	14.	2.485	2.332	2.639	2.485	12.0
38	444	13.	9.6	14.5	2.564	2.262	2.674	2.500	12.2
39	447	15.	12.5	16.	2.708	2.526	2.773	2.669	14.4
40	450	15.5	13.8	17.	2.741	2.625	2.833	2.733	15.4
41	453	15.5	11.4	10.5	2.741	2.434	2.351	2.509	12.3
42	456	9.0	11.5	7.0	2.197	2.442	1.946	2.195	9.0
43	459	5.0	9.0	4.0	1.609	2.197	1.386	1.731	5.6
44	462	4.0	4.5	2.6	1.386	1.504	.916	1.269	3.5_5
45	465	1.5	2.0	1.3	.405	.693	.262	.454	1.6
46	468	1.0	0.8	0.5	.000	-.223	-.693	-.305	0.7

Table 6.3-6

Isothermal Gieseler Plastometry at 410-2°C

time	Pittsburgh #8	Ohio #9	Lower Kittanning	Kentucky #11	Elkhorn #1
T(avg)	412°C	411°C	411°C	410°C	410°C
3	1.	...	...	...	...
4	2.3	0.7	...	0.8	...
5	12.4	1.5	...	1.7	...
6	30.	2.3	0.4	2.5	...
7	61.	3.8	0.4	3.9	...
8	174.	5.8	0.5	7.6	...
9	788.	7.9	0.6	17.8	0.4
10	6440.	12.	0.4	34.	0.5
11	>25,000	17.	0.4	60.	0.5
12	" "	25.	0.5	106.	0.7
13	" "	32.	0.4	187.	0.6
14	" "	39.	0.5	281.	0.8
15	" "	46.	0.4	360.	0.7
16	" "	42.	0.3	453.	0.9
17	" "	38.	0.4	508.	0.8
18	" "	37.	0.4	517.	0.9
19	" "	29.	0.4	522.	1.2
20	" "	25.	0.3	499.	1.0
21	" "	22.	0.3	483.	0.9
22	" "	18.5	0.4	500.	0.9
23	" "	13.5	0.2	456.	1.0
24	" "	11.4	0.2	363.	1.0
25	" "	8.8	0.2	303.	1.0
26	" "	6.3	0.3	244.	1.2
27	" "	4.9	0.3	204.	1.0
28	" "	4.0	0.3	183.	0.9
29	" "	3.3	0.2	137.	1.0
30	" "	2.6	0.3	113.	0.9
31	" "	2.0	0.2	97.	1.0
32	" "	1.8	0.3	82.	0.9
33	" "	1.4	0.3	68.	0.9
34	" "	1.3	0.2	55.	...
35	21,160	1.0	0.2	45.	...
36	19,730	...	...	42.	...
37	18,400	...	...	35.	...
38	23,400	...	...	29.	...
39	17,500	...	...	21.	...
40	13,230	...	...	20.	...

continued

Table 6.3-6, continued

time	Pittsburgh #8	Kentucky #11
41 min	14,185	16.7
42	17,330	16.0
43	15,680	13.7
44	14,185	11.2
45	10,400	9.6
46	10,510	7.9
47	11,730	7.2
48	12,960	6.4
49	11,500	5.2
50	12,460	4.2
51	9,136	4.2
52	9,509	3.0
53	6,836	3.1
54	6,700	2.7
55	6,634	2.3
56	6,003	1.9
57	4,583	1.7
58	4,273	1.55
59	4,230	1.3
60	3,328	1.2
61	2,724	1.06
62	4,146	0.84
63	3,103	...
64	3,328	...
65	2,059	...
66	2,592	...
67	2,253	...
68	1,686	...
69	1,604	...
70	1,737	...
71	1,236	...
72	1,054	...
73	1,033	...
74	907.	...
75	685.	...

time	Pittsburgh #8
76 min	534.
77	498.
78	503.
79	437.
80	321.
81	265.
82	202.
83	174.
84	156.
85	151.
86	129.
87	112.
88	96.
89	93.
90	96.
91	68.
92	69.
93.	61.
94.	58.
95.	48.
96.	41.
97	41.
98	36.
99	29.
100	30.
101	25.
102	24.
103	21.
104	18.5
105	19.9
106	16.0
107	11.5
108	11.7
109	9.5
...	...

Table 6.3-7

Isothermal Gieseler Plastometry at 425-6°C

time	Pittsburgh #8	Ohio #9	Lower Kittanning	Kentucky #11	Elkhorn #1
T(avg)	426°C	426°C	426°	426°C	425°C
3 min	4.9	...	...	...	...
4	30.	1.2	0.4	1.4	...
5	250.	4.7	1.2	4.8	...
6	1,437	10.7	1.7	44.	0.7
7	11,730	21.	1.6	125.	1.1
8	>25,000	44.	1.7	265.	1.9
9	" "	133.	1.9	1,330	2.6
10	" "	324.	1.8	10,680	3.2
11	" "	433.	1.8	>25,000	3.8
12	" "	372.	1.8	" "	4.3
13	" "	273.	1.9	20,830	5.2
14	" "	185.	2.1	17,070	5.8
15	" "	104.	2.0	10,700	5.7
16	" "	59.	2.0	5,844	5.6
17	" "	38.	2.0	5,838	4.3
18	" "	25.	2.1	3,894	3.6
19	" "	14.3	2.0	2,655	3.5
20	" "	9.7	2.1	1,941	2.9
21	" "	5.5	2.0	1,181	2.8
22	" "	3.5	2.0	758.	2.3
23	22,250	2.5	2.2	554.	1.9
24	21,160	1.8	1.9	358.	1.6
25	18,770	1.1	1.9	228.	1.1
26	15,990	0.7	1.6	176.	0.7
27	15,990	...	1.7	123.	...
28	11,160	...	1.5	83.	...
29	10,300	...	1.6	57.	...
30	8,778	...	1.4	41.	...
31	6,836	...	1.3	32.	...
32	6,503	...	1.2	22.	...
33	5,653	...	...	16.9	...
34	4,359	...	...	11.8	...
35	2,951	...	...	9.0	...
36	2,618	...	...	7.2	...
37	2,392	...	...	5.2	...
38	2,080	...	...	4.0	...
39	2,080	...	...	3.1	...
40	1,755		...	2.2	...

continued

Table 6.3-7, continued

time	Pittsburgh #8	Kentucky #11
41 min	1,437	1.9
42	781.	1.6
43	596.	1.3
44	518.	1.0
45	428.	0.8
46	354.	...
47	279.	...
48	279.	...
49	230.	...
50	169.	...
51	164.	...
52	128.	...
53	97.	...
54	75.	...
55	57.	...
56	51.	...
57	36.	...
58	29.	...
59	23.	...
60	18.4	...
61	15.2	...
62	12.6	...
63	9.9	...
64	8.4	...
65	6.9	...
66	5.4	...
67	4.4	...
68	2.9	...
69	2.7	...
70	1.7	...

Table 6.3-8

Isothermal Gieseler Plastometry at 450-2°C

time	Pittsburgh #8	Ohio #9	Lower Kittanning	Kentucky #11	Pocahontas #3	Elkhorn #1
T(avg)	452°C	451°C	450°C	450°C	450°C	450°C
1min	1.3	2.6	...	...	...	...
2	34.	125.	...	1.	...	...
3	1,604	15,200	0.2	28.	...	...
4	11,500	>25,000	1.5	340.	...	0.5
5	>25,000	" "	4.5	2,257	...	2.7
6	" "	8,974	8.2	19,580	...	19.1
7	" "	1,200	11.3	>25,000	...	39.
8	" "	144.	17.7	17,010	...	64.
9	" "	27.	35.	8,773	0.4	158.
10	" "	11.0	59.	2,008	0.4	246.
11	16,300	3.0	77.	484.	0.4	194.
12	10,200	0.6	76.	118.	0.2	103.
13	4,316	...	77.	43.	0.3	45.
14	1,901	...	68.	14.6	0.4	20.
15	837.	...	60.	5.9	0.3	6.8
16	340.	...	51.	2.4	0.3	3.5
17	144.	...	43.	0.9	0.4	1.55
18	57.	...	33.	0.6	0.3	0.7
19	24.	...	32.	...	0.3	...
20	11.1	...	24.	...	0.1	...
21	5.0	...	19.	...	0.2	...
22	2.9	...	16.3	...	0.1	...
23	1.6	...	12.4	...	0.2	...
24	0.8	...	9.7	...	0.4	...
25	...	...	8.1	...	0.1	...
26	...	...	6.5	...	0.2	...
27	...	...	5.0	...	0.2	...
28	...	...	4.5	...	0.1	...
29	...	...	3.4	...	0.2	...
30	...	...	2.4	...	0.0	...
31	...	...	1.8	...	...	...
32	...	...	1.6	...	...	...
33	...	...	1.1	...	...	...
34	...	...	1.0	...	...	...
35	...	...	0.7	...	...	...

Table 6.3-9

Isothermal Plastometry of Pocahontas #3 Coal*

time	450°C		470°C
6 min	0.1 ddpm		0.6 ddpm
7	.15	[0.35]	1.6
8	.5		1.9
9	.4		1.65
10	.35		1.2
11	.35		1.2
12	.15		1.1
13	.25	[0.28]	1.0
14	.35		0.8
15	.3		0.6
16	.25		...
17	.35		...
18	.25	[0.24]	...
19	.25		...
20	.10		...
21	.15		...
22	.10		...
23	.15	[0.17]	...
24	.35		...
25	.10		...
26	.15		...
27	.15		...
28	.10	[0.11]	...
29	.15		...
30	.0		...
31	.10		...
32	.15		...
33	.10	[0.10]	...
34	.0		...
35	.15		...
36	.0		...
37	.0		...
38	.25	[0.05]	...
39	.0		...
40	.0		...

---

* Gieseler plastometer readings of less than 1 ddpm are interpolated and are subject to a reading error of about $\pm$0.15 ddpm.

Bracketed figures are five-minute averages.

Table 6.3-10

Isothermal Gieseler Plastometry (400°C nominal) of Kentucky #11 Seam Coal

time	run 1	run 2	run 3	run 4	ln(1)	ln(2)	ln(3)	ln(4)	avg ln	avg ddpm
[temp]	400.°	400.°	400.°	400.°						400.°C
4	0.5	0.75	0.9	0.25	-0.69	-0.29	-0.11	-1.39	-0.62	0.54
5	0.5	1.5	1.25	0.75	-0.69	0.41	0.22	-0.29	-0.09	0.92
6	1.1	2.	1.25	1.	0.10	0.69	0.22	0.00	0.25	1.3
7	1.65	2.5	2.	1.25	0.50	0.92	0.69	0.22	0.58	1.8
8	2.25	2.75	1.75	1.75	0.81	1.01	0.56	0.56	0.74	2.1
9	2.1	3.	2.5	2.25	0.74	1.10	0.92	0.81	0.89	2.4
10	2.4	3.5	2.25	2.75	0.88	1.25	0.81	1.01	0.99	2.7
11	3.25	4.25	4.	3.	1.18	1.45	1.39	1.10	1.28	3.6
12	3.75	5.5	5.	4.	1.32	1.71	1.61	1.39	1.51	4.5
13	4.5	5.5	6.	4.75	1.50	1.71	1.79	1.56	1.64	5.2
14	5.75	4.75	9.	6.25	1.75	1.56	2.20	1.83	1.83	6.3
15	7.25	3.75	10.	5.5	1.98	1.32	2.30	1.71	1.83	6.2
16	10.	5.5	14.	4.	2.30	1.71	2.64	1.39	2.01	7.5
17	13.	6.	21.	4.5	2.57	1.79	3.05	1.50	2.23	9.3
18	19.	11.5	27.	11.	2.94	2.44	3.30	2.40	2.77	16.0
19	24.	27.	34.	19.	3.18	3.30	3.53	2.94	3.24	25.4
20	30.	39.	39.	34.	3.40	3.66	3.66	3.53	3.56	35.3
21	36.	12.	43.	31.	3.58	2.49	3.76	3.43	3.32	27.5
22	40.	14.	45.	24.	3.69	2.64	3.81	3.18	3.33	27.9
23	44.	33.	51.	47.	3.78	3.50	3.93	3.85	3.77	43.2
24	46.	42.	49.	34.	3.83	3.74	3.89	3.53	3.75	42.4
25	49.	17.	54.	39.	3.89	2.83	3.99	3.66	3.59	36.4
26	57.	28.	50.	50.	4.04	3.33	3.91	3.91	3.80	44.7
27	55.	42.	57.	28.	4.01	3.74	4.04	3.33	3.78	43.8
28	56.	24.	50.	47.	4.03	3.18	3.91	3.85	3.74	42.2
29	52.	20.	51.	37.	3.95	3.00	3.93	3.61	3.62	37.4
30	54.	39.	47.	31.	3.99	3.66	3.85	3.43	3.73	41.9
31	47.	34.	46.	44.	3.85	3.53	3.83	3.78	3.75	42.4
32	49.	13.	39.	27.	3.89	2.57	3.66	3.30	3.35	28.6
33	44.	22.	39.	31.	3.78	3.09	3.66	3.43	3.49	32.9
34	46.	33.	37.	32.	3.83	3.50	3.61	3.47	3.60	36.6
35	41.	30.	36.	27.	3.71	3.40	3.58	3.30	3.50	33.1
36	38.	15.	32.	16.	3.64	2.71	3.47	2.77	3.15	23.2
37	39.	13.	28.	23.	3.66	2.57	3.33	3.14	3.17	23.9
38	35.	21.	27.	25.	3.56	3.05	3.30	3.22	3.28	26.5
39	33.	23.	28.	22.	3.50	3.14	3.33	3.09	3.26	26.1
40	31.	21.	26.	16.	3.43	3.05	3.26	2.77	3.13	22.8
41	29.	13.	22.	11.	3.37	2.57	3.09	2.40	2.86	17.4
42	29.	6.	17.	11.	3.37	1.79	2.83	2.40	2.60	13.4
43	30.	10.	16.	14.	3.40	2.30	2.77	2.64	2.78	16.1
44	28.	10.	16.	13.	3.33	2.30	2.77	2.57	2.74	15.5
45	23.	13.	17.	11.	3.14	2.57	2.83	2.40	2.73	15.4

c o n t i n u e d

Table 6.3-10 Con't.

Isothermal Gieseler Plastometry (400°C nominal) of Kentucky #11 Seam Coal, Continued

time	run 1	run 2	run 3	run 4	ln(1)	ln(2)	ln(3)	ln(4)	avg ln	avg ddpm
46	22.	12.	16.	11.	3.09	2.49	2.77	2.40	2.69	14.7
47	22.	11.	17.	10.	3.09	2.40	2.83	2.30	2.66	14.2
48	23.	10.	13.	10.	3.14	2.30	2.57	2.30	2.58	13.2
49	19.	9.	12.	6.	2.94	2.20	2.49	1.79	2.36	10.5
50	17.	9.	10.	5.	2.83	2.20	2.30	1.61	2.24	9.4
51	15.	7.	8.	4.	2.71	1.95	2.08	1.39	2.03	7.6
52	15.	4.5	7.	4.	2.71	1.50	1.95	1.39	1.89	6.6
53	16.	3.5	7.	3.	2.77	1.25	1.95	1.10	1.77	5.9
54	15.	3.	7.	3.	2.71	1.10	1.95	1.10	1.71	5.5
55	12.	2.5	6.	4.	2.49	0.92	1.79	1.39	1.65	5.2
56	12.	2.	6.	4.	2.49	0.69	1.79	1.39	1.59	4.9
57	11.	2.5	6.	3.75	2.40	0.92	1.79	1.32	1.61	5.0
58	9.	2.5	6.	3.5	2.20	0.92	1.79	1.25	1.54	4.7
59	8.	3.	6.	3.5	2.08	1.10	1.79	1.25	1.56	4.7
60	8.	3.	5.	3.	2.08	1.10	1.61	1.10	1.47	4.4
61	7.	2.5	5.	2.75	1.95	0.92	1.61	1.01	1.37	3.9
62	7.	3.	4.	2.5	1.95	1.10	1.39	0.92	1.34	3.8
63	7.	3.	4.	2.25	1.95	1.10	1.39	0.81	1.31	3.7
64	7.	2.75	3.5	2.25	1.95	1.01	1.25	0.81	1.26	3.5
65	6.	2.25	3.	2.	1.79	0.81	1.10	0.69	1.10	3.0
66	5.	2.	2.5	2.	1.61	0.69	0.92	0.69	0.98	2.7
67	5.	2.5	2.5	1.5	1.61	0.92	0.92	0.41	0.96	2.6
68	5.	1.75	2.	1.5	1.61	0.56	0.69	0.41	0.82	2.3
69	5.	1.75	2.	1.25	1.61	0.56	0.69	0.22	0.77	2.2
70	4.	1.25	2.	1.25	1.39	0.22	0.69	0.22	0.63	1.9
71	4.	1.5	2.	1.	1.39	0.41	0.69	0.00	0.62	1.9
72	3.	1.25	2.	0.75	1.10	0.22	0.69	-0.29	0.43	1.5
73	3.	1.25	1.5	...	1.10	0.22	0.41	...	0.36	[1.4]

Table 6.3-11

Gieseler Plastometry (Isothermal, 410°C nominal) of Western Kentucky #11 Coal

time	run 1	run 2	run 3	ln(1)	ln(2)	ln(3)	avg ln	avg ddpm
4 min	0.8	0.5	1.3	-0.22	-0.69	0.26	-0.22	0.8
5	2.3	1.	2.	0.83	0.00	0.69	0.51	1.7
6	3.	1.5	3.5	1.10	0.41	1.25	0.92	2.5
7	4.	3.	5.	1.39	1.10	1.61	1.36	3.9
8	7.	9.	7.	1.95	2.20	1.95	2.03	7.6
9	14.	27.	15.	2.64	3.30	2.71	2.88	17.8
10	29.	47.	29.	3.37	3.85	3.37	3.53	34.
11	61.	61.	59.	4.11	4.11	4.08	4.10	60.
12	99.	124.	98.	4.60	4.82	4.58	4.67	106.
13	165.	215.	183.	5.11	5.37	5.21	5.23	187.
14	270.	315.	262.	5.60	5.75	5.57	5.64	281.
15	375.	395.	315.	5.93	5.98	5.75	5.89	360.
16	505.	510.	360.	6.22	6.23	5.89	6.12	453.
17	565.	560.	415.	6.34	6.33	6.03	6.23	508.
18	630.	510.	430.	6.45	6.23	6.06	6.25	517.
19	695.	500.	410.	6.54	6.21	6.02	6.26	522.
20	700.	460.	385.	6.55	6.13	5.95	6.21	499.
21	725.	450.	345.	6.59	6.11	5.84	6.18	483.
22	765.	520.	315.	6.64	6.25	5.75	6.22	500.
23	715.	510.	260.	6.57	6.23	5.56	6.12	456.
24	560.	370.	230.	6.33	5.91	5.44	5.89	363.
25	470.	310.	190.	6.15	5.74	5.25	5.71	303.
26	360.	260.	155.	5.89	5.56	5.04	5.50	244.
27	310.	210.	130.	5.74	5.35	4.87	5.32	204.
28	250.	170.	102.	5.52	5.14	4.62	5.09	163.
29	200.	160.	81.	5.30	5.08	4.39	4.92	137.
30	170.	114.	74.	5.14	4.74	4.30	4.73	113.
31	145.	103.	61.	4.98	4.63	4.11	4.57	97.
32	115.	92.	52.	4.74	4.52	3.95	4.41	82.
33	95.	70.	47.	4.55	4.25	3.85	4.22	68.
34	80.	56.	38.	4.38	4.03	3.64	4.01	55.
35	63.	47.	30.	4.14	3.85	3.40	3.80	45.
36	54.	47.	29.	3.99	3.85	3.37	3.74	41.9
37	45.	36.	27.	3.81	3.58	3.30	3.56	35.2
38	38.	33.	19.	3.64	3.50	2.94	3.36	28.8
39	32.	21.	14.	3.47	3.04	2.64	3.05	21.1
40	28.	21.	14.	3.33	3.04	2.64	3.01	20.2
41	23.	17.	12.	3.14	2.83	2.48	2.82	16.7
42	19.	18.	12.	2.94	2.89	2.48	2.77	16.0
43	16.	16.	10.	2.77	2.77	2.30	2.62	13.7
44	13.	12.	9.	2.56	2.48	2.20	2.42	11.2
45	14.	8.	8.	2.64	2.08	2.08	2.27	9.6

c o n t i n u e d

Table 6.3-11 Con't.

Gieseler Plastometry (at 410°C nominal) of Western Kentucky #11 Coal, Continued

time	run 1	run 2	run 3	ln(1)	ln(2)	ln(3)	avg ln	avg ddpm
46 m	11.	6.	7.5	2.40	1.79	2.01	2.07	7.9
47	9.5	6.	6.5	2.25	1.79	1.87	1.97	7.2
48	7.5	7.	5.	2.01	1.95	1.61	1.86	6.4
49	7.	5.	4.	1.95	1.61	1.39	1.65	5.2
50	5.	5.	3.	1.61	1.61	1.10	1.44	4.2
51	6.	4.	3.	1.79	1.39	1.10	1.43	4.2
52	4.	3.5	2.	1.39	1.25	0.69	1.11	3.0
53	4.	3.	2.5	1.39	1.10	0.92	1.13	3.1
54	3.5	3.	1.8	1.25	1.10	0.59	0.98	2.7
55	3.	2.5	1.7	1.10	0.92	0.53	0.85	2.3
56	2.3	2.	1.5	0.83	0.69	0.41	0.64	1.9
57	2.	1.8	1.3	0.69	0.59	0.26	0.51	1.7
58	2.	1.7	1.1	0.69	0.53	0.10	0.44	1.55
59	1.5	1.5	0.9	0.41	0.41	-0.11	0.24	1.3
60	1.5	1.5	[0.8]	0.41	0.41	-0.22	0.20	1.2
61	1.3	1.3	[0.7]	0.26	0.26	-0.36	0.06	1.06
62	1.	1.	[0.6]	0.00	0.00	-0.51	-0.17	0.84
63	1.	1.	[0.5]	0.00	0.00	-0.69	-0.23	0.79
Temp:	409.8° ± 0.4°	410.1° ± 0.4°	410.0° ± 0.2°					410.0°C

Table 6.3-12

Gieseler Plastometry (Isothermal, 425°C nominal) of Western Kentucky #11 Seam Coal

time	run 1	run 2	run 3	run 4	ln(1)	ln(2)	ln(3)	ln(4)	avg ln	avg ddpm
2 min	...	...	...	...	...	...	...	...	...	...
3	...	...	0.3	0.3	...	...	-1.2	-1.2	...	...
4	0.5	2.	2.2	1.8	-0.69	0.69	0.79	0.59	0.34	1.4
5	3.0	5.	6.	6.	1.10	1.61	1.79	1.79	1.57	4.8
6	71.5	41.	31.	41.	4.27	3.71	3.43	3.71	3.78	44.
7	215.	102.	95.	118.	5.37	4.62	4.55	4.77	4.83	125.
8	560.	175.	195.	258.	6.33	5.16	5.27	5.55	5.58	265.
9	2200.	575.	1320.	1875.	7.70	6.35	7.19	7.54	7.19	1330.
10	12950.	4300.	10150.	23000.	9.47	8.37	9.23	10.04	9.28	10680.
11	>25000.	>25000.	23700.	>25000.	>10.1	>10.1	10.07	>10.1	>10.1	>25000.
12	" "	" "	>25000.	" "	" "	" "	>10.1	" "	" "	" "
13	" "	23000.	16200.	20200.	" "	10.04	9.69	9.91	9.94+	20830.+
14	23300.	15400.	14800.	16000.	10.06	9.64	9.60	9.68	9.75	17070.
15	13700.	9600.	11200.	8900.	9.53	9.17	9.32	9.09	9.28	10700.
16	7400.	3400.	7600.	6100.	8.91	8.13	8.94	8.72	8.67	5844.
17	5600.	6000.	6400.	5400.	8.63	8.70	8.76	8.59	8.67	5838.
18	3400.	5000.	4100.	3300.	8.13	8.52	8.32	8.10	8.27	3894.
19	2180.	3800.	2500.	2400.	7.69	8.24	7.82	7.78	7.88	2655.
20	1590.	2500.	2100.	1700.	7.37	7.82	7.65	7.44	7.57	1941.
21	1000.	1600.	1240.	980.	6.91	7.38	7.12	6.89	7.07	1181.
22	540.	1140.	710.	755.	6.29	7.04	6.57	6.63	6.63	758.
23	400.	830.	535.	530.	5.99	6.72	6.28	6.27	6.32	554.
24	280.	570.	350.	295.	5.63	6.35	5.86	5.69	5.88	358.
25	170.	365.	205.	214.	5.14	5.90	5.32	5.37	5.43	228.
26	140.	250.	160.	172.	4.94	5.52	5.08	5.15	5.17	176.
27	103.	175.	113.	114.	4.63	5.16	4.73	4.74	4.82	123.
28	62.	120.	73.	89.	4.13	4.79	4.29	4.49	4.42	83.
29	39.	82.	49.	65.	3.66	4.41	3.89	4.17	4.03	56.5
30	33.	58.	39.	38.	3.50	4.06	3.66	3.64	3.71	41.

c o n t i n u e d

Table 6.3-12 Con't.

Gieseler Plastometry (Isothermal, 425°C nominal) of Western Kentucky #11 Seam Coal, Continued

time	run 1	run 2	run 3	run 4	ln(1)	ln(2)	ln(3)	ln(4)	avg ln	avg ddpm
31 min	25.	44.	25.	40.	3.22	3.78	3.22	3.69	3.48	32.4
32	14.	30.	21.	27.	2.64	3.40	3.04	3.30	3.10	22.1
33	11.	21.	17.5	20.	2.40	3.04	2.86	3.00	2.83	16.9
34	9.	14.	11.	14.	2.20	2.64	2.40	2.64	2.47	11.8
35	6.	12.	8.5	10.5	1.79	2.48	2.14	2.35	2.19	9.0
36	4.5	10.	7.	8.5	1.50	2.30	1.95	2.14	1.97	7.2
37	3.5	8.	4.	6.5	1.25	2.08	1.39	1.87	1.65	5.2
38	2.5	5.	4.	5.	0.92	1.61	1.39	1.61	1.38	4.0
39	2.	4.	3.	4.	0.69	1.39	1.10	1.39	1.14	3.1
40	1.5	2.5	2.	3.3	0.41	0.92	0.69	1.19	0.80	2.2
41	1.3	2.	2.	2.5	0.26	0.69	0.69	0.92	0.64	1.9
42	1.0	2.	1.8	2.	0.00	0.69	0.59	0.69	0.49	1.6
43	[0.7]	2.	1.3	1.5	-0.36	0.69	0.26	0.41	0.25	1.3
44	[0.55]	1.5	1.1	1.3	-0.60	0.41	0.10	0.26	0.04	1.0
45	[0.4]	1.3	0.9	1.	-0.92	0.26	-0.11	0.00	-0.19	0.8
46	...	1.	...	...	...	...	...	...	...	...
Temp:	425.9°C ± 1.0°	425.2°C ± 0.4°	425.5°C ± 0.5°	425.3°C ± 0.6°						425.5°C

Table 6.3-13

Isothermal Gieseler Plastometry (440°C nominal) of Kentucky #11 Seam Coal

TIME	run 1	run 2	run 3	ln(1)	ln(2)	ln(3)	avg ln	avg ddpm
[temp]	440.0°	440.0°	440.0°					440.0°
2	1.1	0.1	0.5	0.10	-2.30	-0.69	-0.97	0.38
3	43.5	0.65	14.25	3.77	-0.43	2.66	2.00	7.4
4	240.	11.25	106.	5.48	2.42	4.66	4.19	66.
5	515.	148.	187.	6.24	5.00	5.23	5.49	242.
6	2500	390	892	7.82	5.97	6.79	6.86	955
7	15000	2050	5900	9.62	7.63	8.68	8.64	5661
8	29700	14900	23900	10.30	9.61	10.08	10.00	21950(+)
9	29600	25500	27200	10.30	10.15	10.21	10.22	27380(+)
10	23000	17800	16600	10.04	9.79	9.72	9.85	18940
11	10400	4700	9500	9.25	8.46	9.16	8.96	7744
12	3900	3100	3950	8.27	8.04	8.28	8.20	3628
13	1625	1100	1570	7.39	7.00	7.36	7.25	1411
14	675	560	615	6.52	6.33	6.42	6.42	615
15	323	265	250	5.78	5.58	5.52	5.63	278
16	164	125	125	5.10	4.83	4.83	4.92	137
17	83	57	57	4.42	4.04	4.04	4.17	65
18	38	35	29	3.64	3.56	3.37	3.52	33.8
19	21	16	15	3.05	2.77	2.71	2.84	17.1
20	11	7	8	2.40	1.95	2.08	2.14	8.5
21	5.5	5.	4.5	1.71	1.61	1.50	1.61	5.0
22	3.5	2.	2.5	1.25	0.69	0.92	0.95	2.6
23	2.25	1.5	1.5	0.81	0.41	0.41	0.54	1.7
24	1.25	1.	0.75	0.22	0.00	-0.29	-0.02	1.0

Table 6.3-14

Gieseler Plastometry (Isothermal, 450°C nominal) of Western Kentucky #11 Seam Coal

time	run 1	run 2	run 3	ln(run 2)	ln(run 3)	avg ln(ddpm)[1]	avg ddpm[1]
1 min	3000.	..	..	...	...	...	...
2	>25000.	1.	1.	0.00	0.00	0.00	1.
3	" "	26.	31.	3.26	3.43	3.35	28.
4	" "	283.	408.	5.65	6.01	5.83	340.
5	8400.	3490.	1460.	8.16	7.27	7.72	2257.
6	22500.	18700.	20500.	9.84	9.93	9.88	19580.
7	>25000.	22800.	>25000.	10.03	>10.13	>10.08	>23900.
8	17500.	10800.	26800.	9.29	10.20	9.74	17010.
9	6600.	4300.	17900.	8.37	9.79	9.08	8773.
10	4300.	900.	4480.	6.80	8.41	7.60	2008.
11	960.	225.	1040.	5.42	6.95	6.18	484.
12	210.	55.	255.	4.01	5.54	4.77	118.
13	65.	24.	78.	3.18	4.36	3.77	43.
14	25.	8.5	25.	2.14	3.22	2.68	14.6
15	8.	3.5	10.	1.25	2.30	1.78	5.9
16	3.5	1.5	4.	0.41	1.39	0.90	2.4
17	1.5	0.5	1.6	-0.69	0.47	-0.11	0.9
18	0.7	[0.4]	0.9	-0.92	-0.11	-0.51	0.6
Temp	450.2° ± 0.8°	449.8° ± 0.6°	450.0° ± 0.2°				449.9°

[1] Data from run 1 were excluded on the basis of erratic behavior during the first five minutes.

Table 6.3-15

Isothermal Gieseler Plastometry (460°C nominal) of Kentucky #11 Seam Coal

time	run 1	run 2	run 3	ln(1)	ln(2)	ln(3)	avg ln	avg ddpm
[temp]	460.0	460.0	460.0					460.0°C
1	0.25	0.5	0.25	-1.39	-0.69	-1.39	-1.16	0.32
2	1.5	37.5	4.25	0.41	3.62	1.45	1.83	6.2
3	5998.	20262.	13395.	8.70	9.92	9.50	9.37	11760.
4	30000+	30000+	29800	10.31+	10.31+	10.30	10.31+	29930+
5	23400	22800	17500	10.16	10.14	9.77	9.96	21060
6	23000	14000	28100	10.14	9.55	10.24	9.95	20840
7	30000+	18700	25900	10.31+	9.84	10.16	10.10	24400+
8	25300	1000	11700	10.14	6.91	9.37	8.81	6665
9	5300	200	1490	8.58	5.30	7.31	7.06	1165
10	692	105	155	6.54	4.65	5.04	5.41	224
11	101	28	26	4.62	3.33	3.26	3.74	41.9
12	18	4	5.5	2.89	1.39	1.71	1.99	7.3
13	5	1	1.5	1.61	0.00	0.41	0.67	2.0
14	2	<1	0.5	0.69	[-1.2]	-0.69	-0.40	[0.7]

6.4.1 Modelling the Isothermal Plastometric Curve

Results are summarized in Section 4.1. Mathematical modelling of the curves shown in Figures 3.3-3 and 4.1-1 makes use of the minicomputer program for successive small incrementation of Equation 2, starting with the initial conditions:

C°	(meltable but not-yet melted fraction)	= 1.00
M°	(molten fraction)	= 0.00
S°	(melted and resolidified fraction)	= 0.00

Integration by successive incrementation is sensitive to mesh. A model was selected for which $k_{init} = 1 \times 10^{-4}$ min^{-1}, $k_{melt} = 1.8$ min^{-1}, and $k_{coke} = 0.2$ min^{-1}, conditions affording a very sharp autoacceleration and hence apt to magnify mesh error. Calculations were conducted for 30-minute time frames at various calculational and printing meshes. Results are summarized in terms of the calculated slopes and values of $t_{max\ flu}$, in Table 6.4-1. These show the calculations to be, in general, insensitive to printing mesh, but systematically sensitive to calculational mesh. The nature of this dependency is shown, for the case of m_{coke}, in Figure 6.4-1.

For subsequent calculations a mesh of 30 min^{-1} has been used.

The database used to develop the relationships among k_{melt}, k_{coke}, and the corresponding slopes is summarized in Table 6.4-2. The values of k_{melt} (0.2 to 2.0 min^{-1}) and of k_{coke} (from 0.1 to 1.0 min^{-1}) cover the low and middle ranges of values derived from experimental data in Table 4.1-2.

Tables 6.4-3 and 6.4-4 show the results of quadratic regression analyses used for the evaluation of k_{coke} and k_{melt}, respectively, from raw experimental data. Table 6.4-5 presents the model data developed for the purpose of estimating values of k_{init}.

The value of k_{init} is of significance for this model analysis. Where $k_{init} < 10^{-5}$ min^{-1} it exerts no significant impact on slopes. As k_{init} increases over the decade 10^{-5} to 10^{-4} min^{-1} its impact becomes noticeable: melting slopes

Table 6.4-1

Modelling the Isothermal Plastometric Behavior of Coals: Some Effects of Calculational and Printing Mesh*

Calcn mesh	Print mesh	melting slope[1]	s.d.	Coking slope[1]	s.d.	Maximum molten fraction (intercept)	Time at maximum fluidity (intercept)
1	1	0.955	.008	[2]		.....	....
2	1	1.178	.014	[2]		.....	....
3	1	1.203	.014	- .2062	.0004	0.8442	7.31 min
4	1	1.348	.014	- .2045	.0001	0.8801	7.13
6	1	1.409	.017	- .2029	.0028	0.9189	6.82
10	1	1.462	.021	- .2016	.0004	0.9519	6.57
12	1	1.475	.021	- .2012	.0004	0.9606	6.51
15	1	1.489	.023	- .2009	.0003	0.9695	6.44
20	1	1.503	.025	- .2006	.0004	0.9784	6.39
30	1	1.562	.013	- .2003	.0004	1.006	6.23
60	1	1.580	.015	- .2000	.0003	1.016	6.16
120	1	1.589	.014	- .1998	.0002	1.021	6.13
2	2	1.178	.0083	[2]		.....	....
4	2	1.333	.0110	- .2045	.0003	0.873	7.16
8	2	1.442	.0112	- .2021	.0003	0.9407	6.66
16	2	1.514	0.151	- .2009	.0003	0.9790	6.396
30	2	1.563	.0128	- .2003	.0002	1.0049	6.234
60	2	1.581	.0140	- .2000	.0003	1.0148	6.168
120	2	1.589	.0138	- .1998	.0003	1.0199	6.134
480	2	1.596	.0142	- .1997	.0004	1.0235	6.109
5	5	1.384	.007	- .2035	.0001	0.9024	6.948
10	5	1.469	.0008	- .2016	.0002	0.9550	6.560
15	5	1.507	.008	- .2009	.0003	0.9765	6.412
30	5	1.547	.007	- .2003	.0002	0.9991	6.263
60	5	1.572	.009	- .2000	.0001	1.0113	6.185
120	5	1.580	.009	- .1998	.0002	1.0163	6.152
480	5	1.587	.009	- .1997	.0002	1.0199	6.127

* For $k_i = .0001$, $k_m = 1.8$, and $k_c = 0.2$ min^{-1}, 30-minute calculations

[1] in units of cycles per minute

[2] program fails, apparently owing to coarseness of calculational mesh

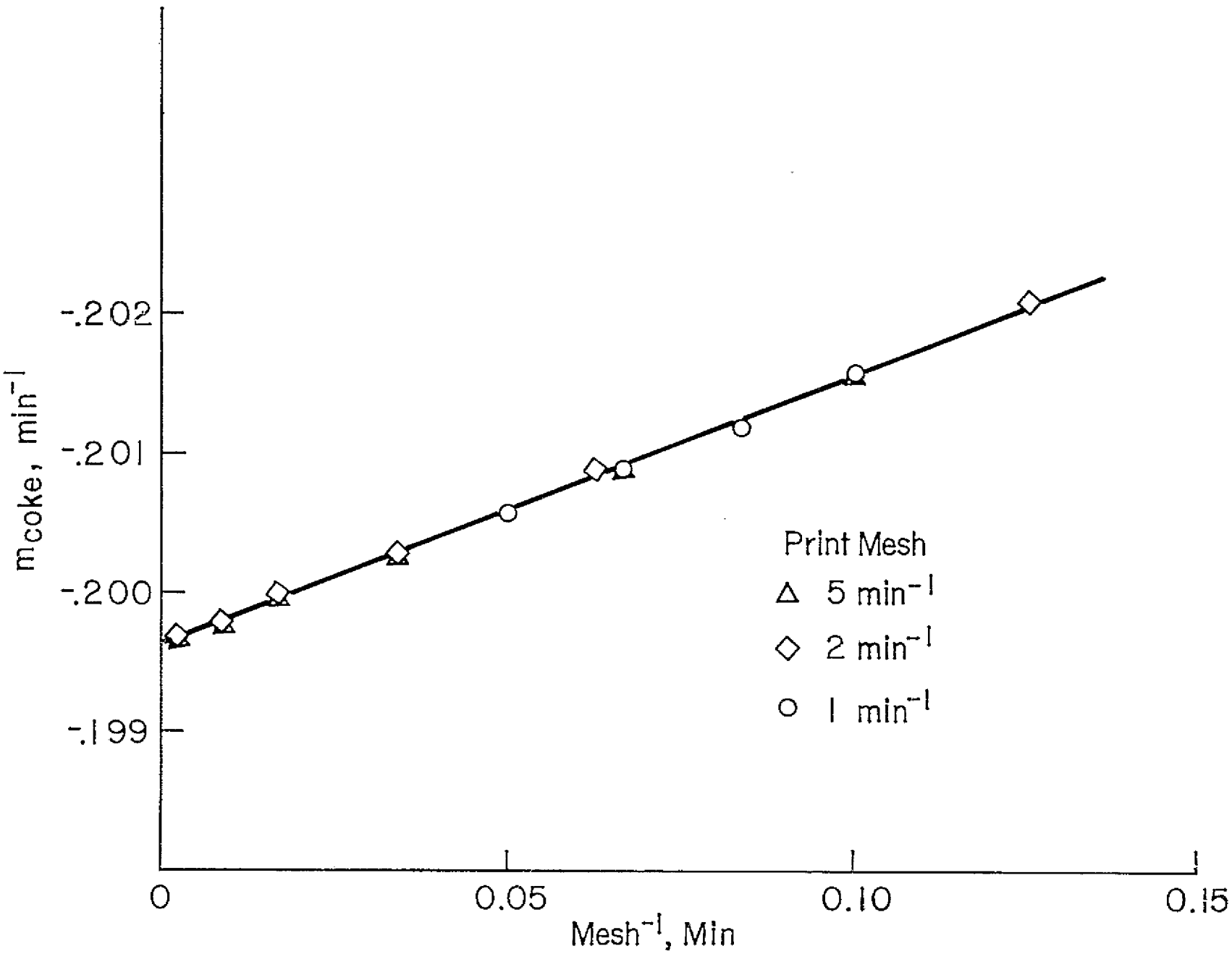

Fig. 6.4-1 Effect of Calculational Mesh Upon Calculated Value of Coking Slope

Table 6.4-2

Model Data Used for Estimates of k(melt) and k(coke)*

k(melt)	k(coke)	m(melt)	-m(coke)	$\frac{-m(coke)}{m(melt)}$	$\frac{k(melt)}{m(melt)}$	$\frac{-k(coke)}{m(coke)}$
0.2	0.1	.1233	.0569	.4615	1.6221	1.7575
0.4	0.1	.3130	.0913	.2916	1.2780	1.0955
0.6	0.1	.5026	.0982	.1955	1.1938	1.0179
0.6	0.15	.4611	.1377	.2987	1.3012	1.0891
0.6	0.2	.4194	.1625	.3876	1.4306	1.2305
0.6	0.25	.3643	.1735	.4762	1.6470	1.4412
0.6	0.3	.3276	.1719	.5247	1.8315	1.7452
0.6	0.35	.2879	.1604	.5573	2.0841	2.1815
0.8	0.1	.6873	.0998	.1452	1.1640	1.0020
0.8	0.2	.6037	.1836	.3042	1.3252	1.0892
0.8	0.4	.4213	.2282	.5417	1.8989	1.7528
1.0	0.1	.8908	.1006	.1130	1.1226	0.9936
1.0	0.15	.8487	.1490	.1755	1.1783	1.0070
1.0	0.2	.7891	.1931	.2447	1.2673	1.0358
1.0	0.25	.7465	.2299	.3080	1.3396	1.0875
1.0	0.3	.6917	.2582	.3733	1.4457	1.1619
1.0	0.35	.6500	.2774	.4268	1.5385	1.2618
1.0	0.4	.6080	.2888	.4750	1.6447	1.3849
1.0	0.6	.4248	.2637	.6208	2.3540	2.2753
1.2	0.1	1.0932	.1002	.0916	1.0977	0.9985
1.2	0.2	0.9873	.1974	.1999	1.2154	1.0131
1.2	0.4	.7971	.3269	.4101	1.5055	1.2236
1.4	0.1	1.2552	.1002	.0798	1.1154	0.9984
1.4	0.15	1.2140	.1502	.1237	1.1532	0.9986
1.4	0.2	1.1721	.1992	.1700	1.1944	1.0039
1.4	0.25	1.1299	.2453	.2171	1.2390	1.0191
1.4	0.3	1.0752	.2869	.2668	1.3021	1.0457
1.4	0.35	1.0443	.3229	.3092	1.3406	1.0841
1.4	0.4	0.9913	.3527	.3558	1.4123	1.1342
1.4	0.6	0.7927	.4107	.5181	1.7661	1.4610
1.4	0.8	.6193	.3835	.6193	2.2606	2.0860
1.4	1.0	.4377	.2884	.6589	3.1985	3.4675
1.6	0.1	1.4668	.1002	.0683	1.0908	0.9983
1.6	0.2	1.3642	.2001	.1467	1.1728	0.9995
1.6	0.4	1.1920	.3695	.3100	1.3423	1.0825
1.6	1.0	0.6231	.4102	.6582	2.5678	2.4381
1.8	0.1	1.6490	.1004	.0609	1.0916	0.9956
1.8	0.15	1.607	.1504	.0936	1.1201	0.9976
1.8	0.2	1.5424	.2004	.1299	1.1670	0.9979
1.8	0.25	1.5017	.2485	.1655	1.1986	1.0061

continued

Table 6.4-2, continued

Model Data Used for Estimates of k(melt) and k(coke), contd.

k(melt)	k(coke)	m(melt)	-m(coke)	$\frac{-m(coke)}{m(melt)}$	$\frac{k(melt)}{m(melt)}$	$\frac{-k(coke)}{m(coke)}$
1.8	0.3	1.4605	.2968	.2032	1.2325	1.0108
1.8	0.35	1.4187	.3405	.2400	1.2688	1.0278
1.8	0.4	1.3584	.3805	.2801	1.3251	1.0513
1.8	0.6	1.1740	.4941	.4209	1.5332	1.2144
1.8	0.8	0.9927	.5337	.5376	1.8132	1.4991
1.8	1.0	.8014	.5076	.6334	2.2461	1.9700
1.8	1.2	.6195	.4263	.6881	2.9056	2.8150
1.8	1.4	.4436	.2991	.6743	4.058	4.681
2.0	0.1	1.8357	.1002	.0546	1.0895	0.9983
2.0	0.4	1.559	.3881	.2489	1.2829	1.0307
2.0	1.0	1.0012	.5878	.5871	1.9976	1.7013

---

* Calculated for k(init) = 1.00×10^{-4} min^{-1}, using a calculational mesh of 30 cycles min^{-1}, taking least-squares slopes from all generated data points for molten fractions between .0005 and one fifth of the maximum melted fraction.

Table 6.4-3

Estimate of k(coke) by a Quadratic Regression*

Coeficients: $a_0 = -8.2709$

$a_1 = +24.0332$

$a_2 = -17.3436$

[-m(coke)/m(melt)]	ln[-k(coke)/m(coke) - 1]	[-k(coke)/m(coke)]
0.05	-7.1126	1.001
.10	-6.0410	1.002
.15	-5.0561	1.006
.20	-4.1580	1.016
.25	-3.3466	1.035
.30	-2.6219	1.073
.35	-1.9839	1.138
.40	-1.4326	1.239
.45	-0.9680	1.380
.50	-0.5902	1.554
.55	-0.2991	1.742
.60	-0.0947	1.910

* for the equation:

$$\ln\left[-\frac{k(coke)}{m(coke)} - 1\right] = a_0 + a_1 \cdot \left[-\frac{m(coke)}{m(melt)}\right] + a_2 \cdot \left[-\frac{m(coke)}{m(melt)}\right]^2$$

Table 6.4-4

Estimate of k(melt) by a Quadratic Regression*

coefficients: $a_0 = +1.1195$

$a_1 = -0.1880$

$a_2 = +2.9015$

[-m(coke)/m(melt)]	[k(melt)/m(melt)]
0.05	1.0952
.10	1.1247
.15	1.1632
.20	1.2108
.25	1.2673
.30	1.3329
.35	1.4075
.40	1.4911
.45	1.5837
.50	1.6873
.55	1.7959
.60	1.9156

* for the equation:

$$\left[\frac{k(melt)}{m(melt)}\right] = a_0 + a_1 \cdot \left[\frac{-m(coke)}{m(melt)}\right] + a_2 \cdot \left[\frac{-m(coke)}{m(melt)}\right]^2$$

Table 6.4-5

Model Data Used for Estimates of k_{init}*

k_{init}	k_{melt}	k_{coke}	m_{melt}	$-m_{coke}$	$\frac{-m_{coke}}{m_{melt}}$	$t_{max\ flu}$
1×10^{-8}	0.6	0.2	.3881	.1636	.4215	44.03 min
	1.0	0.2	.7709	.1911	.2479	23.24
	1.0	0.4	.5790	.2906	.5020	29.81
	1.8	0.2	1.5322	.2003	.1307	12.20
	1.8	0.4	1.3333	.3808	.2856	13.83
	1.8	1.0	.7723	.5168	.6692	22.04
3.162×10^{-8}	0.6	0.2	.3882	.1636	.4214	41.03
1×10^{-7}	0.6	0.2	.3883	.1635	.4211	38.22
	1.0	0.2	.7710	.1923	.2495	20.34
	1.0	0.4	.5800	.2918	.5032	25.95
	1.8	0.2	1.5331	.2003	.1307	10.72
	1.8	0.4	1.3454	.3803	.2826	12.12
	1.8	1.0	.7713	.5164	.6695	19.12
1×10^{-6}	0.6	0.2	.3911	.1637	.4186	32.36
	1.0	0.2	.7733	.1922	.2486	17.40
	1.0	0.4	.5813	.2918	.5019	22.06
	1.8	0.2	1.5342	.2003	.1306	9.24
	1.8	0.4	1.3393	.3811	.2845	10.45
	1.8	1.0	.7729	.5175	.6696	16.21
1×10^{-5}	0.6	0.2	.3951	.1629	.4122	26.44
	1.0	0.2	.7768	.1927	.2481	14.48
	1.0	0.4	.5855	.2914	.4976	18.14
	1.8	0.2	1.5376	.2004	.1303	7.76
	1.8	0.4	1.3333	.3809	.2857	8.79
	1.8	1.0	.7728	.5162	.6680	13.29
1×10^{-4}	0.6	0.2	.4194	.1623	.3869	20.23
	1.0	0.2	.7899	.1928	.2440	11.52
	1.0	0.4	.6030	.2888	.4750	14.07
	1.8	0.2	1.5424	.2004	.1299	6.29
	1.8	0.4	1.3584	.3805	.2801	7.05
	1.8	1.0	.8014	.5113	.6380	10.24
1×10^{-3}	0.6	0.2	.5164	.1526	.2955	13.09
	1.0	0.2	.9379	.1926	.2054	8.04
	1.0	0.4	.8093	.2482	.3067	8.61
	1.8	0.2	1.682	.2004	.1191	4.67
	1.8	0.4	1.5287	.3780	.2472	5.14
	1.8	1.0	1.085	.3988	.3676	5.94

* calculational mesh is 30 min^{-1}; k's in min^{-1}; $t_{max\ flu}$ by intercept of least-squares slopes.

are increased by an average of 0.019 min^{-1} and coking slopes decreased by an average of .0014 min^{-1}. As k_{init} increases over the next decade, from 10^{-4} to 10^{-3} min^{-1}, its impact becomes substantial. Melting slopes are increased by about 0.17 min^{-1} on the average and coking slopes undergo a variable but significant decrease of about 0.03 min^{-1}. Above 10^{-3} the linearity of the melting slope is sufficiently degraded (with standard deviations of slope now typically about 10% of slope) that the assumption of a linear region for ln fluidity vs. time is no longer a very good assumption. In this range the treatment is no longer useful.

KENTUCKY CENTER

FOR

ENERGY RESEARCH

This report was published as part of the Commonwealth-sponsored energy research and demonstration programs under the auspices of The Kentucky Center for Energy Research. The Center was established in 1975 as a cabinet-level state agency to formulate energy plans and strategies and to sponsor related research and demonstration projects. A fifteen-member Energy Research Board guides the activity of the Center. The Kentucky Center for Energy Research is located on Iron Works Pike near Lexington, Kentucky.